Cell Reports
Physical Science

CellPress
OPEN ACCESS

Review

Advances in membranes and electrocatalysts to optimize proton-exchange membrane fuel cells

Naeimeh Rajabalizadeh Mojarrad,[1] Ahmet Can Kırlıoğlu,[2] Burak Ölmez,[3] Ali Ansari Hamedani,[1,4] Merve Buldu-Akturk,[5] Mohammed Ahmed Zabara,[6] Alp Yürüm,[1,4] Cengiz S. Ozkan,[7,*] Selmiye Alkan Gürsel,[1,4,*] Begüm Yarar Kaplan,[1,3,*] and Mihrimah Ozkan[8,*]

[1]Sabanci University SUNUM Nanotechnology Research Center, Istanbul 34956, Türkiye
[2]Vlaamse Instelling voor Technologisch Onderzoek (VITO), Boeretang 200, 2400 Mol, Belgium
[3]Section of Chemistry for Technology, Department of Industrial Engineering, University of Padova, via F. Marzolo 9 35131 Padova, Italy
[4]Faculty of Engineering and Natural Sciences, Sabanci University, Istanbul 34956, Türkiye
[5]Helmholtz-Zentrum Berlin für Materialien und Energie, 14109 Berlin, Germany
[6]Yusuf Hamied Department of Chemistry, University of Cambridge, Lensfield Road, Cambridge CB2 1EW, UK
[7]Department of Mechanical Engineering, University of California, Riverside, Riverside, CA, USA
[8]Department of Electrical and Computer Engineering, University of California, Riverside, Riverside, CA, USA
*Correspondence: cozkan@engr.ucr.edu (C.S.O.), selmiye.gursel@sabanciuniv.edu (S.A.G.), begum.yararkaplan@unipd.it (B.Y.K.), mihri.ozkan@ucr.edu (M.O.)
https://doi.org/10.1016/j.xcrp.2025.102728

SUMMARY

Proton-exchange membrane fuel cells (PEMFCs) have attracted substantial global attention from academia, industry, and policymakers due to their critical role in enabling clean and efficient energy conversion. This momentum is increasingly reflected in real-world applications, including the commercialization of fuel cell vehicles and growing interest in heavy-duty transport solutions. However, PEMFCs still face major barriers to widespread adoption—chief among them are high system costs and limited durability. These challenges largely stem from the membrane electrode assembly (MEA), the functional core of the fuel cell. Accordingly, extensive research efforts have focused on advancing MEA materials, particularly membranes and electrocatalysts, to enhance performance while reducing cost and improving longevity. This review provides a comprehensive overview of recent developments in both state-of-the-art and emerging MEA materials alongside fabrication strategies and their associated trade-offs. By outlining key limitations and proposing future research directions, this work highlights the urgent need for durable, efficient, and scalable solutions to drive PEMFC commercialization in sectors such as transportation, energy storage, and distributed power generation.

INTRODUCTION

Climate change, energy security, and sustainability represent some of the most pressing challenges of our time, elevating hydrogen to an unprecedented level of importance in the global energy landscape. To achieve net-zero carbon emission targets by 2050, countries such as the United States and members of the European Union have introduced comprehensive roadmaps.[1,2] In this context, hydrogen emerges as a promising solution, both as a fuel and as an energy carrier, to meet carbon-free energy goals.[3] In our previous reviews, we have discussed the methods and the current status of hydrogen production.[4,5] Our scope will be fuel cells in this review.

Decarbonizing the transportation sector is particularly critical to achieving the objectives outlined in the Paris Agreement. Governments worldwide are implementing diverse policies to support this transition, as detailed in the International Energy Agency (IEA) Global Electric Vehicle (EV) Policy Explorer.[6] For heavy-duty transportation, the European Commission proposed in 2023 an amendment to the 2019 regulation on CO_2 emission standards, targeting a 90% CO_2 reduction for trucks by 2040 and requiring all city buses to achieve zero emissions by 2030.[7]

Fuel cells play a pivotal role in enabling a sustainable and equitable clean energy future by efficiently converting the chemical energy of clean hydrogen and other fuels into electricity, with heat and water as the only by-products. These versatile systems have applications across numerous sectors, including transportation (road, rail, marine, and aviation), stationary power (industrial, commercial, and residential), and long-duration energy storage for the electricity grid. Furthermore, fuel cell technologies are instrumental in advanced applications such as combined heat and power systems and hybrid approaches like trigeneration, which simultaneously produce power, heat, and hydrogen. By addressing both immediate and long-term challenges, fuel cells represent a cornerstone in the global transition toward sustainable energy solutions.

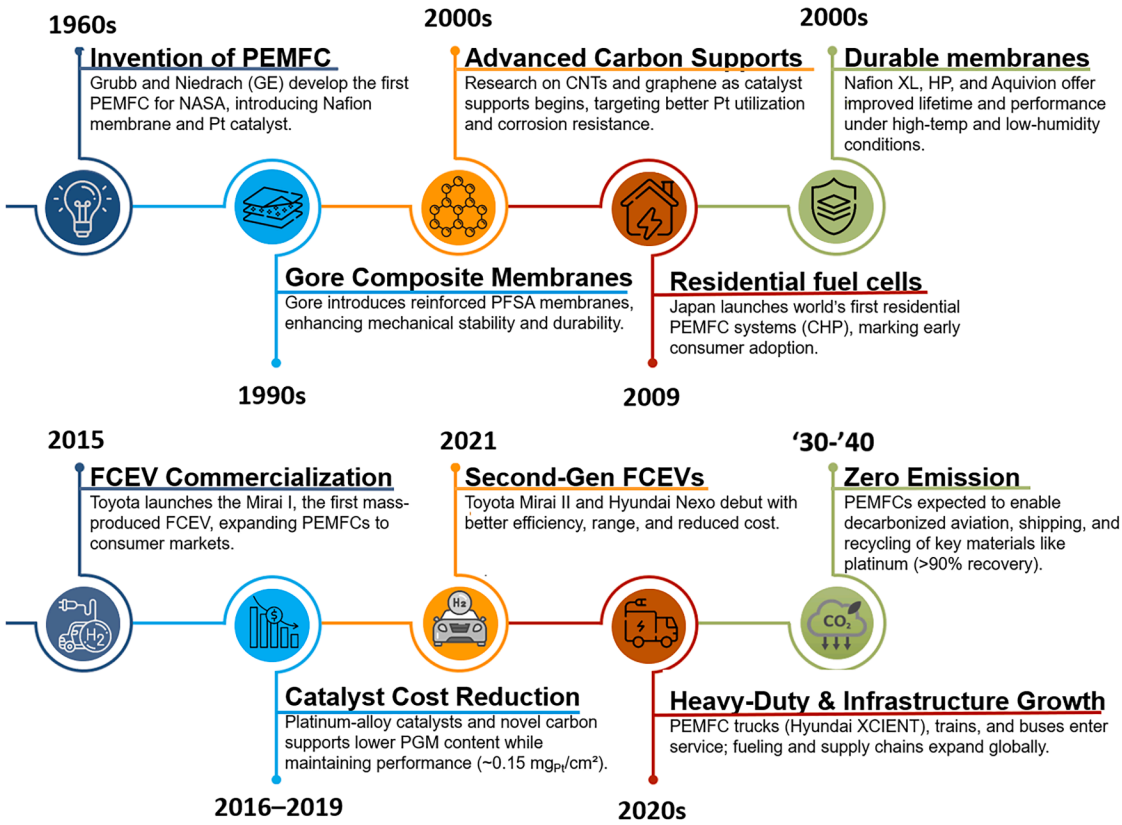

Figure 1. Timeline illustrating the historical evolution and projected milestones of PEMFCs

The evolution begins with their invention in the 1960s for NASA missions, followed by Gore's development of composite membranes in the 1990s and research into advanced carbon supports in the 2000s. Commercialization efforts gained traction with Japan's Ene-Farm residential systems in 2009 and the launch of the first mass-produced FCEV, the Toyota Mirai, in 2015. Progress in the 2010s included chemically stabilized membranes and catalyst innovations that reduced platinum usage. The 2020s mark the emergence of second-generation FCEVs and heavy-duty applications. Looking forward, PEMFC are expected to play a central role in decarbonizing transport and enabling a sustainable, zero-emission energy economy by 2040.

As summarized in Figure 1, proton-exchange membrane fuel cell technology has undergone significant evolution since its inception, addressing long-standing challenges in cost, durability, and system performance. Originally developed in the 1960s by Grubb and Niedrach at General Electric for NASA space missions,[8] proton-exchange membrane fuel cells (PEMFCs) remained limited to specialized applications due to their high cost and platinum dependence. In the 1990s, advancements in membrane electrode assemblies, including Gore's introduction of reinforced composite membranes, and improved platinum-based catalysts marked the first major performance leap.[9,10] The 2000s witnessed the emergence of carbon nanostructures, such as carbon nanotubes and graphene as high-performance catalyst supports,[11] and the first real-world stationary applications, like Japan's Ene-Farm systems.[12] By 2015, the commercialization of the Toyota Mirai I signaled PEMFC readiness for consumer use,[13] followed by the release of second-generation fuel cell electric vehicles (FCEVs) such as the Mirai II and Hyundai Nexo around 2021–2022. Parallel progress in chemically stabilized perfluorinated sulfonic acid (PFSA) membranes and catalyst optimization between 2010 and 2019 further boosted efficiency and durability.[14,15] Entering the 2020s, PEMFCs gained traction in heavy-duty mobility and infrastructure applications, particularly through long-range freight vehicles and buses. Ongoing efforts aim to reduce platinum usage by over 50% and extend stack lifetimes beyond 25,000 h by 2030,[16] setting the stage for zero-emission deployment in aviation, shipping, and industrial sectors by 2040.[17]

Comparison of different types of fuel cell technologies

Fuel cells are categorized into several key types based on their structure, operating mechanisms, and applications (Figure 2). Among the most notable are alkaline fuel cells (AFC), PEMFCs, solid oxide fuel cells (SOFCs), and anion-exchange membrane fuel cells (AEMFCs).[17–19] These technologies differ in various characteristics, including electrolyte type, operating temperature, anode and cathode reactions, power output, and efficiency, as summarized in Table 1.

Among these, PEMFCs stand out as the most effective due to several key advantages, including low-temperature operation (80°C–100°C), compact design, rapid response to load changes, and high efficiency (>60%).[25] These benefits position PEMFCs as promising candidates for next-generation power sources, particularly in the transportation sector.

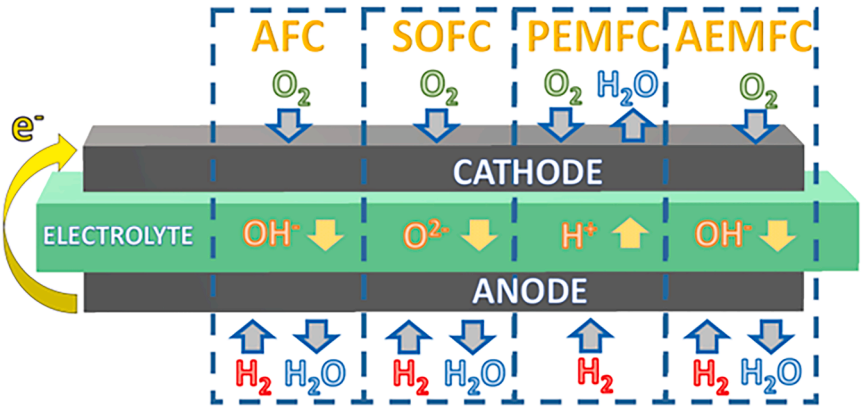

Figure 2. Fuel cell types

Shown is a schematic of the ion conduction mechanisms and reactant/product flows in AFCs, SOFCs, PEMFCs, and AEMFCs. A detailed comparison is provided in Table 1. Arrows indicate the transport of H_2, O_2, H_2O, ions, and electrons.

In recent years, the industrialization of alternative energy vehicles, especially battery electric vehicles (BEVs), has gained momentum due to their low carbon emissions and the growing accessibility of charging infrastructure. However, while BEVs dominate the current market, fuel cell vehicles (FCVs) offer notable advantages, including longer driving ranges (up to 600 km before refueling), shorter refueling times (3–5 min), and superior energy density compared to batteries.[26,27] These attributes make FCVs particularly well suited for heavy-duty applications, long-distance transportation, and sectors such as shipping and aviation, where BEVs face limitations.[3]

Heavy-duty vehicles powered by fuel cells have gained significant interest in recent years. For example, the US Department of Energy (DOE) has set ambitious targets for fuel cell system lifetimes, aiming for 8,000 h for light-duty vehicles and 30,000 h for heavy-duty trucks under operating conditions.[28] The long-distance benefits and rapid refueling of FCVs make them a superior alternative to BEVs for such applications.

The growing demand for PEMFCs is reflected in market projections. The global PEMFC market, valued at US$2,044.73 million in 2020, is expected to reach US$6,270.43 million by 2027.[29] Additionally, PEMFCs in the transportation sector are projected to exceed US$8 billion by 2034.[30] Major FCEV manufacturers, such as Hyundai, Toyota, and Honda, have demonstrated the viability of PEMFC technology by incorporating it into their platforms.[31,32] These factors underline the significant potential of PEMFCs as the leading technology for future clean transportation solutions.

Description of the PEMFC system

As the hydrogen economy gains momentum, the demand for materials used in PEMFCs is expected to rise significantly, particularly in tandem with the expanding FCEV market. The global market for hydrogen FCVs is projected to grow from US$0.2 billion in 2024 to US$2.1 billion by 2030, reflecting a compound annual growth rate (CAGR) of 48%.[33] However, despite this promising growth trajectory, several critical challenges remain, including high manufacturing costs, complex hydrogen storage requirements, and logistical barriers to hydrogen transportation, all of which hinder the widespread adoption of fuel cell technologies in consumer vehicles. Addressing these challenges necessitates the development and deployment of cost-effective, durable, and high-performance materials to facilitate broader applications across various industries.

At the core of a PEMFC system lies the membrane electrode assembly (MEA), often referred to as the "heart" of the fuel cell. The MEA consists of two electronically conductive electrodes –the anode and the cathode– separated by a proton-conductive solid polymer membrane, which functions as the electrolyte (Figure 3A). Typically, PFSA polymers serve as the primary membrane material, while Pt/C and Pt alloy/C catalysts are incorporated into the electrode structures. Although these materials offer acceptable performance and durability, their high cost remains a substantial barrier to the large-scale commercialization of PEMFC-based systems. Within the MEA, two key electrochemical reactions take place:

(1) the hydrogen oxidation reaction (HOR) at the anode, where hydrogen molecules are split into protons and electrons, and
(2) the oxygen reduction reaction (ORR) at the cathode, where oxygen reacts with the protons, forming water as the only by-product.

These reactions occur at specialized active sites known as triple-phase boundaries (TPBs), where the catalyst, reactant gases, and electrolyte interact to facilitate efficient energy conversion.[35] There are various methods in the literature for the preparation of MEAs. Generally, these methods can be categorized into two types: (1) preparation of MEAs using gas diffusion electrodes (Figure 2A), where the catalyst ink is applied onto the gas diffusion layer using different spraying techniques, and (2) the catalyst-coated membrane (CCM) approach, in which the catalyst layer is applied directly onto the membrane (Figure 3B).[36]

The hydrogen and fuel cell markets have witnessed substantial growth in recent years and are poised for further expansion. In the European Union (EU) alone, the hydrogen industry is projected to reach a market valuation of €65 billion by 2030.[37] Similarly, the global hydrogen FCV market, valued at US$2.32 billion in 2024, is anticipated to grow exponentially, reaching US$29.70 billion by 2030.[38] In parallel, the market for PEMFC-powered systems is expected to experience rapid expansion, with estimates placing its valuation at US$7.15 billion by 2028.[39]

These projections underscore the increasing global reliance on hydrogen-based technologies as viable alternatives to conventional fossil fuel systems. However, achieving widespread adoption will require continued advancements in materials

Table 1. Comparative analysis of four major fuel cell technologies

Fuel cell types	AFCs	SOFCs	PEMFC	AEMFCs
Temperature, °C	<100[18]	500–1,000[18]	<120[18]	<80[20]
Common electrolyte	aqueous KOH solution soaked in a matrix	yttria-stabilized zirconia	perfluorinated sulfonic acid polymeric membranes	no common electrolyte, polymers comprising hydrocarbon backbone and $-NR_3^+$ side chain
Anode reaction	$2H_2 + 4OH^- \rightarrow 4H_2O + 4e^-$	$O^{2-} + H_2 \rightarrow H_2O + 2e^-$	$H_2 \rightarrow 2H^+ + 2e^-$	$2H_2 + 4OH^- \rightarrow 4H_2O + 4e^-$
Cathode reaction	$O_2 + 2H_2O + 4e^- \rightarrow 4OH^-$	$1/2\ O_2 + 2e^- \rightarrow O_2^-$	$1/2\ O_2 + 2H^+ + 2e^- \rightarrow H_2O$	$O_2 + 2H_2O + 4e^- \rightarrow 4OH^-$
System output, kW	10–100[17]	<1–3,000[17]	<1–250[17]	–
Lifetime, h	>5,000[21]	40,000–80,000[22]	5,000[23]	300–5,000[21]
Cost	$_{>V}$€104–€170·kW^{-1}[21]	US$0.07–US$0.08·kWh^{-1}[24]	US$76·kW^{-1}[23]	–
Advantages	faster cathode reaction kinetics under alkaline conditions, enhance performance	high efficiency, fuel flexibility, diverse catalyst options, and reduced electrolyte management issues due to solid oxide electrolytes	reduced corrosion, simplified electrolyte management, mild operating temperatures, and rapid start-up	fuel flexibility, compact design, low-cost MEA fabrication, and elimination of perfluorinated polymers and PGM-based catalysts.
Disadvantages	electrolyte management challenges	high temperature operation, corrosion risks, component degradation, and slow start-up	high cost of PGM catalysts, fuel impurity sensitivity	slow HOR kinetics, low AEM ionic conductivity; water management, and the chemical stability of membranes

science, cost reduction strategies, and infrastructure development to support the integration of PEMFCs into mainstream energy and transportation systems.

The role of membranes in PEMFCs

In a PEMFC, the membrane serves a pivotal role by separating the anode and cathode while facilitating selective proton transport.[40] Key characteristics of the proton-exchange membrane (PEM) include (1) high proton conductivity to ensure efficient proton migration under operating conditions; (2) gas impermeability to prevent hydrogen and O_2/air crossover and exceptional chemical and mechanical stability to withstand the demanding PEMFC environment, characterized by acidic, oxidizing, and reducing conditions; (3) utilization of low-cost polymers, which is imperative to support widespread commercialization.

The role of electrocatalysts in PEMFCs

Electrocatalysts in PEMFCs facilitate the electrochemical reactions at the anode and cathode, with the cathode catalyst playing a critical role in performance and stability.[41] The ideal properties of a cathode catalyst include (1) high catalytic activity and selectivity to catalyze the desired reactions while suppressing side reactions, (2) good durability to maintain performance over extended operational periods, (3) resistance to poisoning to minimize performance loss due to impurities like CO in the reactant gases, and (4) utilization of abundant and low-cost materials to ensure economic viability.

Research and development focus

The performance of PEMFCs depends heavily on the properties of both the membrane and electrocatalysts. Current research and development efforts aim to enhance the performance, durability, and cost-effectiveness of these materials. This review will focus on recent advancements in membrane and catalyst technologies for PEMFCs, highlighting their critical roles in achieving a sustainable hydrogen economy and advancing clean energy solutions.

Cost barriers for fuel cell applications

The high cost of PEMFC technology remains one of the primary barriers to its widespread market adoption. These costs stem not only from the expenses associated with individual stack components and their durability but also from the price of hydrogen fuel and the limited availability of hydrogen infrastructure, which are critical for PEMFC operation.[26]

In terms of fuel cell stack costs, the materials used, their manufacturing processes, and their durability significantly influence the overall system cost. MEA, considered the heart of a fuel cell, is the largest contributor to system costs, as illustrated in Figure 4. Among MEA components, the use of platinum-group metals (PGMs) in the electrode structure is a major cost driver, accounting for approximately 40% of the total stack cost.[42,43] However, reducing PGM usage often results in decreased efficiency, durability, and overall performance. Thus, a trade-off between Pt loading and cell performance is essential, highlighting the need for significant advancements in PEMFC electrocatalysts to achieve high power output.[44]

Another expensive MEA component is the membrane, which accounts for approximately 10% of the total stack cost.[26] Currently, PFSA-based membranes, such as Nafion, are extensively employed due to their superior chemical and physical properties. However, these membranes are costly, priced at US$350–US$500 m^{-2}, and perform optimally only under high relative humidity and temperatures below 100°C.[46] These limitations often lead to challenges such as water management issues

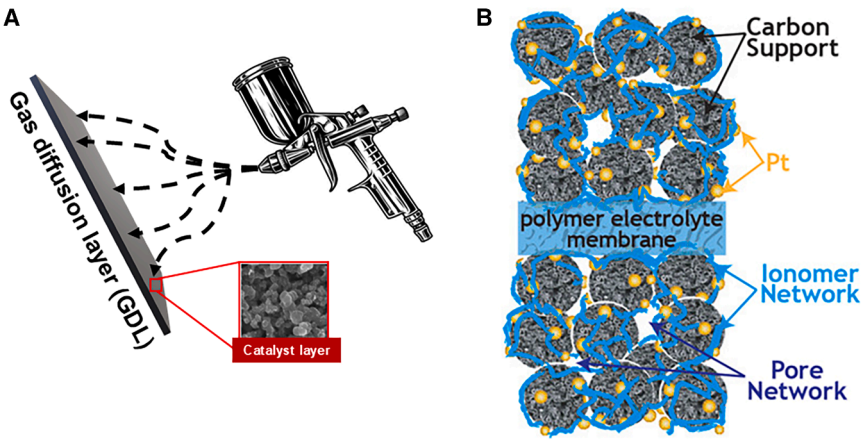

Figure 3. Schematic of MEA fabrication methods

(A) MEA fabrication using sprayed electrodes.

(B) MEA fabrication utilizing a catalyst-coated membrane (CCM) approach.

Adapted with permission from the American Chemical Society.[34]

and Pt poisoning, prompting a need for alternative, cost-effective membrane materials with enhanced performance.

Recent advancements have significantly reduced the cost of PEMFC stacks for FCEVs, which stood at approximately US $75/kW in 2022, representing a 35% reduction over recent years.[47] However, further cost reductions are necessary to achieve the 2030 cost targets for heavy-duty FCV systems.

Cost reduction strategies

To meet the long-term cost goals for heavy-duty FCV systems, research, development, and demonstration efforts must prioritize reducing the costs of stack components, particularly membranes and catalysts. The US DOE's Hydrogen and Fuel Cell Technologies Office Multi-Year Program Plan emphasizes reducing the cost of stack components, including the MEA, to US$27 for a 275 kW PEMFC system.[48] Achieving this goal will require a combination of advanced material development, optimized manufacturing processes, and improved durability to ensure cost-effective and high-performing fuel cell systems for widespread adoption.

The political-economic landscape

The global landscape for hydrogen generation and fuel cell applications is experiencing a significant transformation, driven by a confluence of factors, including technological advancements, policy initiatives, and environmental imperatives. As of 2024, the market size for green hydrogen exceeded US$6.49 billion, with projections indicating a CAGR of over 31% through 2032.[49] This rapid growth is underpinned by substantial governmental support, exemplified by initiatives such as the US DOE's US$750 million funding for 52 hydrogen projects across 24 states and the EU's collaborative efforts with Japan to accelerate hydrogen technology deployment.[50] The economic impact of this burgeoning sector is poised to be substantial, with estimates suggesting that, by 2050, global sales of hydrogen could be worth US$600 billion, while the value chains of green hydrogen could represent a US$11.7 trillion investment opportunity.[51] This economic potential is coupled with significant environmental benefits, as evidenced by California's Hydrogen Hub initiative, which aims to decarbonize public transportation, heavy-duty trucking, and port operations by 2 million metric tons per year.[52] The international collaboration fostered through multilateral partnerships and emerging trade corridors is crucial for establishing industry standards and supporting infrastructure development.[53] However, challenges persist, including unclear demand signals, financing hurdles, and regulatory uncertainties.[54] Despite these obstacles, the trajectory of hydrogen and fuel cell technologies suggests a transformative impact on global gross domestic product (GDP) and a substantial contribution to mitigating environmental challenges worldwide, positioning this sector as a key driver in the transition to a sustainable, low-carbon global economy.[55]

PEMFC components

Each fuel cell stack comprises multiple individual cells connected in series to attain the required power output, as each individual cell can produce only a maximum theoretical voltage of 1 V. As illustrated in Table 1, each single cell within the stack is composed of four primary components: a solid polymeric PEM, two porous conductive catalyst layers (CL), two microporous carbon-based gas diffusion layers, and two bipolar plates (BPs) with flow channels for reactant transport.[56,57] It is crucial to focus on the development of new materials to further enhance the performance and reduce costs of the system. As research efforts increasingly shift toward manufacturing challenges, significant strides are being made to innovate and improve the materials, especially those used in membranes and electrodes.[58]

PEMs

The membrane, as the core component of the MEA in PEMFCs, plays a pivotal role in ensuring efficient operation and overall system performance. It primarily serves as a medium for proton transport from the anode to the cathode, where they combine with oxygen to produce water.[47] Consequently, the success of PEMFC technology heavily depends on the development of high-performance, durable, inexpensive, and environmentally friendly membranes capable of withstanding the demanding conditions of cell operation.

Generally, an ideal PEM must possess high ionic conductivity, robust mechanical strength, and excellent thermal and chemical stability to ensure reliable performance.[59] One of the key factors influencing membrane performance is its ability to maintain a delicate balance between water uptake and proton conductivity.[59] Proper hydration is essential for ensuring the presence of sufficient proton-conducting sites along with well-connected pathways for efficient proton transport, particularly through the vehicle mechanism. However, excessive water uptake can lead to undesirable dimensional changes during hydration and dehydration cycles, resulting in mechanical degradation and eventual structural failure. Moreover,

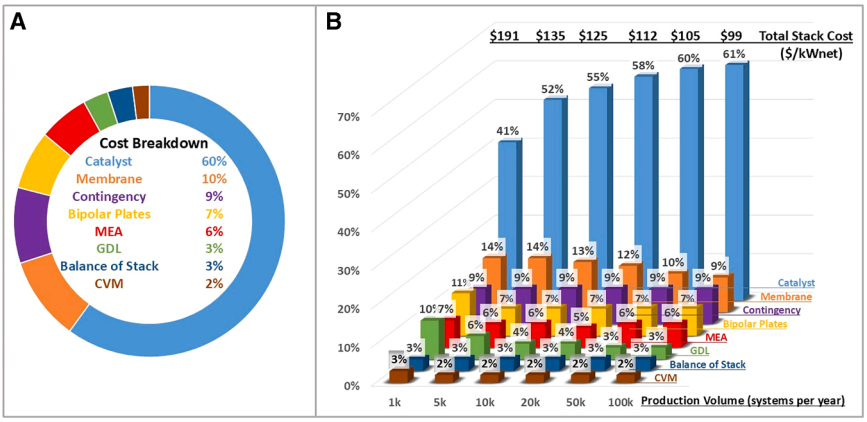

Figure 4. The stack component cost breakdown based on the production volume for HDV application

Information is adapted from the US DOE Hydrogen Program Record: (A) at 50,000 systems/year and (B) at various production volumes (CVM, cell voltage monitor).[45]

excess water can obstruct the transport of reactant gases to the CLs, causing water flooding issues, especially on the cathode side. Recent advancements in water management for PEMFCs have focused on refining this balance between hydration and water transport rate, both of which carry a significant importance for ensuring optimal fuel cell performance and longevity.[25,60,61] For this purpose, water distribution and transport phenomena are extensively studied by employing a combination of advanced computational modeling in parallel with diagnostic and experimental techniques to investigate water dynamics within fuel cell components, aiming to identify optimal operating conditions and develop innovative design strategies. By analyzing the intricate interplay between water distribution, electrochemical reactions, and transport mechanisms, ongoing research is driving the development of next-generation materials, flow control strategies, and operational protocols. Furthermore, while the membrane must be highly permeable to protons and water molecules, it is crucial that it remains impermeable to reactant gases, as gas crossover can lead to the direct mixing of hydrogen and oxygen, resulting in membrane perforation, ultimately compromising both safety and durability.[62,63]

Achieving this balance necessitates an optimized trade-off among three critical factors.

(1) Performance: encompassing efficiency, durability, and adaptability to operating conditions
(2) Safety and environmental impact: addressing concerns related to operation, fabrication, and recycling of membrane materials
(3) Cost: optimizing material selection, fabrication processes, and production scalability to enhance commercial viability

These advancements hold significant potential for improving efficiency, reliability, and durability across a broad spectrum of fuel cell applications, ranging from transportation to stationary power generation. As research continues to refine water management techniques, PEMFC technology is poised to achieve greater commercial viability, supporting the global transition to sustainable and high-performance hydrogen energy systems.

Classification of PEMs

In PEMFCs, the membrane material is typically a solid polymer featuring a backbone integrated with ion-conducting polar moieties.[64,65] These materials are commonly categorized into five main groups based on their chemical structure: perfluorinated, partially fluorinated, non-fluorinated, acid-base blends, and other varieties, such as carbon-based nanomaterials and natural polymer-based membranes. Beyond their chemical characteristics, PEMFC membranes can also be classified based on the fabrication methods, which play a pivotal role in defining their microstructure and, consequently, their performance and properties.[66,67] Common fabrication techniques include solution casting—the most widely used method—alongside extrusion,[67] radiation-induced grafting (RIG),[68] electrospinning, and approaches that combine multiple techniques. Each fabrication method imparts distinct microstructural characteristics to the membrane, influencing its functional properties. This review provides a detailed overview of the application of RIG and electrospinning techniques in the development of membranes for low-temperature PEMFCs.

Perfluorinated membranes

Among the various membrane types, perfluorinated membranes represent the first commercially developed and most mature class for PEMFC applications. These membranes are synthesized through the copolymerization of either aliphatic or aromatic fluorinated monomers, both of which are functionalized with acidic side chains such as sulfonic, carboxylic, or phosphonic acid groups.[69] Structurally, they comprise a hydrophobic polytetrafluoroethylene (PTFE) backbone linked to perfluorinated vinyl ether pendant side chains terminated with hydrophilic acidic groups.[70] The exceptional chemical, mechanical, and thermal stability of perfluorinated membranes is primarily attributed to the hydrophobic PTFE backbone, characterized by its robust carbon–fluorine bonds. Conversely, their high proton conductivity stems from the hydrophilic acidic terminal groups. Within this category, PFSA membranes are the most prominent.

PFSA membranes are categorized by their side-chain length (namely, long side chain and short side chain), resulting in variations in their equivalent weight, inherent properties, and performance. Marketed examples include Nafion, Aquivion, Gore-Select, and Flemion, produced by DuPont, Solvay, W.L. Gore, Brussels, and Asahi Glass, respectively. Nafion, developed by Walther Grot in the late 1960s for aerospace applications, remains the most widely used membrane for PEMFCs in both research and industry.[71] Its popularity stems from its exceptional properties, such as high chemical stability, a lifespan exceeding 60,000 h, adequate ion exchange capacity

Table 2. Commercial PEMs

Membrane	Company	Thickness (μm)	Conductivity (mS·cm^{-1})	IEC	Reference
Aciplex K-101	Asahi Chemical	240	11.4 at 30°C and 100% RH	1.4[a]	Pan et al.[76]
Nafion N117	DuPont	180	13.3 at 30°C and 100% RH	0.9[a]	Pan et al.[76]
Nafion N-901	DuPont	400	10.5 at 30°C and 100% RH	1.1[a]	Pan et al.[76]
Nafion 211	DuPont	254	70 at 25°C	0.98[a]	Pan et al.[76]
Nafion 212	DuPont	50.8	80 at 30°C	0.9[b]	Lee et al.[77]
Nafion N115	DuPont	127	100 at 25°C and 100% RH	0.9[b]	Chemours[78]
Pall R-1010	Pall RAI	100	33.3 at 30°C and 100% RH	1.2[a]	Pan et al.[76]
Gore-Select	W.L. Gore & Associates	18	12.5 at 80°C and 30% RH	–	Gore[79]
Aquivion E87-05S	Solvay-Solexis	50	228 at 80°C and 100% RH	1.12[b]	Solvay[80]

Shown are properties of selected commercial PEMs used in fuel cells, including membrane thickness, proton conductivity under specified conditions, ion exchange capacity (IEC), and manufacturers. Data highlight the variability in performance among different PEM materials based on composition and operating conditions.
[a]mmol·g^{-1}.
[b]meq·g^{-1}.

(IEC = 0.91 mmol·g^{-1}), and excellent ionic conductivity (σ = 80 mS·cm^{-1} at 100% relative humidity [RH] and 30°C), making it the benchmark for PEMFC membrane comparisons.[64,71–73]

Nafion is available in various forms, including films of different thicknesses (e.g., Nafion 112, 115, 117, 211, and 212) and ionomer dispersions at concentrations of 5% and 20% by weight.[74] Despite its unique properties, Nafion has several drawbacks. Its performance is constrained by a narrow operational temperature range (<90°C) and high RH (~100%) requirements, limiting versatility and increasing system costs due to supplementary humidification systems.[74] For instance, the proton conductivity of Nafion 212 decreases nearly 5-fold when the RH drops from 80% to 40% at 80°C and reduces by approximately 1.5 times when the temperature decreases from 80°C to 60°C at 80% RH.[75] Additional challenges include excessive swelling/contraction during hydration cycles, complex manufacturing processes, expensive monomers (>US$500 m^{-2}), and environmental concerns, such as toxic fluoride gas release during degradation.[65] To overcome these issues, various strategies have been developed to address the aforementioned issues by either modifying the properties of Nafion membranes or completely replacing them with alternative options. Nevertheless, Nafion membranes have remained the most used membrane materials for PEMFCs over the past decades.

Table 2 presents a selection of commercial PEMs, key to fuel cell operations, characterized by their thickness, conductivity, and IEC. These membranes exhibit an IEC ranging from approximately from 0.9 to 1.4 mmol·g^{-1}, which is pivotal for their proton conduction efficiency. Conductivities vary from around 10–300 mS·cm^{-1}, typically measured at a standard temperature of 25°C–30°C and 100% RH, but it is essential to note the substantial dependency of these values on temperature and humidity levels. The membrane thickness spans a broad spectrum from 18 to 400 μm, influencing not just the mechanical robustness but also the conduction efficiency of the membrane. Therefore, the choice of membrane for specific fuel cell applications must consider these parameters, aiming to optimize IEC, conductivity, mechanical stability, and sensitivity to environmental conditions.

Partially/non-fluorinated and acid-base membranes

Unlike perfluorinated membranes, which are composed exclusively of fluorocarbon units in both the polymer backbone and side chains, partially fluorinated membranes integrate primarily aliphatic polymer structures with fluorocarbon segments in their backbones. These membranes typically feature side chains comprising non-fluorinated hydrocarbon pendant groups, such as sulfonated aromatic moieties.[81,82] An example of such membranes involves grafting various monomers, such as styrene or its derivatives,[83] onto base polymers like polyvinylidene fluoride (PVDF),[84,85] poly(ethylene-*alt*-tetrafluoroethylene) (ETFE),[86–89] or poly(tetrafluoroethylene-*co*-hexafluoropropylene) (FEP),[90] which have been extensively studied. In certain cases, the resulting copolymer structures are transformed into proton-conducting membranes through acid treatment processes, such as sulfonation[91] or phosphoric acid doping,[86] to incorporate ion-conductive polar groups, enabling proton transport. In contrast to previous types, non-fluorinated membranes are entirely free of fluorocarbon units, with their backbone and side chains composed exclusively of aliphatic or aromatic hydrocarbon units.[92] Notable examples include sulfonated poly(ether ether ketone) (SPEEK),[93] poly(arylene ether sulfone),[94] polyphenylene sulfone,[95,96] and polybenzimidazole.[97,98] Another category includes acid-base blend membranes, which combine an acidic polymer, as a proton donating agent, with a basic compound often containing N-heterocyclic compounds, such as imidazole or pyridine.[99]

The aforementioned membrane types provide a more cost-effective alternative to traditional perfluorinated membranes by partially or entirely replacing fluorine. This substitution significantly lowers the costs associated with the fluorination process and the reliance on expensive fluorine-containing monomers. Nonetheless, ongoing research is focused on optimizing their properties to ensure optimal performance under real operating conditions.

Nafion-based hybrid and composite membranes

A widely adopted strategy for enhancing Nafion membranes involves incorporating organic or inorganic additives,[74] such as ionic liquids, metal oxides, including SiO_2,[100,101] TiO_2,[102] ZrO_2,[103] or their functionalized variants,[72] to create hybrid composite membranes. The properties of these additives—such as size, morphology, surface functionality (e.g., charge type and density), dispersion quality, and compatibility with Nafion—directly influence the membrane's performance.[72,104]

For instance, nanotube-bead additives enhance water retention and diffusion by acting as nanoscale water transport channels.[105] Similarly, incorporating non-functionalized oxides like SiO_2 improves thermochemical stability, dimensional integrity, and fuel crossover resistance.[106] However, these improvements often come at the cost of reduced conductivity due to the disruption of interconnected proton transport channels. In contrast, introducing charged functional groups significantly enhances conductivity by increasing the number of charge carriers and facilitating dynamic interactions with sulfonic acid groups of the Nafion alongside enlarging ion-transport channels.[104,106] Achieving these improvements, however, requires precise and homogeneous nanoscale distribution of additives, which is made possible by advanced fabrication techniques such as sol-gel, self-assembly,[107] and electrospinning[71] approaches that surpass the capabilities of conventional casting techniques.

A second category of state-of-the-art Nafion-based composite membranes utilizes carbon-based nanomaterials, including carbon nanotubes (CNTs), graphene oxide (GO), and their surface-modified derivatives due to their exceptional mechanical strength, optical properties, and stability.[108] Alternatively, an inert polymer can serve as a support for Nafion or vice versa to provide reinforcement. This class of membranes can be developed through various strategies, including the addition of fillers to enhance the Nafion properties, surface modification of Nafion membranes, or replacing Nafion entirely with alternative materials. Fabrication methods such as solution casting, RIG, and electrospinning have been explored for this purpose. While solution casting remains common, challenges such as incompatibility of components and inhomogeneity of the final membrane structure have shifted recent attention toward radiation grafting and electrospinning as promising alternatives. The following sections provide an overview of the principles and equipment and representative examples of membranes produced by these advanced fabrication techniques.

PEMs by RIG

RIG is a versatile and energy-efficient method for producing PEMs with tailored properties, allowing precise control over polymer structure and functional group integration to optimize conductivity and stability. Its scalability, compatibility with diverse materials, and environmentally friendly process make it a promising approach for high-performance fuel cell applications.[88,109–112] The current advancements in the development of PEMs for PEMFCs by RIG reflect a meticulous exploration of materials and fabrication strategies aimed at achieving superior performance across various aspects.[112] These membranes exhibit exceptional potential for fuel cell applications due to their tunable properties.[112] Researchers are concentrating on materials with high ionic conductivity, optimizing the grafting process to enhance ion transport within the membrane matrix.[113] IEC of these membranes is precisely controlled, significantly influencing their ion-conducting capabilities and electrochemical efficiency.[114] Further efforts have been devoted to enhancing the durability of these membranes, ensuring their long-term stability under fuel cell operating conditions.[114] Mechanical properties are optimized to endure mechanical stresses encountered during operation, effectively preventing issues like cracking or delamination. In addition, the electrochemical properties, such as proton conductivity and water uptake, are finely tuned through precise control over the grafting process parameters. Fuel cell performance is significantly enhanced by these advancements, as radiation-induced grafted membranes contribute to enhanced cell efficiency, increased power output, and prolonged operational lifespan. Current research efforts are focused on refining fabrication routes, optimizing material compositions, and structural designs to fully harness the full potential of these membranes and further advance the field of fuel cell technology.[111]

The advancements in PEMs for fuel cell applications highlight the transformative potential of RIG. The studies given in Table 3 showcase diverse and innovative approaches to enhancing membrane performance, stability, and durability across a range of operating conditions.

Earlier studies highlighted the mechanical and oxidative limitations of radiation-grafted FEP-based membranes for PEMFCs, prompting efforts to enhance stability and performance by using ETFE as the base polymer instead of FEP.[88,89,109,110,121] The studies focus on the effects of crosslinking using divinylbenzene (DVB) in styrene-grafted ETFE membranes (25 μm thick), selected for their superior mechanical properties and resistance to radiation-induced damage. Crosslinked membranes with DVB-to-styrene ratios of 5:95 (v/v) demonstrated enhanced oxidative stability, achieving single-cell fuel cell performance comparable to Nafion 112 and a prolonged operational lifespan of 2,185 h during initial testing.[122–124] Another earlier study adapted the concept of short grafted chains and long grafted chains to radiation-grafted membranes, achieving a uniform through-plane distribution for long grafted chain membranes despite high radiation doses. Long grafted chain membranes demonstrated superior swelling behavior and proton conductivity, increasing through-plane conductivity by over 35% at 30% RH, making them ideal for stringent fuel cell applications. These findings enhance our understanding of structure-property relationships and guide synthetic strategies for high-performance membranes using electron-beam grafting.[125]

PEMs developed by grafting a trifluoro styrene derivative onto pre-irradiated ETFE films, followed by hydrolysis emulsion grafting (as developed by Alkan Gürsel et al.), solution grafting, and alcohol-based grafting methods were employed for this monomer film system, and it was shown that the selected monomer facilitated the formation of grafted polymer chains with fluorinated backbones and acid functionalities, enhancing the membrane's stability and performance in fuel cells.[83] Another study by Ben Youcef et al. explored a novel strategy to enhance the intrinsic oxidative stability of uncrosslinked membranes by co-grafting styrene with methacrylonitrile (MAN), which is characterized by its protected α position and strongly dipolar nitrile group,

Table 3. Radiation-grafted PEMs: Preparation parameters and their properties

Base polymer/thickness/ radiation dose (kGy)	Grafting monomer/ crosslinker	Degree of grafting (%)	IEC	Conductivity ($mS \cdot cm^{-1}$)	Performance ($mW \cdot cm^{-2}$)	Water uptake (%)	Reference
ETFE film 25 μm/300	trifluorostyrene derivatives	104–229	1.29–2.15 $meq \cdot g^{-1}$	80–300	–	24.5–72.2	Gürsel et al.[83]
PVDF\1 40 μm/50	styrene	15–35	–	10–70	250 at 60°C	10–60	Sadeghi et al.[85]
ETFE\1 25 μm/100	1-VIm, 4VP	6–60	–	50	237 at 110°C	10–60	Rajabalizadeh Mojarrad et al.[86]
Ultra-thin FEP film 20–25 μm/10 to 50	styrene	12.9–43.3	0.4–1.3 $mmol \cdot g^{-1}$	55.4–207.4 at 80°C	896 at 80°C	15.3–46.5	Li et al.[90]
ETFE film 25 μm/100	styrene/DVB	25–26	0.9–1.4 $mmol \cdot g^{-1}$	uncrosslinked: 100 crosslinked: 18	–	uncrosslinked: 60 crosslinked: 20	Ben Youcef et al.[115]
ETFE film 25 μm/100	styrene, MAN	20–27	1.14–1.46 $mmol \cdot g^{-1}$	42–69	–	25–27	Ben Youcef et al.[115]
ETFE film 50 μm/20-100	4-Vinylpyridine-Tethered Activated Carbon (4-VP-TAC)	40–70	5.7–5.9 $mmol \cdot (repeat\ unit)^{-1}$	39 at 120°C	–	–	Sithambaranathan et al.[116]
PEEK\1 16 μm	styrene	79–114	2.2–2.7 $mmol \cdot g^{-1}$	60–180	–	36–67	Hasegawa et al.[117]
PVDF 12 μm/100	AMS, MGN	43–63	1.23–1.54 $mmol \cdot g^{-1}$	64–89	–	54–65	Nemeth et al.[118]
ETFE 25 μm	4VP, 2VP, NVP	26–93	1.8–2.5 $mmol \cdot g^{-1}$	50-70 at 130°C	450 at 130°C	–	Şanlı et al.[119]
ETFE 25 μm/0.5–4 (irradiation by hard X-rays)	styrene	20–80	–	up to 225	–	43	Farquet et al.[120]

The table summarizes IEC, proton conductivity, water uptake, and fuel cell performance under different operating conditions, highlighting the impact of grafting chemistry and processing parameters on membrane functionality.

significantly improves the oxidative resilience of styrene-grafted ETFE membranes. The incorporation of MAN enhances the lifespan of ETFE-g-styrene/MAN membranes compared to styrene-only membranes, with fuel cell tests showing performance comparable to Nafion 112 and only minor decline at high current densities.[115]

Li et al. devised a membrane featuring an ultra-thin FEP film (20–25 μm) irradiated between 10 and 50 kGy, with PSSA grafting ranging from 12.9% to 43.3%. This membrane exhibited commendable proton conductivity (55.4–207.4 mS cm^{-1} at 80°C) and a peak power density of 0.896 $W{\cdot}cm^{-2}$ at 80°C. However, its less efficient mass transfer compared to Nafion 211 led to higher resistance and reduced performance at high current densities, indicating a need for further optimization.[90] Sithambaranathan et al. reported a novel series of fuel cell membranes created by incorporating 4-VP and TAC as a crosslinker into ETFE films, followed by doping with phosphoric acid (PA). These membranes exhibited proton conductivity of 39 $mS{\cdot}cm^{-1}$ and enhanced mechanical and thermal robustness. The inclusion of the TAC crosslinker played a crucial role in determining the grafting degree and overall membrane efficiency.[116] Hasegawa et al. employed PEEK irradiated at 50 kGy, resulting in a 16 μm membrane with PSSA graftings ranging from 79% to 114%. While the proton conductivity ranged from 60 to 180 $mS{\cdot}cm^{-1}$, specific peak power density information was not provided, necessitating further performance evaluations. Sadeghi et al. demonstrated the versatility of radiation grafting through an innovative approach, presenting PVDF-based membranes starting with PVDF powder (50 kGy, 40 μm) functionalized with PSSA grafts ranging from 15% to 35%. These membranes exhibited impressive proton conductivity of 10–70 $mS{\cdot}cm^{-1}$ and achieved a peak power density of 250 $mW{\cdot}cm^{-2}$ at 0.4 V and 650 $mA{\cdot}cm^{-2}$, highlighting their potential for high-performance electrochemical applications.[85] Gubler et al. investigated fluorine-lean PEMs prepared via the post-sulfonation of co-grafted α-methylstyrene (AMS) and 2-methylene glutaronitrile (MGN) monomers onto a pre-irradiated 12 μm PVDF base film.[118] Their findings revealed that these PEMs not only matched but exceeded the fuel cell performance of Nafion 211. Furthermore, by doping the grafted membranes with Cu-porphyrin as an antioxidant, they achieved enhanced durability under US DOE-like testing conditions without compromising cell performance. This antioxidant strategy represents a universal and effective method for mitigating radical-induced degradation across a broad range of PEMs, offering significant advancements in membrane stability and performance.[112]

Şanlı et al. developed PEMs for high-temperature, low-humidity fuel cell applications by grafting ETFE with various monomers, resulting in high conductivity and mechanical strength. These membranes, tested in PEMFCs, showed promising performance as alternatives to Nafion. They expanded this approach using ETFE with different monomers, achieving notable conductivity and power density, further validating the potential of these membranes in fuel cells.[119,126] Microstructured membranes were prepared using an innovative approach that involved selectively exposing ETFE films to hard X-rays through high-aspect-ratio Ni masks, creating radical patterns for styrene grafting, which were subsequently sulfonated to form proton-conducting membranes. While structuring resulted in a 10% reduction in active area, leading to a slight decrease in fuel cell performance, it notably enhanced the membrane's lifespan without compromising grafting efficiency or proton conductivity.[120,127]

In summary, RIG has been demonstrated to be a highly efficient and versatile technique for creating advanced PEMs with enhanced stability, ion conductivity, and long-term durability for use in fuel cell applications. Key advancements include the transition from FEP- to ETFE-based membranes, crosslinking with DVB, and co-grafting with MAN, enhancing oxidative resilience and proton transport.[88,109,110,112] Alternative monomers, such as trifluorostyrene derivatives and PVDF, have demonstrated promising conductivity and power density.[90,125] Additionally, structural innovations like hard X-ray microstructuring and Cu-porphyrin doping have enhanced membrane lifespan while maintaining high performance.[112,127] These advancements position radiation-grafted PEMs as a scalable and eco-friendly alternative to Nafion, with ongoing research further optimizing their potential for next-generation fuel cells.[111,124]

PEMs for PEMFCs by electrospinning

Electrospinning has recently gained prominence as a versatile and powerful technique for producing high-aspect-ratio fibrous structures at both laboratory and industrial scales.[128,129] This method facilitates the fabrication of ultrafine fibers with customizable morphologies and compositions, featuring diameters ranging from nanometers to submicrons.[128,129] The growing interest over the past decades, particularly in energy-related applications, highlights its effectiveness as a fabrication technique. Its simplicity, speed, versatility, scalability, and cost-effectiveness make it a compelling choice, as evidenced by its widespread adoption across various fields.[130,131] This includes the development of a new generation of high-performance Nafion-based[132] or non-Nafion composite/hybrid membrane materials for PEMFC applications, designed to effectively address the limitations of conventional Nafion membranes.[71,105]

Basically, a typical electrospinning setup consists of a high-voltage power supply, a spinneret, a syringe pump, and a stationary or rotating conductive collector (Figure 5A). The process involves (1) feeding a polymer solution into the spinneret using a syringe pump, (2) applying a high voltage to charge the liquid droplet at the spinneret tip, (3) generating a continuous jet of solution toward the oppositely charged collector, and (4) forming fibers as the liquid jet solidifies through rapid solvent evaporation during elongation toward the collector.[46,128,133] The characteristics of produced fibers, such as size, orientation, and morphology, can be precisely controlled through the adjustment of various parameters.[134,135] These parameters can be classified into three main categories: (1) solution or material-related parameters, including concentration, rheological and electrical properties of the solution, as well as distribution quality of various constitutes (e.g., polymer molecular weight or solution conductivity); (2) process-related parameters, including factors such as applied voltage, humidity, flow rate, needle specifications, and collector properties (Figure 5B); and (3) environmental parameters, primarily consisting of the temperature and RH within the electrospinning chamber. The scanning electron microscopy (SEM) images of a single fiber are shown in Figure 5C, and a free-standing electrospun mat and a compact hot-pressed electrospun membrane are shown in Figure 5D.

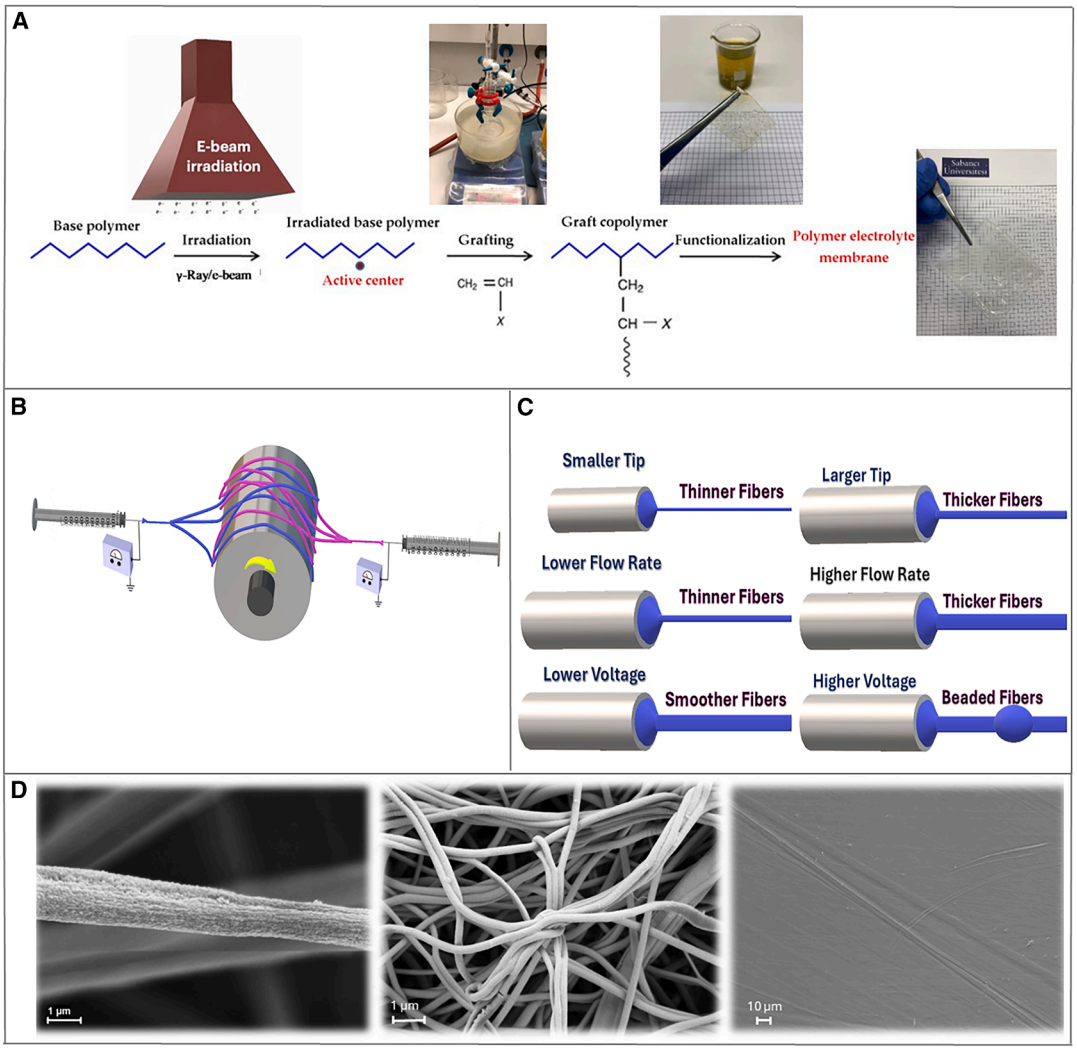

Figure 5. Schematics, SEM images, and various types of electrospinning

(A) RIG and functionalization process for PEM fabrication.

(B) Schematic of a setup for dual-fiber electrospinning.

(C) Effect of process parameters of fiber characteristics.

(D) SEM micrographs of a single fiber, fibrous mat, and compact membrane after hot-pressing.

Adapted from Kırlıoğlu et al.[136]

The membrane fabrication for fuel cells through electrospinning offers several notable advantages, significantly enhancing its applicability in this domain, including the following.

(1) The ability to precisely tailor fiber morphology, size, and orientation[137] and the fine-tuning of its overall composition through multi-layer structure fabrication facilitate the achievement of superior performance.[138]

(2) The flexibility of the setup design has led to the development of various electrospinning techniques, such as single electrospinning, dual electrospinning, and electric field-guided electrospinning, enabling precise tuning of membrane properties.[128]

(3) The ability to fabricate composite membranes comprising mixed fibers from a wide range of otherwise incompatible polymers through dual electrospinning—utilizing multiple spinnerets and a common collector—offers a capability that is challenging to achieve with conventional membrane fabrication methods, such as solution casting.[139–141] Additionally, this method enables the production of membranes with a gradient structure by adjusting the flow rates of the solutions.[138]

(4) These capabilities can be further enhanced by the homogeneous incorporation of functional nanomaterials to enhance properties of electrospun membranes, either as fillers within the fibrous polymer scaffolds or surface decorations. This includes the integration of inorganic nanoparticles to improve properties such as mechanical strength and ionic conductivity.[71]

Table 4. Material selection for single- and dual-electrospun composite membranes and their characteristics

Electrospinning type	Membrane material (nanofiber/matrix)	Thickness (μm)	IEC (mmol·g^{-1})	Water uptake (%)	Conductivity (mS·cm^{-1})	Fuel cell performance (mW·cm^{-2})	Reference
Electric field guide electrospinning	cross-aligned PTFE/Nafion	24.3	–	83.4	210 (at 80°C, >90% RH)	850 (at 80°C, 100% RH)	Hwang et al.[134]
Dual electrospinning	tri-layered 80 wt % PFSA/20 wt % PAI	19 ± 1	–	41.8	134 (at 80°C, 90% RH)	–	Powers et al.[138]
Single electrospinning	PSUT (30 mol %)/Aquivion	30 + 1	0.98	45 ± 3	180 (at 80°C, 95% RH)	520 (at 80°C, 100% RH)	Soad et al.[145]
Single electrospinning	P(VDF-TrFE)- S-SiO_2/Nafion	108	–	34	102 (at 80°C, 100% RH)	–	Rajabalizadeh Mojarrad et al.[146]
Single electrospinning	6IL@HNTs/SPEEK	50 ± 10	2.65	29	139 (at 90°C, 98% RH)	732 (at 80°C, 100% RH)	Xiong et al.[147]
Dual electrospinning	PVDF/S-SiO_2/PFSA	–	1.46	–	89 (at RT, in water)	–	Santos et al.[148]
Dual electrospinning	P(VDF-TrFE)-S-SiO_2/Nafion	–	1.4	55	132 (at 80°C, 100% RH)	344 (at 80°C, 60% RH)	Rajabalizadeh Mojarrad et al.[149]

Data highlight the influence of nanofiber/matrix combinations and fabrication techniques on membrane functionality and fuel cell output.

As a final preparation step, the obtained porous mats are typically transformed into compact structures through several essential post-treatment processes performed for specific purposes prior to characterization. An optimized hot-pressing process,[136] ionomer impregnation,[142] and thermal crosslinking[143] are some of the commonly employed strategies to achieve objectives such as preventing gas crossover, reducing the activation energy for proton hopping by minimizing the distance between hopping sites, and enhancing mechanical strength and dimensional stability.[144]

Table 4 provides an overview of recent advancements in the development of electrospun membranes for PEMFCs. In one notable study, Soad et al. fabricated Aquivion-functionalized polysulfone (PSUT) composite membranes by developing a reinforced scaffold using 4-heptyl-1,2,3-triazole-functionalized PSUT through single electrospinning, subsequently embedding it in an Aquivion ionomer matrix.[145] Their findings revealed that these composite membranes exhibited superior dimensional stability in water and enhanced mechanical strength compared to both non-functionalized polysulfone (PSU)-reinforced membranes and unmodified ionomer membranes, all while maintaining high proton conductivity. Furthermore, the membranes demonstrated a durability five times greater than that of pristine Aquivion membranes, which the authors attributed to the formation of hydrogen bonds arising from acid-base interactions between the matrix and triazole moieties at the fiber-matrix interface.

Additionally, Rajabalizadeh Mojarrad et al. utilized single electrospinning to fabricate sulfonated silica/poly(vinylidene fluoride-co-trifluoroethylene) (S-SiO_2-P(VDF-TrFE)) hybrid membranes with various ratios of S-SiO_2 to carrier polymer.[146] This study highlighted the benefits of integrating highly hydrophilic S-SiO_2 inorganic nanoparticles (NPs), renowned for their exceptional water retention capabilities, which contributed to consistent proton conductivity. Meanwhile, the robust, highly hydrophobic P(VDF-TrFE) fibrous network, serving as both the carrier and reinforcing polymer, ensured the mechanical stability of the membrane. They reported that the membrane containing 70% S-SiO_2 achieved a superior proton conductivity of 102 mS·cm^{-1} at 70°C and 100% RH, surpassing that of the solution-cast Nafion membrane, which showed a conductivity of only 95 mS·cm^{-1}. Xiong et al. synthesized electrospun SPEEK/IL@HNT composite membranes by embedding ionic liquid (IL)-encapsulated halloysite nanotubes (HNTs) within a fully hydrocarbon-based SPEEK matrix using the same method.[147] They reported that the ordered structure of these membranes not only significantly improved their conductivity across a wide range of humidity conditions but also enhanced their mechanical and thermal properties. The through-plane proton conductivity of the SPEEK/6IL@HNT membrane was reported to be 139.2 mS·cm^{-1} at 90°C and 98% RH, significantly surpassing that of pristine SPEEK membranes under the same conditions. Additionally, the maximum power density achieved was 732 mW·cm^{-2}, approximately two orders of magnitude greater than that of Nafion 115.

One of the most effective strategies to overcome the limitations of PFSA-based membranes is reinforcing them with PTFE. Hwang et al. utilized an electric-field-guided electrospinning technique to develop a unique micron-scale, grid-type

PTFE scaffold.[134] This scaffold was subsequently impregnated with a Nafion ionomer, providing proton conductivity along the precisely cross-aligned PTFE channels. This approach effectively addresses the challenges posed by the immiscibility of these two components. The resulting design significantly improves membrane hydration, promotes efficient proton diffusion, and causes minimal swelling. This leads to remarkable single-cell performance, achieving a maximum power density of 0.85 $W{\cdot}cm^{-2}$, which surpasses that of Gore-Select membranes. Furthermore, it demonstrates minimal hydrogen crossover (less than 5 $mA{\cdot}cm^{-2}$ at 0.4 V), far exceeding the durability standards required for transportation applications.

In addition to single electrospinning, it is also beneficial to explore examples of dual electrospinning, which is frequently utilized to create structures unattainable with previous methods, such as blends of multiple non-compatible polymers. Santos et al., pioneers in the use of electrospinning for the preparation of composite membranes for fuel cells,[148] fabricated multilayered PFSA/polyamide-imide (PAI) composite PEMs in one study.[138] These membranes feature both uniform and gradient inner structures along the thickness direction. This was achieved by adjusting the flow rates of solutions to obtain varying PFSA-to-PAI ratios. The impact of these architectural designs on the membranes' final properties was evaluated. They claimed that their 20-μm-thick tri-layer sample, featuring surface layers comprising 95 wt % PFSA and a uniform mixed inner layer of PFSA-PAI, was the best-performing sample, with an ionic conductivity of 89 mS·m, 5% water swelling, tensile strength of 26 MPa, and fuel cell performance comparable to that of Nafion 211.

Rajabalizadeh Mojarrad et al. also employed a combination of dual-electrospinning and sol-gel methods in a single-step process to create well-organized, homogeneous, composite membranes.[149] These membranes comprise Nafion ionomer, reinforcing PVDF or P(VDF-TrFE) fibers, and an S-SiO_2 network created from silica 3-(trihydroxysilyl)-1-propanesulfonic acid and tetraethyl orthosilicate (TEOS). After hot-pressing, the highly conductive S-SiO_2 network and the reinforcing fibers were seamlessly integrated into a pore-free Nafion matrix. They claimed that the P(VDF-TrFE)-based membrane with 60% Nafion (TN60) exhibited a conductivity of 132 $mS{\cdot}cm^{-1}$ at 80°C and a maximum power density of 344 $mW{\cdot}cm^{-2}$ at 60% RH, outperforming the PVDF-containing membrane in terms of both conductivity and maximum power density. Moreover, the TN60 membrane demonstrated an enhanced trend in fuel cell performance with decreasing RH, positioning it as a candidate well suited for operations under lower humidity conditions. Santos et al. used a similar approach to fabricate PFSA/S-SiO_2/PVDF membranes.[148] In this work, they incorporated a non-soluble S-SiO_2 network either into PFSA or PVDF fibers by addition of TEOS as the silica precursor in one of these solutions and electrospun the solutions concurrently onto a common drum to compare the effect of fiber interaction with an inorganic network as well as the matrix type on final properties of these membranes. They claim that the membranes with S-SiO_2 on PFSA fibers showed controlled water swelling and high proton conductivity.[105,145]

In summary, the growing interest in electrospinning is driven by its potential to develop high-performance, nanoscale, ion-conducting composite membranes through this powerful, fast, and tunable technique.[130] This method not only enables the formation of high-aspect-ratio surface nanostructures but also allows for the blending of compatible and non-compatible polymers or simply the incorporation of NPs with tailored properties. Numerous studies in this field consistently demonstrate the superior performance of electrospun membranes compared to their bulk counterparts with the same composition. Notable developments include enhancing dimensional stability and mechanical strength by creating robust fibrous scaffolds,[149] improving ion conductivity and water retention properties through the incorporation of well-dispersed hydrophilic or inorganic compounds, and enabling anisotropic properties in the desired direction, which are not possible with conventional methods.[134,138] Given the aforementioned advantages of these techniques and the enhanced properties of electrospun membranes, electrospinning emerges as a promising fabrication method for commercial PEMFCs.

Reliability and testing

Membrane characterization techniques are crucial for evaluating their inherent characteristics as well as their performance in fuel cells.[110] These techniques can be categorized into three main groups: material-related, functionality-related, and durability tests. The first category evaluates the chemical, physical, thermal, and mechanical properties of the membrane. The second one mostly focuses on transport properties of the bare membrane as the most critical feature and collectively offers insights into the membrane's operational performance in the fuel cell environment. Some of the most significant examples in this category are as follows. Ionic conductivity (σ) refers to a membrane's ability to transport ions under applied electric fields—a critical parameter for assessing its performance in electrochemical applications. In a PEM, conduction of protons takes place through two primary mechanisms: the Grotthuss (or hopping) mechanism, which is dominant under low-humidity conditions, and the vehicle mechanism, which is more predominant under high-humidity conditions.[42,150] In the Grotthuss mechanism, proton transportation occurs via the continuous formation of hydronium ions (H_3O^+) at hydrated sulfonate groups, followed by their sequential hopping to neighboring sulfonate groups. In contrast, the vehicle mechanism relies on the electro-osmotic flow of hydrated ions such as H_3O^+, $H_5O_2^+$, and $H_9O_4^+$ through interconnected nanoscale water clusters, transporting protons along with water molecules from proton-rich to proton-deficient regions. This parameter is determined by measuring the membrane's resistance using either the two-probe or four-probe electrochemical impedance spectroscopy (EIS) method. The test can be performed in either in-plane or through-plane directions across a broad range of temperatures and relative humidities, allowing for the investigation of how these conditions affect the membrane's conductivity.[151] IEC is another key property of a membrane, indicating the number of active functional sites (e.g., sulfonic acid groups) per unit weight of the dry membrane. IEC directly influences crucial performance parameters such as ion conductivity and water uptake. A commonly used method for determining IEC is the acid-base titration method, which involves immersing the membrane in a salt solution to release all protons from the functional groups, followed by titration of the resulting

solution with a strong base.[152] Both conductivity mechanisms are closely linked to the number of acidic groups capable of dissociating to release freely moving protons as well as the sufficient availability of water in the medium to support proton transport. Water uptake is measured as another critical characteristic of the membrane. Water uptake is calculated by comparing the weight of the wet membrane to that of the dry membrane and is expressed as the percentage increase in weight relative to the dry state.[153]

Chemical stability and thermal and mechanical properties of membranes are also significant for fuel cell performance and durability. The melting behavior and crystallinity of the PEMs were analyzed using differential scanning calorimetry, while their thermal stability and degradation characteristics were evaluated through thermogravimetric analysis.[154] The drying process during MEA preparation, which affects membrane water content, was found to be critical. Previously, Brack et al. examined how drying impacts the hydrophilicity, wettability, and surface energies of fuel cell membranes by means of contact angle measurements, and conclusions were drawn on the relationship between drying-induced changes and membrane bonding performance.[155]

In addition to the aforementioned methods, advanced *operando* imaging techniques, such as neutron imaging, are used to monitor the water profile across the membrane. This provides valuable insights into the effects of various conditions, such as applied temperature and pressure, on water distribution within the membrane in an operating fuel cell.[4]

ELECTROCATALYSTS

The HOR and ORR are the main electrochemical reactions that occur in PEMFCs. It is surely beyond doubt that the need for enhanced ORR kinetics and reduction or elimination of Pt used within electrodes are inevitable for mass production of vehicles utilizing PEMFCs.[156] The two main reactions taking place at the anode and cathode side are as follows.

The HOR

$H_2 \rightleftarrows 2H^+ + 2e^-$, has been widely researched on Pt surfaces. According to the Tafel-Heyrovsky-Volmer mechanism, the HOR on Pt surfaces involves three key elementary reaction steps.[157]

(1) Tafel reaction: H_2 dissociates directly into two adsorbed hydrogen atoms on the Pt surface:

$$H_2 \rightleftarrows H_{ad} + H_{ad}.$$

(2) Heyrovsky reaction: one adsorbed hydrogen atom reacts with a proton from the electrolyte and an electron from the electrode to form a hydrogen molecule:

$$H_{ad} + H^+ + e^- \rightleftarrows H_2.$$

(3) Volmer reaction: an adsorbed hydrogen atom on the Pt surface is oxidized, releasing a proton into the solution and transferring an electron to the electrode:

$$H_{ad} \rightleftarrows H^+ + e^-.$$

The ORR

Due to the complex kinetics and the formation of various intermediates throughout the process, understanding the intrinsic ORR mechanism at the atomic or molecular level poses a significant challenge, particularly in the design of Pt-based electrocatalysts. It is widely accepted that a complete four-electron transfer ($4e^-$) mechanism is favorable for the ORR. In contrast, the two-electron pathway is undesirable because it results in the formation of hydrogen peroxide (H_2O_2), which can degrade the Nafion membrane, causing damage to fuel cells.[158]

Theoretical studies suggest that the four-electron pathway is more likely to occur on the Pt (111) crystal facet, especially under oxygen-rich conditions. Therefore, the elemental steps of the ORR are typically described as follows (* indicates an active site of the catalyst):[159]

4 e^- pathway:

$$O_2 + 4\,(H^+ + e^-) \rightarrow 2\,H_2O \quad E = 1.23\ \text{V vs. RHE}, \tag{i}$$

$$1/2\,O_2 + 2\,(H^+ + e^-) \rightarrow *O + 2\,(H^+ + e^-) \rightarrow *OH + (H^+ + e^-) \rightarrow H_2O \tag{ii}$$

$$O_2 + 4\,(H^+ + e^-) \rightarrow *OOH + 3\,(H^+ + e^-) \rightarrow *O + 2\,(H^+ + e^-) \rightarrow *OH + (H^+ + e^-) \rightarrow 2\,H_2O \tag{iii}$$

2 e^- pathway:

$$O_2 + 2\,(H^+ + e^-) \rightarrow H_2O_2 \quad E = 0.70\ \text{V}, \tag{iv}$$

$$O_2 + 2\,(H^+ + e^-) \rightarrow *OOH + (H^+ + e^-) \rightarrow H_2O_2 \tag{v}$$

This 4 e^- pathway avoids the production of harmful peroxide formation and is crucial for efficient PEMFC performance.

Electrocatalyst properties

As mentioned previously, commercial electrocatalysts for PEMFCs are generally Pt based. Table 5 presents a comparison of the electrocatalytic performance of representative commercial Pt/C electrocatalysts. The reported performances reveal notable differences in electrochemical surface area (ECSA), mass activity (MA), and durability. However, direct comparisons are challenging due to variations in testing protocols across different studies. ECSA values vary between 46 and 120 $m^2 \cdot g_{Pt}^{-1}$, and MA values range from 0.05 to 1.05 $A \cdot mg_{Pt}^{-1}$ across the different electrocatalysts. Among selected studies, HiSPEC 3000[160] (20 wt % Pt, Vulcan XC72, Johnson Matthey) stands out, with a notable ECSA of 83.72 $m^2 \cdot g_{Pt}^{-1}$, while TEC10E50E[161] (46.3 wt % Pt, Ketjen Black EC300J, Tanaka Kikinzoku Kogyo [TKK]) follows closely with a similar value of 79.7 $m^2 \cdot g_{Pt}^{-1}$. Durability trends vary due to different AST/accelerated degradation test (ADT) conditions, with TEC10E40E[161] (40 wt % Pt, high-surface-area carbon, TKK) retaining 70% of its initial ECSA after 25,000 cycles, whereas TEC10V20E[162] (20 wt % Pt, Vulcan XC72) experiences a severe 78.4% loss after 5,000 cycles. The data provided by the company

Table 5. Summary of the electrocatalytic performance of representative commercial Pt/C electrocatalysts

Product	Company	Pt content (wt %)	Carbon support	ECSA ($m^2 \cdot g_{Pt}^{-1}$)	MA ($A \cdot gPt^{-1}$)	Durability	Reference
HiSPEC 3000 Pt/C	JM	20	Vulcan XC72	83.72	49	41.6% ECSA loss after 50,000 accelerated stress test (AST) cycles	Alipour Moghadam Esfahani and Easton[160]
HiSPEC 4000 Pt/C		40	Vulcan XC72	53.47	340	–	Moriau et al.[171]
TEC10V20E Pt/C	Tanaka Precious Metals, TKK	20	Vulcan XC72	56	234	78.4% ECSA loss after 5,000 AST cycles	Qiao et al.[172]
TEC10V30E Pt/C		30	Vulcan XC72	57.4	~1050	56% ECSA loss after 15,000 cycles	Yoshii et al.[173]
TEC10E40E Pt/C		40	high-surface-area carbon	57.2	1530	30% ECSA loss after 25,000 cycles	Chen et al.[162]
TEC10E50E Pt/C		46.3	KB EC300J	79.7	480	–	Moriau et al.[171]
TEC10E60TPM Pt/C		60	high-surface-area carbon	46.24	320 ± 10	–	Du et al.[161]
ENYrgy-20	ENY-Mobility	20 ± 0.2 a	high-purity carbon	120 ± 12 a	250 ± 13 a	at least 85% after 5,000 AST cycles[a]	ENY-Mobility[163]
ENYrgy-30		30 ± 0.2 a	high-purity carbon	98 ± 9 a	208 ± 10 a	at least 85% after 5,000 AST cycles[a]	ENY-Mobility[163]
ENYrgy-40		40 ± 0.2 a	high-purity carbon	88 ± 9 a	186 ± 9 a	at least 85% after 5,000 AST cycles[a]	ENY-Mobility[163]
ENYrgy-60		60 ± 0.5 a	high-purity carbon	64 ± 6 a	136 ± 9 a	at least 80% after 5,000 AST cycles[a]	ENY-Mobility[163]
20% Pt/C	E-TEK	20	Vulcan XC72	65	110	–	Gasteiger et al.[164]
40% Pt/C		40	Vulcan XC72	69	100	24% ECSA loss after 10,000 ADT cycles	Kong et al.[174]
20% Pt/C	Fuel Cell Store	20	Vulcan XC72	–	120	19% MA loss after 30,000 ADT cycles	Garsany et al.[165]
Elyst Pt50 0550 Pt/C	Umicore	50	KB EC300J	56.76	240	–	Moriau et al.[171]

Data highlight the trade-offs between activity, stability, and Pt content across commercial products from various suppliers.
[a]Values are derived from company datasheets retrieved from https://eny-mobility.de/assets/files/tds-enyrgy.pdf on June 2, 2025.

on the ENYrgy[163] (ENY-mobility) Pt/C products appears promising; however, further research is needed to evaluate their performance under real fuel cell operating conditions. The variations observed in electrocatalytic performance highlight the impact of Pt loading and the type of carbon support while also emphasizing the need for standardized preparation and testing methods to facilitate more accurate performance comparisons among different Pt/C electrocatalysts.[164,165–170]

PGM-based electrocatalysts

PGM-based electrocatalysts, particularly Pt-based ones, are critically important for the efficiency and performance of PEMFCs.[175] Pt has a unique catalytic activity toward the sluggishness of the ORR, which is a fundamental step in the electrochemical process responsible for generating power in PEMFCs. Therefore, PGM-based electrocatalysts are essential especially at the cathode, where they facilitate the ORR.[176] By reducing overpotentials and maximizing cell voltage, these electrocatalysts enable the system to achieve high power density and efficiency in PEMFCs.

Due to the emphasis of its high cost and low abundance, the mitigation of Pt has been a focal point for researchers working in this field for a long time. As the Pt NPs are small, typically just a few nanometers, they are usually deposited on support materials to enhance their dispersion. In addition to acting as a substrate material for Pt, these supports are influencing the catalytic performance and stability of Pt-based electrocatalysts through metal-support interactions.[177] Carbon materials are highly effective in dispersing Pt NPs and are favored as most commonly utilized supports for Pt-based electrocatalysts due to their large surface area, optimal porosity, excellent electrical conductivity, chemical stability, and low cost.[178–180] The preparation of Pt/C electrocatalysts for the cathode of PEMFCs involves a facile process focused on enhancing electrocatalytic activity and durability. The methodology relies on the integration/impregnation/deposition of Pt NPs onto various carbon materials, serving as supports.[181,182] The commonly used carbon materials are carbon black (CB), CNTs, and graphene. The choice of carbon support material is a critical factor influencing the dispersion and stability of Pt NPs, thereby impacting the overall performance of the catalyst. In the typical synthesis procedure, the process initiates with the dispersion of selected precursor compounds containing Pt onto the specifically high-surface-area carbon support, followed by reduction methods such as chemical reduction or heat treatment.[183] This meticulous approach results in Pt-based electrocatalysts characterized by a considerably increased surface area and improved electrochemical properties. Research on Pt-based electrocatalysts has been focused on optimizing the key parameters, including Pt loading, particle size, distribution on the carbon support, enhancing the durability, and optimum balance between cost, activity, and stability. These efforts play a critical role in advancing the efficiency and life cycle of PEMFCs.[184]

Despite corrosion, CB remains the most prevalent catalyst support for Pt and is frequently utilized as a solution to address the restacking issue of 2D layered carbon materials, including graphene, GO, reduced GO (rGO), and CNTs.[185–188] In our earlier studies, Pt NPs, decorated on various graphene-based supports, including GO, thermally reduced GO, and graphene nanoplatelets (GNPs) by different impregnation-reduction methods deposition, were employed as the catalyst for fuel cell reactions, and the best Pt dispersion and electrocatalytic activity were achieved with GO as support and ethylene glycol reflux as the main impregnation-reduction route.[189,190] Moreover, our group utilized photocatalytic deposition, providing a scalable method for a controlled deposition of Pt NPs on rGO,[191–193] and electrophoretic deposition[194] as the novel approaches for the development of Pt/GO-based electrocatalysts.[195] As an alternative method for the deposition of Pt NPs on GO and GNPs, a supercritical carbon dioxide deposition technique was employed successfully as well.[196] Our subsequent studies proved that GO and CB hybrid supports performed better compared to GO in terms of electrocatalytic activity and fuel cell performance.[197–201]

Arıcı et al. have employed a hybrid support comprising CB and GNPs for the impregnation of Pt NPs with a diameter of ~2 nm, thereby obtaining Pt/CB-GNP electrocatalysts with a homogeneous distribution. By leveraging the synergistic effect of CB and GNPs and preventing the restacking of GNPs, an ECSA of 55 $m^2 \cdot g_{Pt}^{-1}$ and a maximum power density of 377 $mW \cdot cm^{-2}$ were achieved.[202] In another study, Pt-based electrocatalysts were synthesized via a straightforward microwave-assisted method, with utilization of CB and GO hybrid carbon supports. A maximum power density of 1,091 $mW \cdot cm^{-2}$ was achieved with a Pt loading of 0.4 $mg \cdot cm^{-2}$.[200] Tang et al. developed a cost-effective methodology for fabricating a 3D hierarchical material by combining rGO with poly(diallyldimethylammonium-chloride) functionalized CB (FCB) as a support matrix for anchoring Pt NPs, resulting in Pt/rGO-FCB electrocatalysts. The approach involved embedding the FCB between rGO sheets, forming a 3D hierarchical porous rGO/FCB architecture with well-dispersed ultrafine Pt NPs. The electrodes have been demonstrated to exhibit a power density that is 1.25 times greater than that of the conventional Pt/C electrodes, which have a power density of 1,344 $mW \cdot cm^{-2}$, with a maximum mass-specific power density of 7.5 $W \cdot mg_{Pt}^{-1}$.[203]

Significant efforts have been undertaken to improve the efficiency of electrocatalyst production processes, particularly for large-scale industrial applications. Zhang et al. explored the mass production of high-activity and durable Pt/C catalysts using continuous microwave pipeline (CMP) technology alongside conventional methods like chloroplatinic acid reduction with ethylene glycol.[204] Their approach successfully mass produced 50 wt % Pt/C catalysts, achieving a remarkable power density of 1.4 $W \cdot cm^{-2}$ and 0.286 $g_{Pt} \cdot kW^{-1}$.

As displayed in Figure 6, Ott et al. introduced a novel Pt NP/N-modified carbon Ketjen black (KB) catalyst configuration that markedly diminishes local oxygen-related mass transport resistance.[205] The use of chemically modified carbon supports with tailored porosity enables the targeted deposition of Pt NPs on both the outer and inner surfaces of the support particles, thereby boosting the performance of the catalyst. In accordance with the most up-to-date standards for automotive single fuel cell testing, the Pt/N-KB 600°C cathode catalyst demonstrated excellent stability during voltage cycling, outperforming the state-of-the-art reference electrodes. The proposed innovative

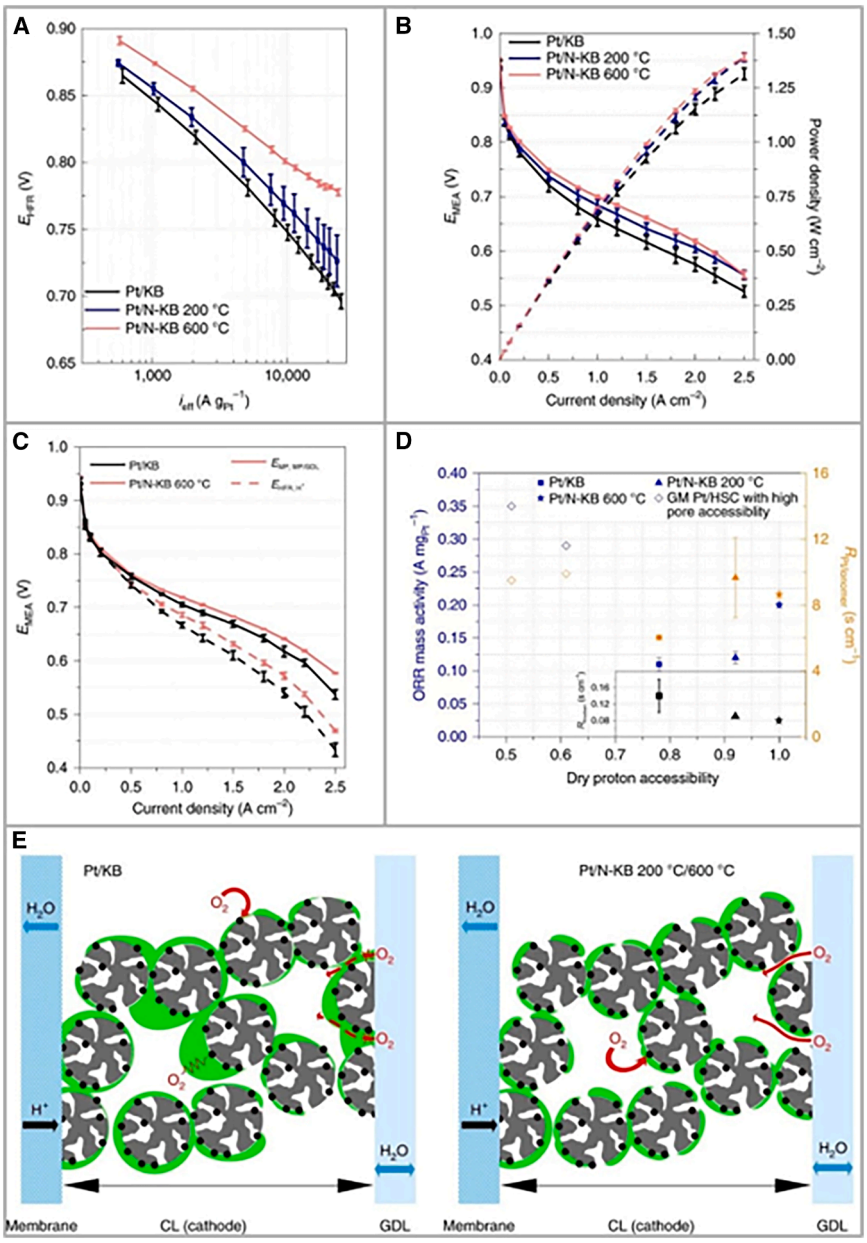

Figure 6. Effect of N modification on ionomer distribution and performance in fuel cells

(A) Pt loading normalized performance curve of 1.4 cm^2 MEAs.

(B) H_2-air fuel cell polarization plots of 1.4 cm^2 MEAs.

(C) Comparison of 43.56 cm^2 MEA polarization curve under stoichiometric flow of 1.5 H_2/2 air at 60°C and $p_a = p_c = 200$ kPa_{abs} and 50% RH of N-KB 600°C (red) versus Pt/KB (black). Solid lines represent high-frequency resistance (HFR)-corrected polarization curves, while dashed ones only include the correction for BP and the contact resistance.

(D) ORR MA at 0.9 V and local O_2 transport resistance ($R_{Pt/ionomer}$) achieved by 1.4 cm^2 cells as a function of dry proton accessibility measured from 43.56 cm^2 ones. The inset reveals the Knudsen resistance ($R_{Knudsen}$) of the synthesized catalysts. For comparison reasons, two high-surface-carbon-based catalysts from the literature are included. Conditions are set as follows: cathode, ~0.11 $mg_{Pt}·cm^{-2}$; anode, 0.15 $mg_{Pt}·cm^{-2}$; total outlet pressure of anode and cathode, respectively, $p_a = p_c = 230$ kPa_{abs} under constant differential flow H_2/Air (or O_2) = 1,000/2,000 normal cubic centimeters (nccm) and the anode and cathode, respectively, $RH_a = RH_c = 100\%$ at 80°C.

(E) Schematic of the $R_{Knudsen}$ for oxygen transport within the catalytic layer (CL) for badly distributed ionomer layers (left) and good ionomer distribution over the entire catalyst (right).

Adapted with permission from Springer Nature.[205]

approach involved doping N atoms into the carbon matrix through ammonolysis under a constant flow of pure NH_3 at varying temperatures, followed by platinizing the N-KB using a polyol method. This approach successfully reduced voltage losses by up to 45 mV at 2 $A·cm^{-2}$ for Pt/N-KB electrocatalysts. Additionally, unmodified Pt-based (Pt/KB) electrocatalysts achieved record power densities of up to 1.39 $W·cm^{-2}$, attributed to the efficient Pt utilization of 0.075 $g_{Pt}·kW^{-1}$ on the cathode side.

Pt-M alloy electrocatalysts

To reduce the cost of the electrocatalysts and enhance their performance in the fuel cells, the partial substitution of PGMs with non-noble transition metals (e.g., Fe, Co, Ni, Mo, and Cu) has been the subject of numerous recent studies,[206–208] and one of the most important application examples is the use of PtCo in the commercial Toyota Mirai vehicle. The Mirai PtCo alloy has demonstrated lower activation resistance with respect to the previous 2008 FCV models.[209] In the recently launched Toyota Mirai, it has further enhanced the performance of PtCo alloy catalyst by coating them with an IL to decrease the diffusion resistance of the ionomer and simultaneously slowing the rate of Co dissolution in them.[210] Other recent 3d transition metals (TMs) block substitution for PGM metals studies have focused on the synthesis and electrochemical characterization of PtTi- and PtMn-based alloys[211,212] and on coating PtCo- and PtFe-based alloys on the surface of frameworks such as Fe-N_x-enriched nanocubes (Fe-N-C) and zeolite-derived supports.[213,214] The main challenges regarding the partial substitution of Pt are (1) maintaining the stability of M in the Pt-M alloy under highly acidic conditions and (2) the growth of the catalyst particle size and subsequent decrease of the ECSA. To address the former issue, Li et al. have demonstrated an efficient core-shell structure with 2–3 atomic layers of Pt shell (Figure 7A).[207] The latter issue has been alleviated through methods such as nitrogen doping of the catalyst support.[215] Moreover, using the

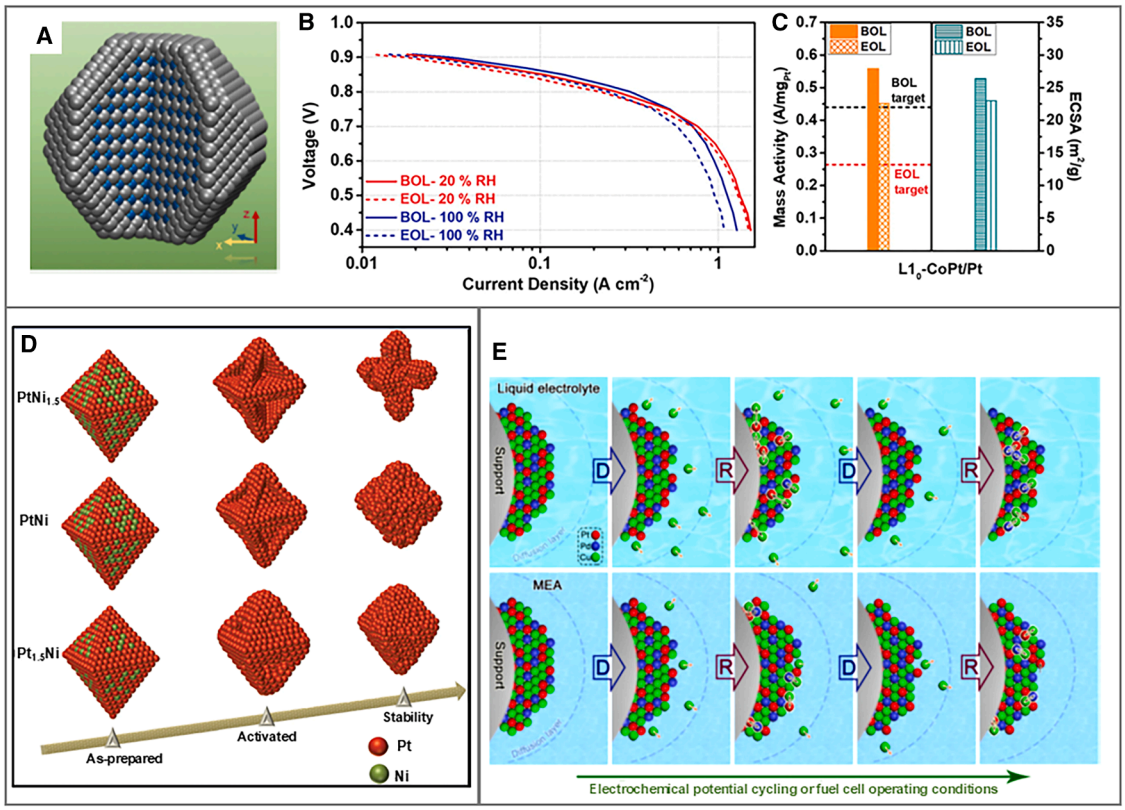

Figure 7. Selected state-of-the-art Pt-M alloy electrocatalysts

(A) Hard-magnet core/shell L10-CoPt/Pt NPs with 2–3 atomic layers of Pt shell.

(B) The corresponding polarization curves under 20% and 100% relative humidity (RH) at the beginning and end of life (BOL and EOL, respectively).

(C) Surpassing the US DOE's BOL and EOL target mass activity criteria. Adapted with permission from Elsevier.[207]

(D) The dealloying of Pt_xNi_y alloys shows higher dealloying as the Pt is decreased. Adapted with permission from Springer Nature.[217]

(E) The dealloying-realloying (self-healing) of electrocatalysts is observed for the case of Pd-containing $Pt_{20}Pd_{20}Cu_{60}$ alloys. Adapted with permission from Springer Nature.[206]

synergistic effect of GNPs in hybrid structures has been shown to address instability and activity issues of Pt-M catalysts.[201,216] The dealloying studies of Pt-Ni alloy-type electrocatalyst NPs by Cui et al. (Figure 7B) have confirmed that the loss in ORR activity is due to the surface adsorption of oxygen.[217] To address the dealloying, Wu et al. introduced palladium (Pd) as a component and made a $Pt_{20}Pd_{20}Cu_{60}$/C catalyst that demonstrated a dealloying/realloying (self-healing) behavior (Figure 7C).

To the best of our knowledge, in the studies related to the Pt-M based ORR electrocatalysts, the common practice is to perform the rotating disc electrode (*ex situ*) tests first to assure the proof of concept and screen non-active devised materials.[211] This is the reason why the performance data from MEA or *in situ* tests are available less frequently. Moreover, even in some studies where *in situ* tests are performed, the maximum power densities are not reported. Considering the aforementioned circumstances, what proceeds is a comparison between different Pt-M alloy-based electrocatalysts only based on the *ex situ* test results (reported in Table 6). Among the explored studies in this review, the highest $E_{1/2}$ is attributed to hard magnet $L1_0$-CoPt alloy NPs that demonstrate $E_{1/2}$ of 0.967 V vs. reversible hydrogen electrode (RHE) and an MA of 2.25 $A{\cdot}mg_{Pt}^{-1}$.[207] The tungsten-doped $L1_0$-PtCo shows a performance on par with the hard magnet non-doped counterpart ($E_{1/2}$ of 0.953 V vs. RHE and an MA of 2.25 $A{\cdot}mg_{Pt}^{-1}$).[218]

Although the focus of most of the studies has been to substitute 3d TMs such as Co, Fe, Ni, and Mn for PGM metals,[212–214,217] there also have been studies on less frequent substitutions, such as Ti and La.[211,224] There are also studies of Pt-M catalysts that are in ultrathin-walled nanotube form, such as the catalyst developed by Liu et al.[225] The current state-of-the-art Pt-M alloy ORR electrocatalysts are reviewed in more detailed reviews, like the one by Zhou et al. for Pt and Fe-group transition metals (Fe, Co, Ni),[226] the review by Pan et al. focusing on shape-controlled dealloyed Pt alloy nanocatalysts,[227] the review by Sun et al. discussing the low-PGM electrocatalysts and TPB design,[177] and the review by Lim et al. on the role of transition metals in the Pt alloy catalysts of the ORR.[228]

PGM-free electrocatalysts

The high price of PGM-based electrocatalysts led researchers to develop an alternative solution.[229–231] PGM-free electrocatalysts were proposed as a result of this research. In terms of current density, PGM-free M-N-C electrocatalysts can deliver >30

Table 6. Comparison of the electrochemical performance of representative PGM-based and Pt-M alloy-based electrocatalysts for PEMFC applications

		ex situ			*in situ*				
					Pt loading (mg/cm^2)				
Catalyst	Preparation method	ECSA ($m^2 \cdot g^{-1}$)	MA ($mA \cdot mg_{Pt}^{-1}$)	Half-wave potential for ORR catalyst $E_{1/2}$ (V)	Cathode	Anode	Maximum power density ($mW \cdot cm^{-2}$)	Single-cell test conditions	Reference
Pt/rGO	Pt/rGO by ethylene glycol reflux	138	–	–	0.25	0.25	320	temperature: 60°C; H_2 (anode)/O_2 (cathode); flow rate: at stoichiometric ratios of 1.5/2 for H_2/O_2	Şanlı et al.[189]
Pt/rGO-CB	microwave-assisted synthesis of Pt NPs on CB-rGO hybrid support	65	147 @0.8 V	0.797	0.4	0.4	1091	temperature: 80°C; H_2 (anode)/O_2 (cathode); flow rate: 0.5 $L \cdot min^{-1}$ (anode)/0.5 $L \cdot min^{-1}$ (cathode)	Yarar Kaplan et al.[200]
Pt/CB-GNP	direct impregnation of $Pt(dba)_3$ complexes on the carbonaceous support and reducing it under H_2 at room temperature	55	120 @0.8 V	–	0.5	0.5	377	temperature: 80°C; H_2 (anode)/O_2 (cathode); flow rate: 0.5 $L \cdot min^{-1}$ (anode)/0.5 $L \cdot min^{-1}$ (cathode)	Arıcı et al.[202]
Pt/rGO-FCB	self-assembly and solvothermal reaction	62.1	249 @0.9 V	0.89	0.18	0.3	1344	temperature: 65°C; H_2 (anode)/O_2 (cathode)	Tang et al.[203]
Pt/CB	CMP for mass production of Pt/C catalysts	71.9	137 @0.9 V	0.92	0.3	0.1	1400	temperature: 70°C; H_2 (anode)/air (cathode); flow rate: at stoichiometric ratios of 1.5/2.5 for H_2/air	Zhang et al.[204]
Pt/N-KB	deposition of Pt NPs on the outer and inner surface of the chemically modified carbon supports	83	350 @0.9 V	~0.9	0.105	0.15	1390	temperature: 80°C; H_2 (anode) O_2/N_2 (cathode); flow rate: H_2:1,000 nccm O_2/N_2: 2000 nccm	Ott et al.[205]

(*Continued on next page*)

Table 6. *Continued*

Catalyst	Preparation method	*ex situ* ECSA ($m^2 \cdot g^{-1}$)	*ex situ* MA ($mA \cdot mg_{Pt}^{-1}$)	*ex situ* Half-wave potential for ORR catalyst $E_{1/2}$ (V)	*in situ* Pt loading (mg/cm^2) Cathode	*in situ* Pt loading (mg/cm^2) Anode	*in situ* Maximum power density ($mW \cdot cm^{-2}$)	*in situ* Single-cell test conditions	Reference
Pt/CNF-CB	microwave-assisted reduction of Pt NPs on CNF-CB hybrid support	108.2	272 @0.8 V	0.8	0.4	0.4	907	temperature: 80°C; H_2 (anode)/O_2 (cathode); flow rate: 0.5 $L \cdot min^{-1}$ (anode)/0.5 $L \cdot min^{-1}$ (cathode)	Yarar Kaplan et al.[219]
Pt/rGO-VC	surfactant-mediated chemical reduction route to obtain self-assembled Pt/rGO-VC	87	149 @0.8 V	0.81	0.35	0.35	857	temperature: 80°C; H_2 (anode)/O_2 (cathode); flow rate: 0.5 $L \cdot min^{-1}$ (anode)/0.5 $L \cdot min^{-1}$ (cathode)	Sevim Yılmaz et al.[220]
Pt/KB_{IW}	incipient wetness impregnation	70 ± 2	336 ± 7 @0.9 V	–	0.064	0.1	–	temperature: 80°C; H_2 (anode)/O_2 (cathode); flow rate: H_2/O_2 (2,000/5,000 nccm)	Harzer et al.[221]
CTAB-assisted Pt	microwave-assisted polyol process	94.0	72 @0.9 V	0.87	0.4	0.2	1142	temperature: 80°C; H_2 (anode)/O_2 (cathode); flow rate: both 0.2 L/min	Shen et al.[222]
Pt-aniline complex-coated C nanofibers	encapsulation of Pt catalyst in a thin, uniform N-containing carbon layer supported on a carbon nanofiber	178 ± 13	116.7@0.9V	0.91	0.1	0.025	~610	temperature: 80°C; H_2 (anode)/air (cathode); flow rate: H_2/air (150/800 sccm)	Karuppanan et al.[223]
PtPdCu NPs	wet chemical synthesis	~60.7 $m^2 \cdot g_{Pt+Pd}^{-1}$	1,660	~0.92	–	–	–	–	Wu et al.[206]
Tungsten-doped $L1_0$-PtCo	wet chemical synthesis	63.1	2250	0.953	0.02	0.02	–	temperature: 80°C; H_2 (anode)/O_2 (cathode); back pressure: both 150 kPa_{abs}	Liang et al.[218]

(*Continued on next page*)

Table 6. ***Continued***

Catalyst	Preparation method	*ex situ* ECSA ($m^2 \cdot g^{-1}$)	*ex situ* MA ($mA \cdot mg_{Pt}^{-1}$)	*ex situ* Half-wave potential for ORR catalyst $E_{1/2}$ (V)	*in situ* Pt loading (mg/cm^2) Cathode	*in situ* Pt loading (mg/cm^2) Anode	*in situ* Maximum power density ($mW \cdot cm^{-2}$)	*in situ* Single-cell test conditions	Reference
Hard-magnet $L1_0$-CoPt NPs	wet chemical synthesis	27.3	2250	0.967	0.105	0.105	–	temperature: 80°C; H_2 (anode)/O_2 (cathode); flow rate: H_2/O_2 (500/1,000 sccm); back pressure: both 150 kPa_{abs}	Li et al.[207]
Pt_5La	self-assembly into MOF + Pt precursor adsorption + annealing	–	490	0.92	0.1	0.1	1250	H_2 (anode)/O_2 (cathode); back pressure: both 2 atm_{abs}	Zhu et al.[224]
PtTi	impregnation in commercial Pt/C catalyst Ti-precursor to form $PtTiO_x$ and subsequent reductive annealing	54.6	680	~0.9	0.02	–	–	–	Herzog et al.[211]
PtMn	platinum (II) acetylacetonate + manganese (III) acetylacetonate sonication and subsequent heating at 200°C	53.0	520	~0.9	0.1	N/A	1360	H_2 (anode)/O_2 (cathode); back pressure: both 150 kPa_{abs}	Nie et al.[212]
PtFe on Fe-N_x-enriched nanocubes (FeNCs)	impregnation of Pt and Fe precursors on the surface of FeNC support	N/A	1157	0.889	0.065	0.1	1,050	temperature: 80°C; H_2 (anode)/O_2 (cathode); flow rate: H_2/O_2 (200/300 sccm); back pressure: both 1 bar_{abs}	Wu et al.[213]
PtCo on N-doped composite carbon supports)	impregnation of Pt and Co precursors on the surface of carbon support derived from ZIF-67 and KB composite	93.1	860	0.933	0.15	0.05	1,830	temperature: 80°C; back pressure: 200 kPa_{abs}	Zhang et al.[214]

Results highlight the trade-offs between activity, platinum utilization, and synthetic complexity, providing insights into the development of next-generation high-performance fuel cell catalysts.

mA·cm^{-2}, lower than the US DOE target, which is 44 mA·cm^{-2}, but close to the commercial Pt/C electrocatalyst; therefore, M-N-C electrocatalysts need to be improved more in terms of performance before they can be offered commercially.[232] The main types of non-PGM catalysts include (1) core-shell catalysts, (2) metal (oxy) nitrides, and (3) heteroatom-doped carbon. Among these, nitrogen-coordinated TM embedded in a carbon matrix (i.e., M-N-C electrocatalysts) is the most popular. These electrocatalysts in general comprise >90% disordered carbon, small amounts of TM, and small amounts of nitrogen.[232]

The main problem facing applications of M-N-C electrocatalysts is instability. These electrocatalysts degrade by 40%–80% after 100 h of continuous operation.[232] They suffer from Fenton reactions, which occur due to H_2O_2 formation, and consequent carbon corrosion and demetallation, leading to faster carbon degradation and a significant amount of performance loss. They also have thicker CLs than PGM-based electrocatalysts, meaning more carbon content, worse mass transfer, and less stability.

Different TMs can be used for manufacturing M-N-C electrocatalysts. The most common TMs, with their electrochemical activity order from high to low, are Fe, Co, Mn, Cu, and Ni.[229] Even though Fe is the most electrochemically active among them, it has more of a tendency to participate in Fenton reactions than the others, making it more vulnerable to long-lasting durability tests.[230]

The type of carbon sources used for Fe-N-C electrocatalysts that are studied in the literature involve different synthesis routes and lead to different results (Table 7; Figure 8). There are three main approaches to synthesize Fe-N-C electrocatalysts. The first approach, which produced the earliest examples of Fe-N-C electrocatalysts that yielded moderate performance, is to dope iron and nitrogen to a polymer-based carbon source. One of the earliest studies included an FeN_4-doped porphyrin-based electrocatalyst made by Wuan et al.[233]; subsequent tests resulted in 0.73 V of half-wave potential, 730 mW·cm^{-2} maximum power density, and 10 h of continuous operation. Polyaniline (PANI)-based Fe-N-C electrocatalysts are also extensively studied, delivering better performance than the previously discussed porphyrin-based one. Fu et al.[234] synthesized a PANI-coated Fe-N-C electrocatalyst with porous graphene-like frameworks, resulting in 0.80 V of half-wave potential and 1,060 mW·cm^{-2} maximum power density. Zhang et al.[235] created a Fe- and N-doped dual-pyridine coordinated polymer and then pyrolyzed the mixture, resulting in an electrocatalyst that yielded 0.81 V of high half-wave potential but a lower maximum power density of 650 mW·cm^{-2}.

In addition to polymers, other carbon-based materials such as carbon nanotubes (CNTs) and graphene can serve as carbon sources in the second approach for synthesizing Fe–N–C electrocatalysts. However, this method typically results in lower power density. For example, an alternative electrocatalyst, Fe–N–CNT, was synthesized by Xia et al.[236] involves a CNT-like structure, which is made by doping $FeCl_3$ into a melamine sponge and the subsequent heat treatments, promising a high surface area and activity. The electrochemical tests resulted in 0.77 V of half-wave potential, a low maximum power density value of 360 mW·cm^{-2}, and 30 h of continuous operation. Using graphene as the carbon source for Fe-N-C catalysts is becoming popular owing to the high surface area and excellent conducting properties of graphene. Sibul et al.[241] synthesized a Fe-N-graphene electrocatalyst using Fe- and N-doped GO by pyrolyzing the precursor mixture. The resulting electrocatalyst yielded 0.77 V of half-wave potential and 243 mW·cm^{-2} of a very low maximum power density, showing that graphene-based non-PGM catalyst research should be improved. Another GO-based Fe-N-C electrocatalyst development using three different iron precursors ($FeCl_2$, $FeCl_3$, and $FeSO_4$) and subsequent investigation of the effect of CeO_2 addition was reported by Kırlıoğlu et al.[242] Of the resulting Fe-N-C electrocatalysts, the one made of $FeCl_3$ precursor and without CeO_2 addition showcased the highest half-wave potential of 0.62 V; on the other hand, the highest maximum power density of 86.6 mW·cm^{-2} of these electrocatalysts was exhibited by the one made of $FeCl_3$ precursor and doped with CeO_2. This shows that CeO_2 addition affects the half-wave potential negatively, but max. power density positively. Both half-wave potential and maximum power density values are very low compared to the other works, showing that additional research on GO-based Fe-N-C electrocatalysts and potential dopants must be carried out.

The third approach utilizes the zeolitic imidazolate framework (ZIF-8)-based non-PGM catalysts, and this approach is commonly studied in PEMFC catalyst research due to the easier modification of the transition metal, their decent electrochemical performance, and their long continuous operation. Liu et al.[239] synthesized an Fe-N-C electrocatalyst using pyrolysis of Fe-doped ZIF-8 under an argon atmosphere at 1,000°C. The resulting Fe2-Z8-C electrocatalyst exhibited 0.81 V of half-wave potential, 1,141 mW·cm^{-2} of high maximum power density, as well as 167 h of continuous operation. Even with lower Fe loadings, the power density remained close owing to the densely distributed Fe particles on the electrocatalyst. As mentioned, different transition metals, such as Co and Mn, can be used in non-PGM electrocatalysts. Co-based electrocatalysts demonstrate a solid performance under alkaline conditions but they are weak under acidic conditions; therefore, synthesizing cobalt-based electrocatalysts for PEMFCs is challenging, requiring a solution to make them able to work better under acidic conditions. Wang et al.[230] developed a Co-N-C electrocatalyst that is produced using pyrolysis of Co-doped ZIF-8 under an argon atmosphere at 1,000°C and achieved 20% Co doping. 0.80 V half-wave potential, and 560 mW·cm^{-2} of maximum power density was observed during testing. After 100 h of continuous operation, potential loss is 60 mV due to instability of active sites or electrode structures after long operation. Different from Co-based electrocatalysts, Mn-based electrocatalysts perform better in harsh acidic media, and the contribution of Mn to Fenton reactions are negligible compared to Fe and Co. Li et al.,[240] by means of these advantages of Mn, developed an Mn-N-C electrocatalyst using pyrolysis of 20% Mn-doped ZIF-8 under an N_2 atmosphere at 1,100°C and an after treatment with acid leaching and thermal activation at 1,100°C. After subsequent tests, the Mn-N-C electrocatalyst yielded 0.80 V of half-wave potential, 460 mW·cm^{-2} of maximum power density, and only 17 mV loss of potential after 30,000 cycles of accelerated durability testing. The latter shows that the Mn-N-C electrocatalyst is more durable than its Fe and Co counterparts.

Table 7. Electrochemical and PEMFC single-cell test performance of non-PGM electrocatalysts

Catalyst	Preparation method	$E_{1/2}$ (V)	Catalyst loading ($mg \cdot cm^{-2}$)		Maximum power density ($mW \cdot cm^{-2}$)	Single-cell test conditions	Durability (h)	Reference
			Cathode	Anode (Pt)				
FeN_4 in polyporphyrin	polymerizing PTTPP with implementing iron atoms inside, forming FeN_4 moieties	0.73	4	0.25	730	temperature: 80°C; H_2 (anode)/O_2 (cathode); flow rate: both 0.3 $L \cdot min^{-1}$; back pressure: both 1.4 bar_{abs}	10	Wuan et al.[233]
Fe-N-C-Phen-PANI	embedding Phen and Fe $(Ac)_2$ to the carbon particles, then addition of aniline and subsequent pyrolysis	0.80	4	0.2	1060	temperature: 80°C; H_2 (anode)/O_2 (cathode); flow rate: 0.3 $L \cdot min^{-1}$ (H_2), 0.4 $L \cdot min^{-1}$ (O_2)	–	Fu et al.[234]
Fe-dual pyridine-derived Fe-N-C	creating a polymer from DMP and DPD and adding N_2 and $FeCl_2$ into this polymer, then pyrolysis at 900°C	0.81	4	0.5	650	temperature: 80°C; H_2 (anode)/O_2 (cathode); flow rate: both 0.3 $L \cdot min^{-1}$; back pressure: both 2 bar_{abs}	–	Zhang et al.[235]
Fe-N-CNT	doping $FeCl_3$ into melamine sponge (MS), then two-stage heat treatment of the resulting $FeCl_3$/MS precursor	0.77	4	0.25	360	temperature: 75°C; H_2 (anode)/O_2 (cathode); flow rate: both 0.4 $L \cdot min^{-1}$; back pressure: both 1.5 bar_{abs}	30	Xia et al.[236]
S-doped Fe-N-C	grafting CB with sulfophenyl group, then mixing with m-PDA and $FeCl_3$, polymerizing and pyrolyzing at 950°C	0.84	4	0.4	1030	temperature: 80°C; H_2 (anode)/O_2 (cathode); flow rate: both 0.3 $L \cdot min^{-1}$ (0.2 $L \cdot min^{-1}$ for durability test); back pressure: both 2 bar_{abs} (1 bar_{abs} for durability test)	10	Wang et al.[237]
Fe-N-C/CO_2	pyrolysis in CO_2/Ar atmosphere, then acid leaching of polymer-coated and ironized CB	0.80	4	0.4	1230	temperature: 80°C; H_2 (anode)/O_2 (cathode); flow rate: both 0.3 $L \cdot min^{-1}$; back pressure: both 2 bar_{abs}	–	Wan et al.[238]
ZIF-8-based Fe-N-C	pyrolysis of Fe-doped ZIF-8 precursor at 1000°C under Ar atmosphere	0.81	2.8	0.25	1141	temperature: 65°C; H_2 (anode)/O_2 (cathode)	167	Liu et al.[239]
ZIF-8-based Co-N-C	pyrolysis of Co-doped ZIF-8 precursor at 1100°C under Ar atmosphere	0.80	4	0.2	560	temperature: 80°C; H_2 (anode)/O_2 (cathode); flow rate: both 0.2 $L \cdot min^{-1}$	100	Wang et al.[230]
ZIF-8-based Mn-N-C	pyrolysis of Mn-doped ZIF-8 precursor at 1100°C under Ar atmosphere, then heat treatment at 900°C under N_2 atmosphere	0.80	4	0.25	460	temperature: 80°C; H_2 (anode)/O_2 (cathode); flow rate: 0.3 $L \cdot min^{-1}$ (H_2), 0.5 $L \cdot min^{-1}$ (O_2)	100	Li et al.[240]

(*Continued on next page*)

Table 7. *Continued*

Catalyst	Preparation method	$E_{1/2}$ (V)	Catalyst loading (mg·cm^{-2})		Maximum power density (mW·cm^{-2})	Single-cell test conditions	Durability (h)	Reference
			Cathode	Anode (Pt)				
Fe-N-graphene	pyrolysis of a solution containing GNPs, 1,10-phenanthroline, and iron (II) acetate at 800°C under N_2 atmosphere for 1 h	0.77	4	0.8	243	temperature: 80°C; H_2 (anode)/O_2 (cathode); flow rate: 0.3 L·min^{-1} (H_2), 0.2 L·min^{-1} (O_2)	–	Sibul et al.[241]
Fe-N-graphene with CeO_2 additive	synthesis and reduction of nano-sized GO and doping of this GO with N and Fe, then adding different amounts of CeO_2	0.62	3.9	0.4	86.6	temperature: 80°C; H_2 (anode)/O_2 (cathode); flow rate: 1 L·min^{-1} (H_2), 1.5 L·min^{-1} (O_2)	–	Kirlioğlu et al.[242]

These data provide insight into the viability of non-precious metal catalysts for sustainable and cost-effective PEMFC applications.

The approach of doping Fe-N-C electrocatalysts with different materials to increase the surface area or improving the mass transport properties of the resulting electrocatalysts has also been studied in the literature.[237,238,243] Yang et al.[243] doped SiO_2 into a ZIF-8-based Fe-N-C electrocatalyst, modifying the mass transport properties of the catalyst and obtaining a more hydrophobic surface. This operation improved the performance of the pristine Fe-N-C electrocatalyst by 25%. Wang et al.[237] synthesized an S doped Fe-N-C electrocatalyst, $Fe(SCN)_3$, by coating an m-phenylenediamine (m-PDA) monomer with sulfophenyl-grafted CB followed by subsequent polymerization and pyrolysis. The resulting electrocatalyst yielded 0.84 V of half-wave potential and 1,030 mW·cm^{-2} of maximum power density. These results showed that S doping increased the performance of the pristine Fe-N-C electrocatalyst by nearly 30%. Wan et al.[238] applied a mild CO_2 etching to another m-PDA-based Fe-N-C electrocatalyst by pyrolyzing the electrocatalyst in a CO_2 atmosphere, increasing the pore size and, therefore, the surface area of the electrocatalyst. This operation resulted in 0.80 V of half-wave potential and a superior maximum power density of 1,230 mW·cm^{-2} but inferior stability due to a lower graphitization degree caused by CO_2 over etching.

In conclusion, the ZIF-8-based Fe-N-C electrocatalyst is currently the best-performing non-PGM electrocatalyst among the reviewed works, with the highest maximum power density and longest duration of continuous operation, yielding performance closer to its PGM-based counterparts. The performance of this type of M-N-C electrocatalyst can be amplified further by doping different materials to boost their mass transport rate, improve their resistance against acidic media, and eventually solve their instability issues and increase their durability. Although the graphene-based Fe-N-C electrocatalysts currently exhibit comparably poor performance, there are some examples surpassing the target of the US DOE.[244–246] Furthermore, strategies like stabilizing the catalyst with hydrogen passivation are proposed in the literature,[247] and more strategies are likely to be introduced in the future.

Reliability and testing

Electrocatalysts are characterized by their chemical, physical, thermal, morphological as well as electrochemical properties. Since, in this review, the focus is electrocatalysts for PEMFCs, fuel cell-relevant properties are emphasized by utilizing electrochemical characterization methods. The most common electrochemical characterization methods for electrocatalysts and electrodes in PEMFCs include cyclic voltammetry (CV), linear sweep voltammetry (LSV), and EIS.[248,249] Some of the most significant examples of these types and the applied techniques are as follows. CV facilitates the evaluation of electrocatalytic activity by measuring the current response as a function of potential, which aids in elucidating reaction mechanisms and assessing electroactive surface area. LSV with a rotating disk electrode system allows the precise determination of catalytic performance under well-controlled mass transport conditions, providing critical insights into the effects of diffusion on reaction kinetics. EIS is employed to investigate the kinetics and transport phenomena within the fuel cell, yielding insights into the system's resistance and capacitance characteristics. Collectively, these characterization methods provide very important

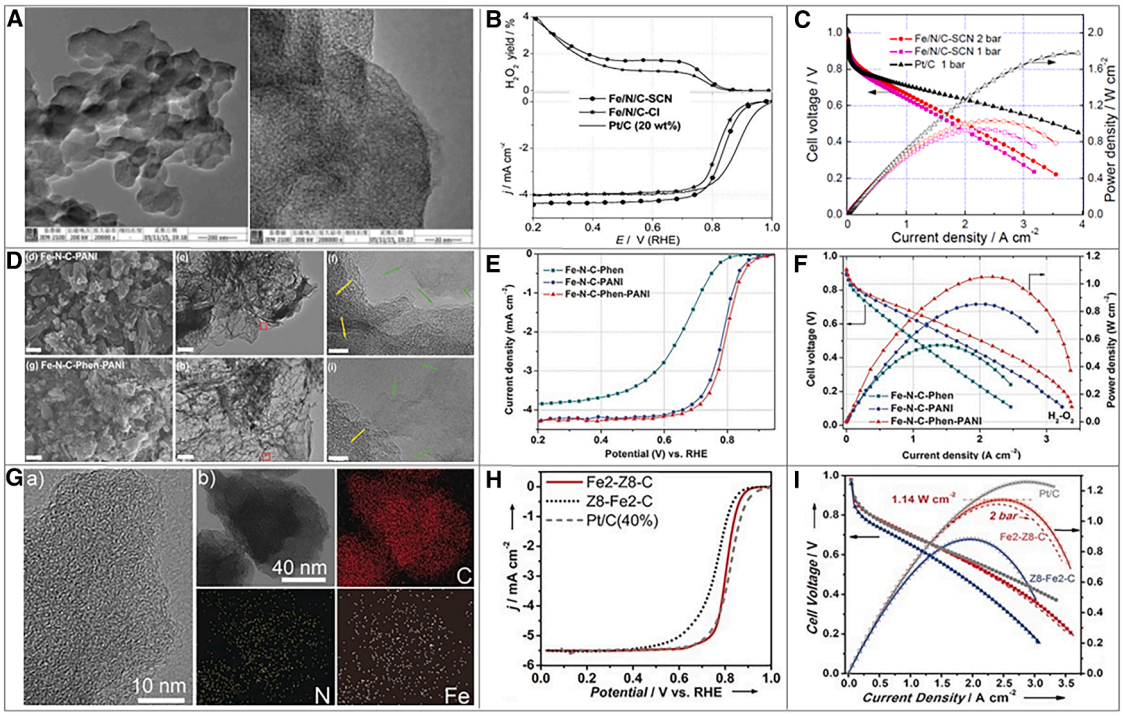

Figure 8. Selected state-of-the-art non-PGM electrocatalysts

(A–C) HR-TEM images (A), LSV curves (B), and polarization curves (C) of an S-doped Fe-N-C catalyst. Adapted with permission from John Wiley and Sons.[237]
(D–F) HR-TEM images (D), LSV curves (E), and polarization curves (F) of an Fe-N-C-Phen-PANI catalyst. Adapted with permission from John Wiley and Sons.[234]
(G–I) HR-TEM and EDS images (G), LSV curves (H), and polarization curves (I) of a ZIF-8-based Fe-N-C catalyst. Adapted with permission from John Wiley and Sons.[239]

information for optimizing the catalytic activity of electrocatalysts and electrode materials, thereby enhancing the overall efficiency and durability of PEMFCs.

A major issue in the development of PEMFCs is the degradation of electrodes and membranes, linked to catalyst properties, device design, or radical formation during catalysis. ADTs are crucial for assessing stability by simulating real-world conditions and predicting device lifespan.[250] *Ex situ* testing of half-cells offers a faster, cost-effective way to study catalyst aging. Variability in test conditions makes it difficult to compare results, prompting the US DOE and the Fuel Cell Commercialization Conference of Japan to propose standardized ADT protocols.[251] The DOE's Hydrogen and Fuel Cell Technologies Office studies degradation mechanisms under realistic stresses, such as impurities, freezing, and start-stop cycles. Key degradation pathways include carbon corrosion during start-stop cycles and Pt dissolution in load cycles, often measured by the loss of ECSA.[252]

The CL|PEM interface

The CL|PEM interface serves as the critical locus for the ORR and HOR in fuel cells. This interface comprises three essential components—catalysts, carbon support, and ionomer film—that function synergistically to facilitate efficient redox reactions.[253] The ionomer film, which envelops both catalyst and support particles, is crucial for proton and water transport, channeling these species to the reaction site at the TPB. The TPB represents the unique interface where fuel, ionomer, and catalyst converge, enabling the transfer of protons and electrons necessary for efficient reaction kinetics.[254] Despite its significance, the CL|PEM interface has received relatively limited attention in the scientific literature, with few studies comprehensively investigating its structure, electrochemical processes, and contribution to fuel cell performance. This paucity of research can be attributed to the inherent complexity of studying interfaces within multi-component systems.[255–257]

Structure and composition of the CL|PEM interface. The CL|PEM interface is a complex, heterogeneous structure comprising three primary components: catalyst NPs, carbon support, and ionomer. The catalyst NPs, typically Pt or Pt alloys, are dispersed across a high-surface-area carbon support and enveloped by an ionomer layer that facilitates proton and water mass transfer. The region where the fuel contacts the catalyst, enabling the redox reaction and subsequent electron transfer to the support, is termed the TPB.[258,259] The microscopic structure of the CL|PEM interface, as illustrated in Figure 9A, reveals the intricate spatial relationships between these components. The carbon support, being the largest component, provides electronic conductivity, porosity, and stability in both acidic and basic environments. Catalyst particles are distributed both on the surface and within the micropores of the support. The ionomer film, crucial for reactant and product mass transport, covers the catalyst and support surfaces.[260,261]

Optimization of the CL|PEM interface. Optimizing the CL|PEM interface requires careful consideration of both microscopic

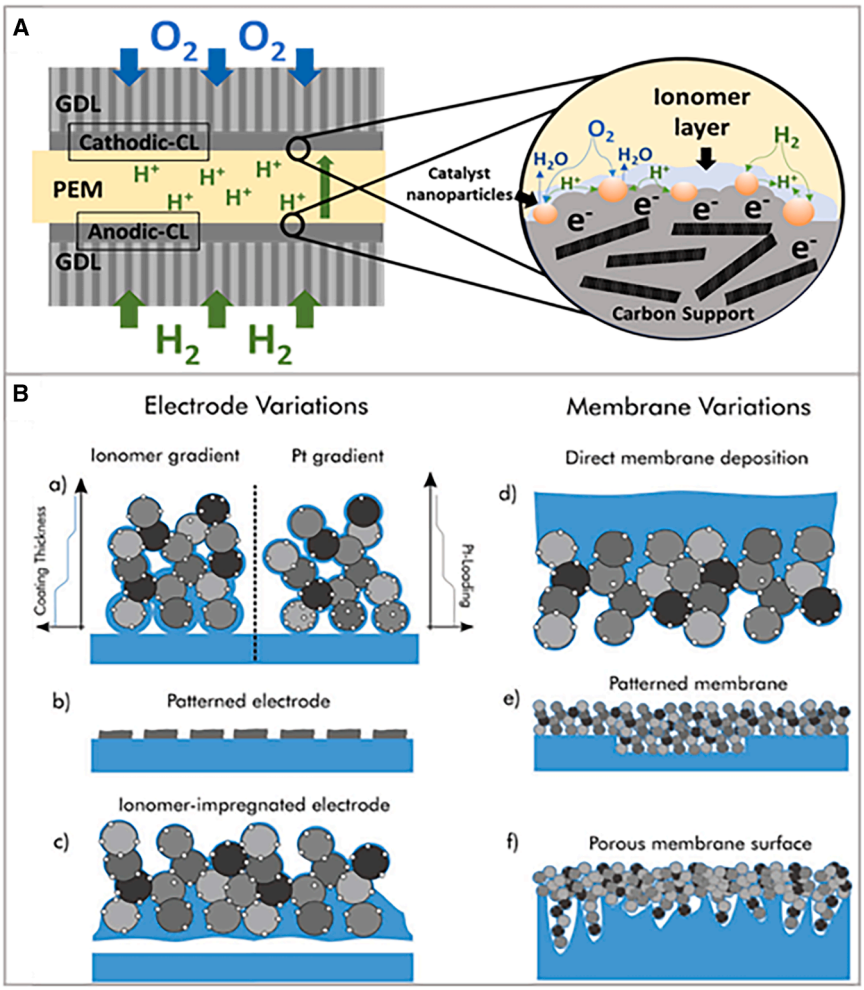

Figure 9. CL|PEM interface structure and optimization techniques

(A) Schematic of the CL|PEM interface.

(B) CL|PEM interface manufacturing techniques including, (a) graded electrodes (ionomer/Pt-content), (b) patterned electrodes, (c) ionomer-impregnated electrodes, (d) direct membrane deposition (DMD), (e) patterned membranes, and (f) porous membrane surfaces. Adapted with permission from John Wiley and Sons.[262]

and macroscopic parameters. At the microscopic level, the interactions between catalyst/support, catalyst/ionomer, and support/ionomer must be finely tuned. Macroscopically, the overall connectivity and homogeneity of the CL|PEM interface are critical factors.[263,264] Research data so far suggest that the highest-performing CL|PEM interfaces exhibit the following characteristics/process metrics: uniform distribution of 2- to 5-nm Pt catalyst particles, carbon support thickness of 20–30 nm, and ionomer film thickness of 4–10 nm covering both catalyst and support. Maintaining this homogeneous distribution across the entire interface presents a significant challenge, largely dependent on macroscopic fabrication methods.[261,265]

Electrochemical processes and performance evaluation. The fuel cell's redox reactions, including the ORR and HOR, occur at the CL|PEM interface. The efficiency of these reactions is contingent upon facile mass transport of reactants and products to and from the TPB as well as minimal resistance to electron transfer from the catalyst through the support. EIS has emerged as a powerful technique for evaluating charge and mass transfer processes at the CL|PEM interface. EIS enables spatial separation of processes based on their characteristic time constants, providing invaluable insights into interface dynamics.[266,267]

Advanced techniques for CL|PEM interface optimization. Recent advancements in membrane deposition methods have shown promise in optimizing CL|PEM interfaces, as detailed by Breitweiser et al.[262] These techniques, illustrated in Figure 9B, include the following: (1) surface-patterned membranes, which includes the utilization of micro- or nano-patterned surfaces to create controlled interface structures, enhancing proton and oxygen transport pathways[268,269]; (2) direct-deposited membrane manufacturing, which includes the direct deposition of ionomer films onto the CL, resulting in highly controlled and compact structures with optimized ionomer thickness[270,271]; (3) porous membrane design, based on incorporation of porosity within the membrane to improve gas and liquid transport, particularly beneficial under high current densities[269,272]; and (4) ionomer-impregnated assembly, which is based on impregnation of the CL with ionomer, creating a finely distributed ionomer network that enhances proton conductivity and structural stability.[273] These techniques have demonstrated significant improvements in fuel cell performance by creating more controlled and homogeneous structures, thereby enhancing TPB exposure and reaction efficiency.

Recent studies have further expanded these techniques, including a methodology for gradient-structured interfaces based on implementation of compositional gradients across the CL|PEM interface to optimize both catalytic activity and mass transport properties.[274] In addition, 3D-printed electrode structures were developed, based on the utilization of additive manufacturing techniques to create precisely controlled electrode architectures, useful for enhancing the TPB area and mass transport characteristics.[275] Furthermore, atomic layer deposition methods were employed for interface engineering to create highly controlled, ultra-thin, conformal coatings on catalyst particles and support structures to improve interface stability and performance.[276]

Overall, the CL|PEM interface represents a critical frontier in fuel cell research and development. Its optimization through advanced fabrication techniques and precise control of

component distribution holds the key to realizing substantial improvements in fuel cell efficiency and longevity. As the field progresses, continued focus on interface engineering will be essential for advancing sustainable energy technologies. Future research directions may include the development of *in situ* characterization techniques for real-time interface monitoring and the exploration of novel materials and structures that can further enhance the performance and durability of fuel cell systems.

Advanced micro-scale *operando* techniques include combining micro X-ray computed tomography (X-CT), X-ray radiography, and computed tomography X-ray absorption near edge structure (CT-XANES) to investigate water diffusion through the gas diffusion electrode, the current-density dispersion inside the catalyst and microporous layers, and the degradation of MEA.[277] These analyses can be combined with deep learning to get a better modeling of each component of a PEMFC stack.[278] Furthermore, the evolution and the effects of TPBs inside a PEMFC can be monitored by coupling PEMFC testing with high-frequency impedance analysis and subsequent circuit modeling.[263]

SUMMARY AND FUTURE TRENDS

PEMFC membranes and electrocatalysts have garnered significant attention in recent years due to their critical roles in enhancing fuel cell performance, durability, and efficiency. In this respect, state-of-the-art and next generation proton-conductive polymers for membranes and Pt- and non-PGM-based electrocatalysts were summarized within this review. A thorough examination of the fabrication/synthesis methods, type of materials, and structure-property relationships of PEMFC membranes and electrocatalysts was provided. The selection of the materials for MEA significantly influences performance, and therefore these materials are a vital area of research for improving fuel cell technologies. To overcome the key challenges, the enhancement of properties such as ionic conductivity, optimizing catalytic activity, and improving long-term stability, including materials used in membrane and electrode structure, is crucial. In closure, we would like to provide the following conclusions and future trends.

Recent trends in PEMFC research and development

Membranes and electrocatalysts for PEMFCs have been the focus of extensive research efforts in recent years owing to their pivotal roles in determining fuel cell performance, longevity, and overall efficiency. While the field has experienced a relative deceleration in research intensity since 2020, the imperative for continued advancements remains paramount. Here we summarize several key developments in PEMFC membrane technology.

(1) High-temperature membranes. Efforts have been made to develop membranes capable of operating at elevated temperatures (120°C–300°C), which offer advantages such as enhanced CO tolerance and simplified water management.[279] These high-temperature PEMFCs (HT-PEMFCs) show promise for addressing hydrogen source challenges and contributing to carbon reduction goals.

(2) Reinforced membranes. The advent of mechanically reinforced membranes has led to improved durability and operational stability, addressing one of the critical challenges in PEMFC longevity.[280]

(3) Phosphoric acid-doped membranes. Studies have focused on mitigating the negative effects of phosphoric acid on platinum catalysts in HT-PEMFCs with novel approaches to catalyst design and membrane composition.[279]

For the area of electrocatalysts, significant progress has been reported.

(1) PGM-free catalysts. Efforts to replace expensive platinum catalysts with more cost-effective alternatives have intensified, with particular focus on Fe-N-C systems for the ORR.[281]

(2) Nanostructured catalysts. Advanced nanostructuring techniques have been employed to enhance catalyst activity and durability, including the development of core-shell structures and alloys.[279]

(3) Support material innovations. Research has explored alternative support materials to carbon, aiming to mitigate carbon corrosion issues and enhance overall catalyst stability.[281,282]

The apparent deceleration in research intensity since 2020 can be attributed to several factors.

(1) Maturation of certain technologies. Some areas of PEMFC research have reached a plateau in terms of incremental improvements, leading to a shift in focus toward other emerging energy technologies.

(2) Economic factors. Fluctuations in funding and market dynamics have influenced research priorities and resource allocation.

(3) The COVID-19 pandemic. The global health crisis has disrupted research activities and collaborations, potentially slowing progress in the field.

However, the need for continued advancements in PEMFC technology remains critical for several reasons.

(1) Cost reduction. Despite progress, further cost reductions are necessary to make PEMFCs economically competitive with conventional energy technologies.[281]

(2) Durability enhancement. Improving the long-term stability of membranes and catalysts under real-world operating conditions remains a significant challenge.[280]

(3) Performance optimization. Enhancing power density, efficiency, and operational flexibility is crucial for expanding the application range of PEMFC.[264]

(4) Sustainability goals. The potential of PEMFCs to contribute to decarbonization efforts and renewable energy integration underscores the importance of continued research and development in this field.

While the pace of PEMFC membrane and electrocatalyst research may have moderated since 2020, the fundamental

importance of these components in advancing clean energy technologies necessitates sustained scientific inquiry and innovation. Future research directions should focus on addressing the upcoming challenges in cost, especially in the light of rising inflationary impacts worldwide as well as availability of resources, durability, and performance to fully realize the potential of PEMFCs in a sustainable energy landscape. The following section will provide a 5-year and a 10-year outlook for membrane technology development.

Projected outlook for membrane development

The future prospects for PEMFC membranes are indeed promising, with significant technological advancements expected in the next 5–10 years. These developments will be crucial in addressing the current challenges and driving widespread adoption of PEMFCs.

In the next 5 years, we anticipate significant progress in the following areas.

(1) Hydrocarbon-based membranes. Research will intensify to develop high-performance hydrocarbon-based membranes as alternatives to Per- and Polyfluoroalkyl (PFAS)-containing membranes. These materials are expected to offer performance comparable to PFSA membranes while being more cost-effective and environmentally friendly.[279]
(2) Nanocomposite membranes. Advanced nanocomposite membranes incorporating materials such as GO, CNTs, and metal-organic frameworks (MOFs) will likely emerge, offering enhanced proton conductivity and mechanical stability.[281]
(3) Improved durability. Membrane durability will be significantly enhanced through the development of novel polymer blends and reinforcement techniques, extending the operational lifetime of PEMFCs.[280]
(4) Advanced manufacturing techniques. Adoption of 3D printing and other advanced manufacturing techniques for MEAs will increase, allowing more precise control over membrane properties and reduced production costs.[263]

Looking further ahead to 2034, we can expect more transformative developments.

(1) Self-healing membranes. Development of self-healing membrane materials that can autonomously repair minor damage could significantly extend PEMFC lifetimes and reduce maintenance requirements.
(2) Bio-inspired membranes. Biomimetic approaches may lead to the creation of highly efficient proton-conducting membranes inspired by natural systems, potentially revolutionizing PEMFC performance.
(3) Integrated smart membranes. Membranes with integrated sensors and adaptive properties could optimize performance in real time based on operating conditions.
(4) Zero-PFAS membranes. Complete transition away from PFAS-containing membranes to environmentally benign alternatives without compromising performance is expected.[279]
(5) High-temperature membranes. Development of membranes capable of efficient operation at temperatures above 200°C could expand the application range of PEMFCs.[279]

According to recent market reports, the global PEMFC market is projected to grow at a CAGR of 28% between 2024 and 2034, reaching a value of over US $8 billion by 2034.[30] This growth will be driven by advancements in membrane technology, increased adoption in the transportation sector, and supportive government policies.

Projected outlook for electrocatalyst development

The forthcoming decade presents significant opportunities for advancing electrocatalysts for hydrogen fuel cells, propelled by increasing global commitments to clean energy transitions and decarbonization strategies. Research efforts will prioritize the optimization of performance, durability, and cost-effectiveness. Platinum, the current benchmark for the HOR and ORR, will remain central to investigations due to its superior catalytic properties. However, its high cost and limited availability are expected to drive substantial progress in alternative non-precious metal catalysts, including TM-N-C frameworks, metal oxides, single-atom catalysts, and high-entropy alloys.

Innovations in electrocatalyst development will likely harness the capabilities of nanotechnology, computational modeling, and machine learning to enhance catalytic activity and long-term stability.[283] Furthermore, advances in catalyst-support interactions and electrode architecture are anticipated to improve the durability and efficiency of fuel cells under practical operating conditions. Parallel efforts will focus on sustainable manufacturing practices for catalyst production, aligning with global objectives of environmental sustainability and resource efficiency. These developments will collectively enable the widespread adoption of hydrogen fuel cells as a key technology in the clean energy landscape.

Pt and Pt-M

Reducing reliance on precious (Pt remains a central research priority, as its high cost and scarcity present significant barriers to the widespread commercialization of PEMFCs. A promising strategy to address this challenge involves the development of multi-metal composite catalysts incorporating more cost-effective transition metals, such as Fe, Co, and Ni. However, the dissolution and dealloying of these transition metals during fuel cell operation raise durability concerns, necessitating advanced structural engineering approaches, such as core-shell architectures, to enhance catalyst stability. Among the investigated Pt-M alloy electrocatalysts, $L1_0$-CoPt NPs have demonstrated the most promising performance to date.[207,218] Furthermore, the integration of artificial intelligence (AI) and machine learning (ML) in catalyst design is revolutionizing the field by accelerating the discovery of high-performance, low-cost alternatives to Pt. ML models can analyze extensive datasets, predict optimal catalyst compositions, and simulate performance characteristics, significantly reducing the time and cost associated with traditional experimental trial-and-error methods. By leveraging AI-driven insights alongside advancements in material synthesis,

researchers can systematically develop catalysts that combine high catalytic activity, improved stability, and reduced cost, thereby expediting the commercialization of PEMFCs and reinforcing their role as a pivotal technology in the transition to sustainable energy systems.

In parallel, optimizing CL deposition techniques is critical for maximizing catalyst utilization and enhancing PEMFC efficiency. Conventional methods, such as drop-casting and manual airbrushing,[284] often lead to inhomogeneous catalyst distribution and NP aggregation, which negatively impact fuel cell performance. Future advancements are expected to focus on precision engineering techniques such as spray pyrolysis,[285] electrospinning,[286] or inkjet printing,[287] which enable the fabrication of uniform, thin CLs with controlled nanostructures. Achieving greater homogeneity in CLs will minimize energy loss, enhance fuel utilization, and extend PEMFC durability, ultimately driving the technology toward higher operational efficiency and broader commercial viability.

Non-PGM

Non-PGM catalysts have emerged as cost-effective alternatives to their expensive PGM-based counterparts. Among these, M-N-C catalysts—where M represents a transition metal such as Fe, Co, or Mn—have garnered significant attention due to their potential for sustainable and economically viable fuel cell applications. While these catalysts demonstrate promising catalytic activity, their widespread practical implementation remains hindered by several critical challenges, including instability caused by Fenton reactions, suboptimal mass transport properties, and insufficient long-term durability. Consequently, ongoing research efforts continue to focus on enhancing the stability and performance of M-N-C catalysts with the ultimate goal of achieving performance metrics comparable to those of PGM-based catalysts.

Currently, ZIF-8-derived M-N-C catalysts have gained substantial interest among researchers due to their well-established and scalable synthesis process. These catalysts exhibit superior power density and prolonged continuous operation compared to other non-PGM alternatives. Furthermore, the incorporation of graphene-based structures as a carbon support in M-N-C catalysts has been explored as a strategy to improve stability and mass transport. While these modifications have yet to yield significant breakthroughs in overall performance, graphene remains a highly promising candidate due to its exceptional specific surface area and high electrical conductivity. With further optimization, the development of an efficient synthesis route for high-performance M-N-graphene catalysts could significantly enhance the viability of M-N-C catalysts by addressing their key limitations.

In parallel, the emphasis on sustainability and cost reduction continues to drive progress toward the broader adoption of PEMFCs. Green manufacturing processes and the development of recyclable materials are expected to mitigate environmental impact while reducing production costs. Additionally, advancements in hybrid energy systems and comprehensive system-level optimizations will likely improve overall efficiency and long-term performance. These technological innovations are poised to accelerate the deployment of PEMFCs across various sectors, including transportation, stationary power generation, and portable energy applications. As the hydrogen economy expands, with global hydrogen consumption projected to increase 6-fold by 2050 compared to 2020 levels,[288,289] PEMFCs are expected to play an increasingly pivotal role in the transition toward a sustainable and economically viable energy future.

AUTHOR CONTRIBUTIONS

B.Y.K. and M.O. proposed the topic of the manuscript. N.R.M., A.C.K., S.A.G., B.Ö., A.A.H., M.B.-A., M.A.Z., A.Y., C.S.O., B.Y.K., and M.O. investigated the literature, discussed the structure and sections, and wrote the manuscript. All authors critically revised the review article for complete and comprehensive intellectual content. All authors read and approved the final version of the manuscript. B.Y.K. and M.O. managed the manuscript team.

DECLARATION OF INTERESTS

The authors declare no competing interests.

REFERENCES

1. U.S. Department of Energy (2022). DOE National Clean Hydrogen Strategy and Roadmap. Online at: https://www.hydrogen.energy.gov/docs/hydrogenprogramlibraries/pdfs/clean-hydrogen-strategy-roadmap.pdf.
2. European Comission (2019). The European Green Deal. https://commission.europa.eu/strategy-and-policy/priorities-2019-2024/european-green-deal_en.
3. (2021). EU Hydrogen Policy: Hydrogen as an energy carrier for a climate-neutral economy. https://www.europarl.europa.eu/RegData/etudes/BRIE/2021/689332/EPRS_BRI(2021)689332_EN.pdf.
4. Kaplan, B.Y., Kırlıoğlu, A.C., Alinezhadfar, M., Zabara, M.A., Mojarrad, N. R., Iskandarani, B., Yürüm, A., Özkan, C.S., Özkan, M., and Gürsel, S.A. (2023). Hydrogen production via electrolysis: Operando monitoring and analyses. Chem Catal. *3*, 100601. https://doi.org/10.1016/j.checat.2023.100601.
5. Zabara, M.A., Ölmez, B., Buldu-Akturk, M., Yarar Kaplan, B., Kırlıoğlu, A. C., Alkan Gürsel, S., Özkan, M., Özkan, C.S., and Yürüm, A. (2024). Photoelectrocatalytic Hydrogen Generation: Current Advances in Materials and Operando Characterization. Glob. Chall. *8*, 2400011. https://doi.org/10.1002/gch2.202400011.
6. International Energy Agency. IEA - Global EV Policy Explorer. https://www.iea.org/data-and-statistics/data-tools/global-ev-policy-explorer.
7. European Commission (2023). Regulation of the European Parliament and of the Council. https://eur-lex.europa.eu/TodayOJ/.
8. Lucia, U. (2014). Overview on fuel cells. Renew. Sustain. Energy Rev. *30*, 164–169. https://doi.org/10.1016/j.rser.2013.09.025.
9. Barbir, F. (2005). CHAPTER 4 - Main Cell Components, Materials Properties and Processes. In PEM Fuel Cells: Theory and Practice, pp. 73–113. https://doi.org/10.1016/B978-012078142-3/50005-7.
10. Steele, B.C., and Heinzel, A. (2001). Materials for fuel-cell technologies. Nature *414*, 345–352. https://doi.org/10.1038/35104620.
11. Shao, M., Chang, Q., Dodelet, J.P., and Chenitz, R. (2016). Recent Advances in Electrocatalysts for Oxygen Reduction Reaction. Chem. Rev. *116*, 3594–3657. https://doi.org/10.1021/acs.chemrev.5b00462.
12. Ishikawa, H., Sugawara, Y., and Tsuji, Y. (2014). Development of Residential Fuel Cell System of Panasonic and Approaches to Enhance Durability. ECS Meeting Abstracts *MA2014-01 785*, 785. https://doi.org/10.1149/MA2014-01/18/785.
13. Toyota Motor Corporation (2015). Toyota Global Newsroom. https://global.toyota/en/newsroom/.
14. Mauritz, K.A., and Moore, R.B. (2004). State of Understanding of Nafion. Chem. Rev. *104*, 4535–4585. https://doi.org/10.1021/cr0207123.

15. Debe, M.K. (2012). Electrocatalyst approaches and challenges for automotive fuel cells. Nature *486*, 43–51. https://doi.org/10.1038/nature11115.

16. U.S. Department of Energy (2020). Program Record #21003. https://www.hydrogen.energy.gov/docs/hydrogenprogramlibraries/pdfs/21003-life-cycle-ghg-emissions-small-suvs.pdf?sfvrsn=4da4525a_1.

17. Mekhilef, S., Saidur, R., and Safari, A. (2012). Comparative study of different fuel cell technologies. Renew. Sustain. Energy Rev. *16*, 981–989. https://doi.org/10.1016/j.rser.2011.09.020.

18. U.S. Department of Energy (2016). Comparison of Fuel Cell Technologies. https://www.energy.gov/eere/fuelcells/articles/comparison-fuel-cell-technologies-fact-sheet.

19. Das, G., Choi, J.H., Nguyen, P.K.T., Kim, D.J., and Yoon, Y.S. (2022). Anion Exchange Membranes for Fuel Cell Application: A Review. Polymers *14*, 1197–1231. https://doi.org/10.3390/polym14061197.

20. Yassin, K., Rasin, I.G., Willdorf-Cohen, S., Diesendruck, C.E., Brandon, S., and Dekel, D.R. (2021). A surprising relation between operating temperature and stability of anion exchange membrane fuel cells. Journal of Power Sources Advances *11*, 100066. https://doi.org/10.1016/j.powera.2021.100066.

21. Ferriday, T.B., and Middleton, P.H. (2021). Alkaline fuel cell technology - A review. Int. J. Hydrogen Energy *46*, 18489–18510. https://doi.org/10.1016/j.ijhydene.2021.02.203.

22. Zarabi Golkhatmi, S., Asghar, M.I., and Lund, P.D. (2022). A review on solid oxide fuel cell durability: Latest progress, mechanisms, and study tools. Renew. Sustain. Energy Rev. *161*, 112339. https://doi.org/10.1016/j.rser.2022.112339.

23. Hua, Z., Zheng, Z., Pahon, E., Péra, M.C., and Gao, F. (2022). A review on lifetime prediction of proton exchange membrane fuel cells system. J. Power Sources *529*, 231256. https://doi.org/10.1016/j.jpowsour.2022.231256.

24. (2013). U.S. Department of Energy - Cost Study for Manufacturing of Solid Oxide Fuel Cell Power Systems. https://www.pnnl.gov/main/publications/external/technical_reports/PNNL-22732.pdf.

25. Liu, Q., Lan, F., Chen, J., Zeng, C., and Wang, J. (2022). A review of proton exchange membrane fuel cell water management: Membrane electrode assembly. J. Power Sources *517*, 230723. https://doi.org/10.1016/j.jpowsour.2021.230723.

26. Pollet, B.G., Kocha, S.S., and Staffell, I. (2019). Current status of automotive fuel cells for sustainable transport. Curr. Opin. Electrochem. *16*, 90–95. https://doi.org/10.1016/j.coelec.2019.04.021.

27. Cunanan, C., Tran, M.K., Lee, Y., Kwok, S., Leung, V., and Fowler, M. (2021). A Review of Heavy-Duty Vehicle Powertrain Technologies: Diesel Engine Vehicles, Battery Electric Vehicles, and Hydrogen Fuel Cell Electric Vehicles. Clean Technol. *3*, 474–489. https://doi.org/10.3390/cleantechnol3020028.

28. U.S. Department of Energy - Fuel Cells. https://www.energy.gov/eere/fuelcells/fuel-cells.

29. Mordor Intelligence (2024). Polymer Electrolyte Membrane Fuel Cell Market Size & Share Analysis - Growth Trends & Forecasts (2025 - 2030). https://www.mordorintelligence.com/industry-reports/global-polymer-electrolyte-membrane-pem-fuel-cells-market-industry.

30. IDTechEx (2023). Materials for PEM Fuel Cells 2024-2034: Technologies, Markets, Players. https://www.idtechex.com/en/research-report/materials-for-pem-fuel-cells-2024-2034-technologies-markets-players/987.

31. Aminudin, M.A., Kamarudin, S.K., Lim, B.H., Majilan, E.H., Masdar, M.S., and Shaari, N. (2023). An overview: Current progress on hydrogen fuel cell vehicles. Int. J. Hydrogen Energy *48*, 4371–4388. https://doi.org/10.1016/j.ijhydene.2022.10.156.

32. Selmi, T., Khadhraoui, A., and Cherif, A. (2022). Fuel cell–based electric vehicles technologies and challenges. Trend Editorial *29*, 78121–78131. https://doi.org/10.1007/s11356-022-23171-w.

33. Market & Market (2024). Hydrogen Fuel Cell Vehicle Market Size, Share & Analysis. https://www.marketsandmarkets.com/Market-Reports/automotive-fuel-cell-market-14859789.html.

34. Sassin, M.B., Garsany, Y., Gould, B.D., and Swider-Lyons, K.E. (2017). Fabrication Method for Laboratory-Scale High-Performance Membrane Electrode Assemblies for Fuel Cells. Anal. Chem. *89*, 511–518. https://doi.org/10.1021/acs.analchem.6b03005.

35. Karuppanan, K.K., Panthalingal, M.K., and Biji, P. (2018). Chapter 26 - Nanoscale, Catalyst Support Materials for Proton-Exchange Membrane Fuel Cells. In Handbook of Nanomaterials for Industrial Applications, C. M. Hussain, ed. (Elsevier), pp. 468–495. https://doi.org/10.1016/B978-0-12-813351-4.00027-4.

36. Xing, Y., Liu, L., Fu, Z., Li, Y., and Li, H. (2023). Preparation of an Integrated Membrane Electrode Assembly for Proton Exchange Membrane Fuel Cells Using a Novel Wet-Bonding Strategy. Energy Fuels *37*, 12360–12368. https://doi.org/10.1021/acs.energyfuels.3c01800.

37. Statista (2022). Forecast key economic indicators of the hydrogen industry in the European Union in 2030. https://www.statista.com/statistics/859106/eu-hydrogen-market-size-by-indicator/.

38. Precedence Research (2024). Hydrogen Fuel Cell Vehicle Market Size, Share, and Trends 2024 to 2034. https://www.precedenceresearch.com/hydrogen-fuel-cell-vehicle-market.

39. Advanced Propulsion Centre. Behind the scenes: The 2020 Automotive Fuel Cell Roadmap. https://www.apcuk.co.uk/news-events/news/behind-the-scenes-the-2020-automotive-fuel-cell-roadmap/.

40. Shimpalee, S., Lilavivat, V., Xu, H., Rowlett, J.R., Mittelsteadt, C., and Van Zee, J.W. (2018). The Effect of Membrane Properties on Performance and Transports inside Polymer Electrolyte Membrane Fuel Cells. J. Electrochem. Soc. *165*, F1019–F1026. https://doi.org/10.1149/2.0081813jes.

41. Litster, S., and McLean, G. (2004). PEM Fuel Cell Electrodes. J. Power Sources *130*, 61–76. https://doi.org/10.1016/j.jpowsour.2003.12.055.

42. Wang, Y., Pang, Y., Xu, H., Martinez, A., and Chen, K.S. (2022). PEM Fuel cell and electrolysis cell technologies and hydrogen infrastructure development – a review. Energy Environ. Sci. *15*, 2288–2328. https://doi.org/10.1039/D2EE00790H.

43. Mancino, A., Menale, C., Vellucci, F., Pasquali, M., and Bubbico, R. (2023). PEM Fuel Cell Applications in Road Transport. Energies *16*, 6129. https://doi.org/10.3390/en16176129.

44. Cai, F., Cai, S., and Tu, Z. (2024). Proton exchange membrane fuel cell (PEMFC) operation in high current density (HCD): Problem, progress and perspective. Energy Convers. Manag. *307*, 118348. https://doi.org/10.1016/j.enconman.2024.118348.

45. US Department of Energy (2024). U.S. Department of Energy Hydrogen Program Record. https://www.hydrogen.energy.gov/docs/hydrogenprogramlibraries/pdfs/review24/24004-hd-fuel-cell-system-cost-2023.pdf?sfvrsn=70ff384f_3.

46. Yusoff, Y.N., and Shaari, N. (2021). An overview on the development of nanofiber-based as polymer electrolyte membrane and electrocatalyst in fuel cell application. Int. J. Energy Res. *45*, 18441–18472. https://doi.org/10.1002/er.7020.

47. Ogungbemi, E., Wilberforce, T., Ijaodola, O., Thompson, J., and Olabi, A. G. (2020). Review of operating condition, design parameters and material properties for proton exchange membrane fuel cells. Int. J. Energy Res. *45*, 1227–1245. https://doi.org/10.1002/er.5810.

48. U.S. Department of Energy (2024). Hydrogen and Fuel Cell Technologies Office Multi-Year Program Plan. https://www.energy.gov/sites/default/files/2024-05/hfto-mypp-2024.pdf.

49. The Rise of Green Hydrogen: Stats, Trends, and Future Projections. https://www.plugpower.com/blog/the-rise-of-green-hydrogen-stats-trends-and-future-projections/.

50. U.S. Department of Energy (2024). Bipartisan Infrastructure Law: Clean Hydrogen Electrolysis, Manufacturing, and Recycling FOA Selections.

https://www.energy.gov/sites/default/files/2024-03/DE-FOA-0002922-bil-foa-selections.pdf.

51. Zhang, Q., Tong, Z., Tong, S., and Cheng, Z. (2022). Research on performance of liquid drive fan cooling system for hydrogen fuel cell forklift. Int. J. Hydrogen Energy *47*, 9690–9705. https://doi.org/10.1016/j.ijhydene.2022.01.034.

52. Kiviranta, K., Thomasson, T., Hirvonen, J., and Tähtinen, M. (2020). Connecting circular economy and energy industry: A techno-economic study for the Åland Islands. Appl. Energy *279*, 115883. https://doi.org/10.1016/j.apenergy.2020.115883.

53. Maier, M., Owen, R.E., Pham, M.T.M., Dodwell, J., Majasan, J., Robinson, J.B., Hinds, G., Shearing, P.R., and Brett, D.J.L. (2021). Acoustic time-of-flight imaging of polymer electrolyte membrane water electrolysers to probe internal structure and flow characteristics. Int. J. Hydrogen Energy *46*, 11523–11535. https://doi.org/10.1016/j.ijhydene.2021.01.077.

54. Ahmad, S., Jia, H., Chen, Z., Li, Q., and Xu, C. (2020). Water-energy nexus and energy efficiency: A systematic analysis of urban water systems. Renew. Sustain. Energy Rev. *134*, 110381. https://doi.org/10.1016/j.rser.2020.110381.

55. Brandão, L.M.d.S., Barbosa, M.d.S., De Jesus, R.A., Bharad, P.A., Lima, Á.S., Soares, C.M.F., Yerga, R.M.N., Bilal, M., Ferreira, L.F.R., Iqbal, H. M., et al. (2022). Enhanced hydrogen fuel production using synergistic combination of solar radiation and TiO_2 photocatalyst coupled with Burkholderia cepacia lipase. Int. J. Hydrogen Energy *47*, 14483–14492. https://doi.org/10.1016/j.ijhydene.2022.02.220.

56. Duan, Y., Liu, H., Zhang, W., Khotseng, L., Xu, Q., and Su, H. (2023). Materials, components, assembly and performance of flexible polymer electrolyte membrane fuel cell: A review. J. Power Sources *555*, 232369. https://doi.org/10.1016/j.jpowsour.2022.232369.

57. Mench, M.M. (2008). Fuel Cell Engines (John Wiley & Sons). https://doi.org/10.1002/9780470209769.

58. Gubler, L., Rajesh, B., Wokaun, A., Scherer, G.G., Steiger, B., Reiner, A., Kramer, D., Hajbolouri, F., Gürsel, S.A., Beck, N., and Thampi, K.R. (2004). Materials for Polymer Electrolyte Fuel Cells. Chimia *58*, 826. https://doi.org/10.2533/000942904777677128.

59. Wang, Y., Ruiz Diaz, D.F., Chen, K.S., Wang, Z., and Adroher, X.C. (2020). Materials, technological status, and fundamentals of PEM fuel cells – A review. Mater. Today *32*, 178–203. https://doi.org/10.1016/j.mattod.2019.06.005.

60. Wang, X.R., Ma, Y., Gao, J., Li, T., Jiang, G.Z., and Sun, Z.Y. (2021). Review on water management methods for proton exchange membrane fuel cells. Int. J. Hydrogen Energy *46*, 12206–12229. https://doi.org/10.1016/j.ijhydene.2020.06.211.

61. Wang, X., Ni, Z., Yang, Z., Wang, Y., and Han, K. (2024). Optimization of PEMFC operating parameters considering water management by an integrated method of sensitivity analysis, multi-objective optimization and evaluation. Energy Convers. Manag. *321*, 119057. https://doi.org/10.1016/j.enconman.2024.119057.

62. Zhang, J., Zhang, H., Wu, J., and Zhang, J. (2013). Chapter 6 - Hydrogen Crossover. In PEM Fuel Cell Testing and Diagnosis (Elsevier), pp. 171–185. https://doi.org/10.1016/B978-0-444-53688-4.00006-1.

63. Xie, Z., Wang, J., Zhao, G., Zhang, Q., Fan, H., Zeng, A., and Ding, W. (2024). A review on durability of key components of PEM fuel cells. Catal. Sci. Technol. *14*, 4420–4431. https://doi.org/10.1039/D4CY00351A.

64. Maiyalagan, T., and Pasupathi, S. (2010). Components for PEM Fuel Cells: An Overview. Mater. Sci. Forum *657*, 143–189. https://doi.org/10.4028/www.scientific.net/MSF.657.143.

65. Ahmad, S., Nawaz, T., Ali, A., Orhan, M.F., Samreen, A., and Kannan, A. M. (2022). An overview of proton exchange membranes for fuel cells: Materials and manufacturing. Int. J. Hydrogen Energy *47*, 19086–19131. https://doi.org/10.1016/j.ijhydene.2022.04.099.

66. Wong, C.Y., Wong, W.Y., Ramya, K., Khalid, M., Loh, K.S., Daud, W.R. W., Lim, K.L., Walvekar, R., and Kadhum, A.A.H. (2019). Additives in proton exchange membranes for low- and high-temperature fuel cell applications: A review. Int. J. Hydrogen Energy *44*, 6116–6135. https://doi.org/10.1016/j.ijhydene.2019.01.084.

67. Mbarek, S., El Kissi, N., Baccouch, Z., and Iojoiu, C. (2019). Extrusion of Nafion and Aquivion membranes: environmentally friendly procedure and good conductivities. Polym. Bull. *76*, 1151–1166. https://doi.org/10.1007/s00289-018-2427-6.

68. Nasef, M.M. (2022). Radiation Grafted Ion Conducting Membranes for Electrochemical Energy Systems: Status of Developmental and Upscaled Membranes. Journal of Applied Membrane Science & Technology *26*, 51–76. https://doi.org/10.11113/amst.v26n1.233.

69. Souzy, R., and Ameduri, B. (2005). Functional fluoropolymers for fuel cell membranes. Prog. Polym. Sci. *30*, 644–687. https://doi.org/10.1016/j.progpolymsci.2005.03.004.

70. Hickner, M.A., Ghassemi, H., Kim, Y.S., Einsla, B.R., and McGrath, J.E. (2004). Alternative Polymer Systems for Proton Exchange Membranes (PEMs). Chem. Rev. *104*, 4587–4611. https://doi.org/10.1021/cr020711a.

71. Shang, Z., Wycisk, R., and Pintauro, P. (2021). Electrospun Composite Proton-Exchange and Anion-Exchange Membranes for Fuel Cells. Energies *14*, 6709. https://doi.org/10.3390/en14206709.

72. Prykhodko, Y., Fatyeyeva, K., Hespel, L., and Marais, S. (2021). Progress in hybrid composite Nafion®-based membranes for proton exchange fuel cell application. Chem. Eng. J. *409*, 127329. https://doi.org/10.1016/j.cej.2020.127329.

73. Primachenko, O.N., Marinenko, E.A., Odinokov, A.S., Kononova, S.V., Kulvelis, Y.V., and Lebedev, V.T. (2021). State of the art and prospects in the development of proton-conducting perfluorinated membranes with short side chains: A review. Polym. Adv. Technol. *32*, 1386–1408. https://doi.org/10.1002/pat.5191.

74. Zhu, L.Y., Li, Y.C., Liu, J., He, J., Wang, L.Y., and Lei, J.D. (2022). Recent developments in high-performance Nafion membranes for hydrogen fuel cells applications. Pet. Sci. *19*, 1371–1381. https://doi.org/10.1016/j.petsci.2021.11.004.

75. Barique, M.A., Tsuchida, E., Ohira, A., and Tashiro, K. (2018). Effect of Elevated Temperatures on the States of Water and Their Correlation with the Proton Conductivity of Nafion. ACS Omega *3*, 349–360. https://doi.org/10.1021/acsomega.7b01765.

76. Pan, M., Pan, C., Li, C., and Zhao, J. (2021). A review of membranes in proton exchange membrane fuel cells: Transport phenomena, performance and durability. Renew. Sustain. Energy Rev. *141*, 110771. https://doi.org/10.1016/j.rser.2021.110771.

77. Lee, K.H., Chu, J.Y., Kim, A.R., and Yoo, D.J. (2018). Facile Fabrication and Characterization of Improved Proton Conducting Sulfonated Poly (Arylene Biphenylether Sulfone) Blocks Containing Fluorinated Hydrophobic Units for Proton Exchange Membrane Fuel Cell Applications. Polymers *10*, 1367–1381. https://doi.org/10.3390/polym10121367.

78. Chemours (2016). Nafion™ N115, N117, N1110. https://fuelcellearth.com/pdf/nafion-N115-N117-N1110.pdf.

79. Gore (2023). GORE AES Fuel Cell Portfolio - Datasheet. https://www.gore.com/system/files/2023-08/GORE-AES-Fuel-Cell-Portfolio-Datasheet-EN_0.pdf.

80. Solvay (2020). Aquivion® E87-05S Technical Data Sheet. https://www.fuelcellstore.com/spec-sheets/solvay-aquivion-e87-05s-membrane.pdf.

81. Smitha, B., Sridhar, S., and Khan, A.A. (2005). Solid polymer electrolyte membranes for fuel cell applications—a review. J. Membr. Sci. *259*, 10–26. https://doi.org/10.1016/j.memsci.2005.01.035.

82. Li, Y., Roy, A., Badami, A.S., Hill, M., Yang, J., Dunn, S., and McGrath, J. E. (2007). Synthesis and characterization of partially fluorinated hydrophobic–hydrophilic multiblock copolymers containing sulfonate

groups for proton exchange membrane. J. Power Sources *172*, 30–38. https://doi.org/10.1016/j.jpowsour.2007.04.046.

83. Gürsel, S.A., Yang, Z., Choudhury, B., Roelofs, M.G., and Scherer, G.G. (2006). Radiation-Grafted Membranes Using a Trifluorostyrene Derivative. J. Electrochem. Soc. *153*, A1964. https://doi.org/10.1149/1.2335626.

84. Golubenko, D.V., Korchagin, O.,V., Voropaeva, D.Y., Bogdanovskaya, V. A., and Yaroslavtsev, A.B. (2022). Membranes Based on Polyvinylidene Fluoride and Radiation-Grafted Sulfonated Polystyrene and Their Performance in Proton-Exchange Membrane Fuel Cells. Polymers *14*, 3833–3848. https://doi.org/10.3390/polym14183833.

85. Sadeghi, S., Işıkel Şanlı, L., Güler, E., and Alkan Gürsel, S. (2018). Enhancing proton conductivity via sub-micron structures in proton conducting membranes originating from sulfonated PVDF powder by radiation-induced grafting. Solid State Ionics *314*, 66–73. https://doi.org/10.1016/j.ssi.2017.11.017.

86. Rajabalizadeh Mojarrad, N., Sadeghi, S., Yarar Kaplan, B., Güler, E., and Alkan Gürsel, S. (2019). Metal-Salt Enhanced Grafting of Vinylpyridine and Vinylimidazole Monomer Combinations in Radiation Grafted Membranes for High-Temperature PEM Fuel Cells. ACS Appl. Energy Mater. *3*, 532–540. https://doi.org/10.1021/acsaem.9b01777.

87. Tap, T.D., Hasegawa, S., Yoshimura, K., Yen, V.T.K., Tue, N.H.M., Tuan, N.M., Hieu, D.T.T., Tuan, H.A., Hao, L.H., Nguyen, L.L., et al. (2024). Phase separation and water channels in graft-type polymer electrolyte membranes for hydrogen fuel cell. Int. J. Hydrogen Energy *59*, 777–790. https://doi.org/10.1016/j.ijhydene.2024.02.082.

88. Gubler, L., Prost, N., Gürsel, S.A., and Scherer, G.G. (2005). Proton exchange membranes prepared by radiation grafting of styrene/divinylbenzene onto poly(ethylene-alt-tetrafluoroethylene) for low temperature fuel cells. Solid State Ionics *176*, 2849–2860. https://doi.org/10.1016/j.ssi.2005.09.045.

89. Ben youcef, H., Gürsel, S.A., Wokaun, A., and Scherer, G.G. (2008). The influence of crosslinker on the properties of radiation-grafted films and membranes based on ETFE. J. Membr. Sci. *311*, 208–215. https://doi.org/10.1016/j.memsci.2007.12.015.

90. Li, X., Zhang, H., Lin, C., He, Z., and Ramani, V. (2022). Quantitative analysis of proton exchange membrane prepared by radiation-induced grafting on ultra-thin FEP film. Int. J. Hydrogen Energy *47*, 1874–1887. https://doi.org/10.1016/j.ijhydene.2021.10.234.

91. Mohammedi, M., and Mehdipour-Ataei, S. (2020). Durable sulfonated partially fluorinated polysulfones as membrane for PEM fuel cell. Renew. Energy *158*, 421–430. https://doi.org/10.1016/j.renene.2020.05.124.

92. Nguyen, H., Klose, C., Metzler, L., Vierrath, S., and Breitwieser, M. (2022). Fully Hydrocarbon Membrane Electrode Assemblies for Proton Exchange Membrane Fuel Cells and Electrolyzers: An Engineering Perspective. Adv. Energy Mater. *12*, 2103559. https://doi.org/10.1002/aenm.202103559.

93. Segale, M., Seadira, T., Sigwadi, R., Mokrani, T., and Summers, G. (2024). A new frontier towards the development of efficient SPEEK polymer membranes for PEM fuel cell applications: a review. Mater. Adv. *5*, 7979–8006. https://doi.org/10.1039/D4MA00628C.

94. Chae, J.E., Yoo, S.J., Kim, J.Y., Jang, J.H., Lee, S.Y., Song, K.H., and Kim, H.J. (2020). Hydrocarbon-based electrode ionomer for proton exchange membrane fuel cells. Int. J. Hydrogen Energy *45*, 32856–32864. https://doi.org/10.1016/j.ijhydene.2020.03.003.

95. Adamski, M., Peressin, N., and Holdcroft, S. (2021). On the evolution of sulfonated polyphenylenes as proton exchange membranes for fuel cells. Mater. Adv. *2*, 4966–5005. https://doi.org/10.1039/D1MA00511A.

96. Miyake, J., Watanabe, T., Shintani, H., Sugawara, Y., Uchida, M., and Miyatake, K. (2021). Reinforced Polyphenylene Ionomer Membranes Exhibiting High Fuel Cell Performance and Mechanical Durability. ACS Mater. Au *1*, 81–88. https://doi.org/10.1021/acsmaterialsau.1c00002.

97. Wu, J., Liao, C., Li, T., Zhou, J., Zhang, L., Wang, J.Q., Li, G., and Li, X. (2023). Metal-coordinated polybenzimidazole membranes with preferential K^+ transport. Nat. Commun. *14*, 1149. https://doi.org/10.1038/s41467-023-36711-w.

98. Maiti, T.K., Singh, J., Majhi, J., Ahuja, A., Maiti, S., Dixit, P., Bhushan, S., Bandyopadhyay, A., and Chattopadhyay, S. (2022). Advances in polybenzimidazole based membranes for fuel cell applications that overcome Nafion membranes constraints. Polymer *255*, 125151. https://doi.org/10.1016/j.polymer.2022.125151.

99. Sithambaranathan, P., Nasef, M.M., Ahmad, A., Abbasi, A., and Ting, T. M. (2023). Composite Proton-Conducting Membrane with Enhanced Phosphoric Acid Doping of Basic Films Radiochemically Grafted with Binary Vinyl Heterocyclic Monomer Mixtures. Membranes *13*, 105. https://doi.org/10.3390/membranes13010105.

100. Liu, S., Yu, J., Hao, Y., Gao, F., Zhou, M., and Zhao, L. (2024). Impact of SiO_2 Modification on the Performance of Nafion Composite Membrane. Int. J. Polym. Sci. *2024*, 6309923. https://doi.org/10.1155/2024/6309923.

101. Niu, J., Zhang, S., Li, Y., Li, X., Zhang, J., Lu, S., and He, Q. (2023). Effects of microstructure on the retention of proton conductivity of Nafion/SiO2 composite membranes at elevated temperatures:An in situ SAXS study. Polymer *273*, 125869. https://doi.org/10.1016/j.polymer.2023.125869.

102. Thmaini, N., Charradi, K., Ahmed, Z., Aranda, P., and Chtourou, R. (2022). Nafion/SiO_2@TiO_2-palygorskite membranes with improved proton conductivity. J. Appl. Polym. Sci. *139*, e52208. https://doi.org/10.1002/app.52208.

103. Parnian, M.J., Rowshanzamir, S., and Alipour Moghaddam, J. (2018). Investigation of physicochemical and electrochemical properties of recast Nafion nanocomposite membranes using different loading of zirconia nanoparticles for proton exchange membrane fuel cell applications. Mater. Sci. Energy Technol. *1*, 146–154. https://doi.org/10.1016/j.mset.2018.06.008.

104. Porozhnyy, M.V., Shkirskaya, S.A., Butylskii, D.Y., Dotsenko, V.V., Safronova, E.Y., Yaroslavtsev, A.B., Deabate, S., Huguet, P., and Nikonenko, V.V. (2021). Physicochemical and electrochemical characterization of Nafion-type membranes with embedded silica nanoparticles: Effect of functionalization. Electrochim. Acta *370*, 137689. https://doi.org/10.1016/j.electacta.2020.137689.

105. Soad, R., Cavaliere, S., Jones, D.J., and Rozière, J. (2016). Electrospun nanofibre composite polymer electrolyte fuel cell and electrolysis membranes. Nano Energy *26*, 729–745. https://doi.org/10.1016/j.nanoen.2016.06.027.

106. Li, J., Xu, G., Luo, X., Xiong, J., Liu, Z., and Cai, W. (2018). Effect of nanosize of functionalized silica on overall performance of swelling-filling modified Nafion membrane for direct methanol fuel cell application. Appl. Energy *213*, 408–414. https://doi.org/10.1016/j.apenergy.2018.01.052.

107. Jalali, S., Seyedghayem, M.M., Hooriabad Saboor, F., Venkatramani, A., and Asgari, M. (2023). Proton Exchange Membrane Fuel Cells: Focused on Organic-Inorganic Nanocomposite Membranes. Period. Polytech. - Chem. Eng. *67*, 472–489. https://doi.org/10.3311/PPch.21632.

108. Vinothkannan, M., Kim, A.R., and Yoo, D.J. (2021). Potential carbon nanomaterials as additives for state-of-the-art Nafion electrolyte in proton exchange membrane fuel cells: a concise review. RSC Adv. *11*, 18351–18370. https://doi.org/10.1039/d1ra00685a.

109. Gubler, L., Gürsel, S.A., and Scherer, G.G. (2005). Radiation Grafted Membranes for Polymer Electrolyte Fuel Cells. Fuel Cells *5*, 317–335. https://doi.org/10.1002/fuce.200400078.

110. Gürsel, S.A., Gubler, L., Gupta, B., and Scherer, G.G. (2008). Radiation Grafted Membranes. In Fuel Cells I, G.G. Scherer, ed. (Springer Berlin Heidelberg), pp. 157–217.

111. Nasef, M.M., Gürsel, S.A., Karabelli, D., and Güven, O. (2016). Radiation-grafted materials for energy conversion and energy storage applications.

Prog. Polym. Sci. *63*, 1–41. https://doi.org/10.1016/j.progpolymsci.2016.05.002.

112. Yarar Kaplan, B., KIRLIOĞLU, A.C., JAMİL, E., Yürüm, A., RAJABALİZADEH, N., HAGHMORADİ, N., İSKANDARANİ, B., SALİMKHANİ, H., and Alkan Gürsel, S. (2020). Radiation-Grafted Polymer Electrolyte Membranes for Fuel Cells. Hacettepe Journal of Biology and Chemistry *48*, 483–506. https://doi.org/10.15671/hjbc.813239.

113. Ke, X., Drache, M., Gohs, U., Kunz, U., and Beuermann, S. (2018). Preparation of Polymer Electrolyte Membranes via Radiation-Induced Graft Copolymerization on Poly(ethylene-alt-tetrafluoroethylene) (ETFE) Using the Crosslinker N,N′-Methylenebis(acrylamide). Membranes *8*, 102. https://doi.org/10.3390/membranes8040102.

114. Nasef, M.M. (2014). Radiation-Grafted Membranes for Polymer Electrolyte Fuel Cells: Current Trends and Future Directions. Chem. Rev. *114*, 12278–12329. https://doi.org/10.1021/cr4005499.

115. Ben youcef, H., Gubler, L., Gürsel, S.A., Henkensmeier, D., Wokaun, A., and Scherer, G.G. (2009). Novel ETFE based radiation grafted poly(styrene sulfonic acid-co-methacrylonitrile) proton conducting membranes with increased stability. Electrochem. Commun. *11*, 941–944. https://doi.org/10.1016/j.elecom.2009.02.047.

116. Sithambaranathan, P., Nasef, M.M., Ahmad, A., and Ripin, A. (2017). Crosslinked composite membrane by radiation grafting of 4-vinylpyridine/triallyl-cyanurate mixtures onto poly(ethylene-co-tetrafluoroethylene) and phosphoric acid doping. Int. J. Hydrogen Energy *42*, 9333–9341. https://doi.org/10.1016/j.ijhydene.2016.03.140.

117. Hasegawa, S., Hiroki, A., Ohta, Y., Iimura, N., Fukaya, A., and Maekawa, Y. (2020). Thermally stable graft-type polymer electrolyte membranes consisting based on poly (ether ether ketone) and crosslinked graft-polymers for fuel cell applications. Radiat. Phys. Chem. *171*, 108647. https://doi.org/10.1016/j.radphyschem.2019.108647.

118. Nemeth, T., Han, Z., and Gubler, L. (2024). High-Performance Fluorine-Lean Thin Aromatic Hydrocarbon Membranes Based on Polyvinylidene Fluoride for Hydrogen Fuel Cells. Membranes *14*, 263. https://doi.org/10.3390/membranes14120263.

119. Şanlı, L.I., Taş, S., Yürüm, Y., and Gürsel, S.A. (2014). Water Free Operated Phosphoric Acid Doped Radiation-Grafted Proton Conducting Membranes for High Temperature Polymer Electrolyte Membrane Fuel Cells. Fuel Cells *14*, 914–925. https://doi.org/10.1002/fuce.201300110.

120. Farquet, P., Padeste, C., Börner, M., Youcef, H.B., Gürsel, S.A., Scherer, G.G., Solak, H.H., Saile, V., and Wokaun, A. (2008). Microstructured proton-conducting membranes by synchrotron-radiation-induced grafting. J. Membr. Sci. *325*, 658–664. https://doi.org/10.1016/j.memsci.2008.08.040.

121. Gürsel, S.A., Youcef, H.B., Wokaun, A., and Scherer, G.G. (2007). Influence of reaction parameters on grafting of styrene into poly(ethylene-alt-tetrafluoroethylene) films. Nucl. Instrum. Methods Phys. Res. Sect. B Beam Interact. Mater. Atoms *265*, 198–203. https://doi.org/10.1016/j.nimb.2007.08.050.

122. Gubler, L., Youcef, H.B., Gürsel, S.A., Wokaun, A., and Scherer, G.G. (2008). Cross-Linker Effect in ETFE-Based Radiation-Grafted Proton-Conducting Membranes: I. Properties and Fuel Cell Performance Characteristics. J. Electrochem. Soc. *155*, B921. https://doi.org/10.1149/1.2951919.

123. Gubler, L., Youcef, H.B., Yamaki, T., Sawada, S., Gürsel, S.A., Wokaun, A., and Scherer, G.G. (2009). Cross-Linker Effect in ETFE-Based Radiation-Grafted Proton-Conducting Membranes: II. Extended Fuel Cell Operation and Degradation Analysis. J. Electrochem. Soc. *156*, B532. https://doi.org/10.1149/1.3082109.

124. Ben youcef, H., Alkan Gürsel, S., Buisson, A., Gubler, L., Wokaun, A., and Scherer, G.G. (2010). Influence of Radiation-Induced Grafting Process on Mechanical Properties of ETFE-Based Membranes for Fuel Cells. Fuel Cells *10*, 401–410. https://doi.org/10.1002/fuce.200900200.

125. Sproll, V., Schmidt, T.J., and Gubler, L. (2015). Grafting design: a strategy to increase the performance of radiation-grafted membranes. Polym. Int. *65*, 174–180. https://doi.org/10.1002/pi.5041.

126. Şanlı, L.I., and Gürsel, S.A. (2010). Synthesis and characterization of novel graft copolymers by radiation-induced grafting. J. Appl. Polym. Sci. *120*, 2313–2323. https://doi.org/10.1002/app.33419.

127. Brack, H.P., Padeste, C., Slaski, M., Gürsel, S.A., and Solak, H.H. (2004). Preparation of Micro- and Nanopatterns of Polymer Chains Grafted onto Flexible Polymer Substrates. J. Am. Chem. Soc. *126*, 1004–1005. https://doi.org/10.1021/ja0379870.

128. Keirouz, A., Wang, Z., Reddy, V.S., Nagy, Z.K., Vass, P., Buzgo, M., Ramakrishna, S., and Radacsi, N. (2023). The History of Electrospinning: Past, Present, and Future Developments. Adv. Mater. Technol. *8*, 2201723. https://doi.org/10.1002/admt.202201723.

129. Ji, D., Lin, Y., Guo, X., Ramasubramanian, B., Wang, R., Radacsi, N., Jose, R., Qin, X., and Ramakrishna, S. (2024). Electrospinning of nanofibres. Nat. Rev. Methods Primers *4*, 1. https://doi.org/10.1038/s43586-023-00278-z.

130. Waldrop, K., Wycisk, R., and Pintauro, P.N. (2020). Application of electrospinning for the fabrication of proton-exchange membrane fuel cell electrodes. Curr. Opin. Electrochem. *21*, 257–264. https://doi.org/10.1016/j.coelec.2020.03.007.

131. Sarkar, A., Bidu, J.M., Panda, J., Kwon, Y.J., Bak, S., Cho, K.Y., Byun, S., and Cheong, J.Y. (2025). Applications of electrospinning for fuel cell and electrolysis cell applications in hydrogen technologies. Energy Rev. *4*, 100119. https://doi.org/10.1016/j.enrev.2024.100119.

132. Sigwadi, R., Mokrani, T., and Msomi, P.F. (2021). Nafion reinforced with polyacrylonitrile nanofibers/zirconium-graphene oxide composite membrane for direct methanol fuel cell application. J. Polym. Res. *29*, 18. https://doi.org/10.1007/s10965-021-02854-x.

133. Al-Dhabebi, A.M., Ling, J.K., Krishnan, S.G., Yousefzadeh, M., Elumalai, N.K., Saheed, M.S.M., Ramakrishna, S., and Jose, R. (2022). Electrospinning research and products: The road and the way forward. Appl. Phys. Rev. *9*, 011319. https://doi.org/10.1063/5.0077959.

134. Hwang, C.K., Lee, K.A., Lee, J., Kim, Y., Ahn, H., Hwang, W., Ju, B.K., Kim, J.Y., Yeo, S.Y., Choi, J., et al. (2022). Perpendicularly stacked array of PTFE nanofibers as a reinforcement for highly durable composite membrane in proton exchange membrane fuel cells. Nano Energy *101*, 107581. https://doi.org/10.1016/j.nanoen.2022.107581.

135. Ramakrishna, S., Fujihara, K., Teo, W.E., Yong, T., Ma, Z., and Ramaseshan, R. (2006). Electrospun nanofibers: solving global issues. Mater. Today *9*, 40–50. https://doi.org/10.1016/S1369-7021(06)71389-X.

136. Kırlıoğlu, A.C., Rajabalizadeh Mojarrad, N., Alkan Gürsel, S., Güler, E., and Yarar Kaplan, B. (2024). New generation radiation-grafted PVDF-g-VBC based dual-fiber electrospun anion exchange membranes. Int. J. Hydrogen Energy *51*, 1390–1401. https://doi.org/10.1016/j.ijhydene.2023.05.345.

137. Ren, G., Qu, Z., Wang, X., Zhang, G., and Wang, Y. (2024). Electrospun fabrication and experimental characterization of highly porous microporous layers for PEM fuel cells. Int. J. Hydrogen Energy *55*, 455–463. https://doi.org/10.1016/j.ijhydene.2023.11.226.

138. Powers, D., Wycisk, R., and Pintauro, P.N. (2019). Electrospun tri-layer membranes for H2/Air fuel cells. J. Membr. Sci. *573*, 107–116. https://doi.org/10.1016/j.memsci.2018.11.046.

139. Li, Y., Zhu, J., Cheng, H., Li, G., Cho, H., Jiang, M., Gao, Q., and Zhang, X. (2021). Developments of Advanced Electrospinning Techniques: A Critical Review. Adv. Mater. Technol. *6*, 2100410. https://doi.org/10.1002/admt.202100410.

140. Karanfil, G. (2022). Preparation and characterization of electrospun sulfonated polysulfone/ZrO2 composite nanofiber membranes. Int. J. Mater. Res. *113*, 243–252. https://doi.org/10.1515/ijmr-2021-8318.

141. Zhang, C.L., and Yu, S.H. (2014). Nanoparticles meet electrospinning: recent advances and future prospects. Chem. Soc. Rev. *43*, 4423–4448. https://doi.org/10.1039/C3CS60426H.

142. Mohammedi, M., and Mehdipour-Ataei, S. (2022). Preparation and properties of composite membranes of fully fluorinated nanofibrous electrospun mat impregnated with highly sulfonated polysulfone: Effect of thermal treatment on the mat and the membranes thereof. Int. J. Hydrogen Energy *47*, 17313–17328. https://doi.org/10.1016/j.ijhydene.2022.03.184.

143. Hossain, M., Shang, Z., Wycisk, R., and Pintauro, P.N. (2020). Pore-Filled PEMs from Poly(Phenylene Sulfonic Acid)s and Electrospun Poly (Phenylene Sulfone) Fiber Mats. ECS Trans. *98*, 367–373. https://doi.org/10.1149/09809.0367ecst.

144. Shang, Z., Hossain, M.M., Wycisk, R., and Pintauro, P.N. (2022). Poly (phenylene sulfonic acid)-expanded polytetrafluoroethylene composite membrane for low relative humidity operation in hydrogen fuel cells. J. Power Sources *535*, 231375. https://doi.org/10.1016/j.jpowsour.2022.231375.

145. Soad, R., Giancola, S., Donnadio, A., Zatoń, M., Donzel, N., Rozière, J., Jones, D.J., and Cavaliere, S. (2021). Active electrospun nanofibers as an effective reinforcement for highly conducting and durable proton exchange membranes. J. Membr. Sci. *622*, 119037. https://doi.org/10.1016/j.memsci.2020.119037.

146. Rajabalizadeh Mojarrad, N., Iskandarani, B., Taşdemir, A., Yürüm, A., Alkan Gürsel, S., and Yarar Kaplan, B. (2021). Nanofiber based hybrid sulfonated silica/P(VDF-TrFE) membranes for PEM fuel cells. Int. J. Hydrogen Energy *46*, 13583–13593. https://doi.org/10.1016/j.ijhydene.2020.08.005.

147. Xiong, C., Ling, Z., Wang, B., Yu, Y., Liu, Q., Fu, X., Wu, C., Zhang, R., Hu, S., Bao, X., and Yang, J. (2024). Electrospinning-assisted construction of rapid proton conduction channels in halloysite nanotube-encapsulated ionic liquid-embedded sulfonated poly(ether ether ketone) proton exchange membranes. Fuel *362*, 130814. https://doi.org/10.1016/j.fuel.2023.130814.

148. Santos, L.D., Powers, D., Wycisk, R., and Pintauro, P.N. (2020). Electrospun Hybrid Perfluorosulfonic Acid/Sulfonated Silica Composite Membranes. Membranes *10*, 250. https://doi.org/10.3390/membranes10100250.

149. Rajabalizadeh Mojarrad, N., Kırlıoğlu, A.C., and Yarar Kaplan, B. (2023). P (VDF-TrFE) reinforced composite membranes fabricated via sol-gel and dual-fiber electrospinning for reduced relative humidity operation of PEM fuel cells. Solid State Ionics *392*, 116152. https://doi.org/10.1016/j.ssi.2023.116152.

150. G.G. Scherer, ed. (2010). Fuel Cells I (Springer Berlin), p. 215. https://doi.org/10.1007/978-3-540-69757-2.

151. Lee, C.H., Park, H.B., Lee, Y.M., and Lee, R.D. (2005). Importance of Proton Conductivity Measurement in Polymer Electrolyte Membrane for Fuel Cell Application. Ind. Eng. Chem. Res. *44*, 7617–7626. https://doi.org/10.1021/ie0501172.

152. Elerian, A.F., Mohamed, A.A., Elnaggar, E.M., and Abu-Saied, M.A. (2024). Development of novel proton exchange membranes based on cross-linked polyvinyl alcohol (PVA)/5-sulfosalicylic acid (SSCA) for fuel cell applications. Discov. Appl. Sci. *6*, 341. https://doi.org/10.1007/s42452-024-05940-z.

153. Ogungbemi, E., Ijaodola, O., Khatib, F.N., Wilberforce, T., El Hassan, Z., Thompson, J., Ramadan, M., and Olabi, A.G. (2019). Fuel cell membranes – Pros and cons. Energy *172*, 155–172. https://doi.org/10.1016/j.energy.2019.01.034.

154. Brack, H.P., Ruegg, D., Bührer, H., Slaski, M., Gürsel, S.A., and Scherer, G.G. (2004). Differential scanning calorimetry and thermogravimetric analysis investigation of the thermal properties and degradation of some radiation-grafted films and membranes. J. Polym. Sci. B Polym. Phys. *42*, 2612–2624. https://doi.org/10.1002/polb.20137.

155. Brack, H.P., Slaski, M., Gubler, L., Scherer, G.G., Gürsel, S.A., and Wokaun, A. (2004). Characterisation of Fuel Cell Membranes as a Function of Drying by Means of Contact Angle Measurements. Fuel Cells *4*, 141–146. https://doi.org/10.1002/fuce.200400018.

156. Camacho, M.d.l.N., Jurburg, D., and Tanco, M. (2022). Hydrogen fuel cell heavy-duty trucks: Review of main research topics. Int. J. Hydrogen Energy *47*, 29505–29525. https://doi.org/10.1016/j.ijhydene.2022.06.271.

157. Shao, M. (2011). Palladium-based electrocatalysts for hydrogen oxidation and oxygen reduction reactions. J. Power Sources *196*, 2433–2444. https://doi.org/10.1016/j.jpowsour.2010.10.093.

158. Wang, Y., Wang, D., and Li, Y. (2021). A fundamental comprehension and recent progress in advanced Pt-based ORR nanocatalysts. SmartMat *2*, 56–75. https://doi.org/10.1002/smm2.1023.

159. Keith, J.A., and Jacob, T. (2010). Theoretical Studies of Potential-Dependent and Competing Mechanisms of the Electrocatalytic Oxygen Reduction Reaction on Pt(111). Angew. Chem. Int. Ed. *49*, 9521–9525. https://doi.org/10.1002/anie.201004794.

160. Alipour Moghadam Esfahani, R., and Easton, E.B. (2020). Exceptionally durable Pt/TOMS catalysts for fuel cells. Appl. Catal. B Environ. *268*, 118743. https://doi.org/10.1016/j.apcatb.2020.118743.

161. Du, S., Guan, S., Mehrazi, S., Zhou, F., Pan, M., Zhang, R., Chuang, P.Y. A., and Sui, P.C. (2021). Effect of Dispersion Method and Catalyst on the Crack Morphology and Performance of Catalyst Layer of PEMFC. J. Electrochem. Soc. *168*, 114506. https://doi.org/10.1149/1945-7111/ac3598.

162. Chen, M., Li, C., Zhang, B., Zeng, Y., Karakalos, S., Hwang, S., Xie, J., and Wu, G. (2022). High-Platinum-Content Catalysts on Atomically Dispersed and Nitrogen Coordinated Single Manganese Site Carbons for Heavy-Duty Fuel Cells. J. Electrochem. Soc. *169*, 034510. https://doi.org/10.1149/1945-7111/ac58c7.

163. ENY-Mobility (2020). ENYrgy Technical Data Sheet. https://eny-mobility.de/assets/files/tds-enyrgy.pdf.

164. Gasteiger, H.A., Kocha, S.S., Sompalli, B., and Wagner, F.T. (2005). Activity benchmarks and requirements for Pt, Pt-alloy, and non-Pt oxygen reduction catalysts for PEMFCs. Appl. Catal. B Environ. *56*, 9–35. https://doi.org/10.1016/j.apcatb.2004.06.021.

165. Garsany, Y., Singer, I.L., and Swider-Lyons, K.E. (2011). Impact of film drying procedures on RDE characterization of Pt/VC electrocatalysts. J. Electroanal. Chem. *662*, 396–406. https://doi.org/10.1016/j.jelechem.2011.09.016.

166. Inaba, M., Zana, A., Quinson, J., Bizzotto, F., Dosche, C., Dworzak, A., Özaslan, M., Simonsen, S.B., Kuhn, L.T., and Arenz, M. (2021). The Oxygen Reduction Reaction on Pt: Why Particle Size and Interparticle Distance Matter. ACS Catal. *11*, 7144–7153. https://doi.org/10.1021/acscatal.1c00652.

167. Kocha, S.S., Shinozaki, K., Zack, J.W., Myers, D.J., Kariuki, N.N., Nowicki, T., Stamenkovic, V., Kang, Y., Li, D., and Papageorgopoulos, D. (2017). Best Practices and Testing Protocols for Benchmarking ORR Activities of Fuel Cell Electrocatalysts Using Rotating Disk Electrode. Electrocatalysis *8*, 366–374. https://doi.org/10.1007/s12678-017-0378-6.

168. Wei, C., Rao, R.R., Peng, J., Huang, B., Stephens, I.E.L., Risch, M., Xu, Z. J., and Shao-Horn, Y. (2019). Recommended Practices and Benchmark Activity for Hydrogen and Oxygen Electrocatalysis in Water Splitting and Fuel Cells. Adv. Mater. *31*, 1806296. https://doi.org/10.1002/adma.201806296.

169. Makharia, R., Kocha, S., Yu, P., Sweikart, M.A., Gu, W., Wagner, F., and Gasteiger, H.A. (2006). Durable PEM Fuel Cell Electrode Materials: Requirements and Benchmarking Methodologies. ECS Trans. *1*, 3–18. https://doi.org/10.1149/1.2214540.

170. Ahn, C.Y., Park, J.E., Kim, S., Kim, O.H., Hwang, W., Her, M., Kang, S.Y., Park, S., Kwon, O.J., Park, H.S., et al. (2021). Differences in the Electrochemical Performance of Pt-Based Catalysts Used for Polymer

Electrolyte Membrane Fuel Cells in Liquid Half- and Full-Cells. Chem. Rev. *121*, 15075–15140. https://doi.org/10.1021/acs.chemrev.0c01337.

171. Moriau, L.J., Hrnjić, A., Pavlišič, A., Kamšek, A.R., Petek, U., Ruiz-Zepeda, F., Šala, M., Pavko, L., Šelih, V.S., Bele, M., et al. (2021). Resolving the nanoparticles' structure-property relationships at the atomic level: a study of Pt-based electrocatalysts. iScience *24*, 102102. https://doi.org/10.1016/j.isci.2021.102102.

172. Qiao, Z., Hwang, S., Li, X., Wang, C., Samarakoon, W., Karakalos, S., Li, D., Chen, M., He, Y., Wang, M., et al. (2019). 3D porous graphitic nanocarbon for enhancing the performance and durability of Pt catalysts: a balance between graphitization and hierarchical porosity. Energy Environ. Sci. *12*, 2830–2841. https://doi.org/10.1039/C9EE01899A.

173. Yoshii, K., Yamaji, K., Tsuda, T., Matsumoto, H., Sato, T., Izumi, R., Torimoto, T., and Kuwabata, S. (2016). Highly durable Pt nanoparticle-supported carbon catalysts for the oxygen reduction reaction tailored by using an ionic liquid thin layer. J. Mater. Chem. A *4*, 12152–12157. https://doi.org/10.1039/C6TA04859E.

174. Kong, F., Liu, S., Li, J., Du, L., Banis, M.N., Zhang, L., Chen, G., Doyle-Davis, K., Liang, J., Wang, S., et al. (2019). Trimetallic Pt–Pd–Ni octahedral nanocages with subnanometer thick-wall towards high oxygen reduction reaction. Nano Energy *64*, 103890. https://doi.org/10.1016/j.nanoen.2019.103890.

175. Liu, M., Zhao, Z., Duan, X., and Huang, Y. (2019). Nanoscale Structure Design for High-Performance Pt-Based ORR Catalysts. Adv. Mater. *31*, 1802234. https://doi.org/10.1002/adma.201802234.

176. Sui, S., Wang, X., Zhou, X., Su, Y., Riffat, S., and Liu, C.j. (2017). A comprehensive review of Pt electrocatalysts for the oxygen reduction reaction: Nanostructure, activity, mechanism and carbon support in PEM fuel cells. J. Mater. Chem. A *5*, 1808–1825. https://doi.org/10.1039/C6TA08580F.

177. Sun, Y., Polani, S., Luo, F., Ott, S., Strasser, P., and Dionigi, F. (2021). Advancements in cathode catalyst and cathode layer design for proton exchange membrane fuel cells. Nat. Commun. *12*, 5984. https://doi.org/10.1038/s41467-021-25911-x.

178. Meng, Q.H., Hao, C., Yan, B., Yang, B., Liu, J., Shen, P.K., and Tian, Z.Q. (2022). High-performance proton exchange membrane fuel cell with ultra-low loading Pt on vertically aligned carbon nanotubes as integrated catalyst layer. J. Energy Chem. *71*, 497–506. https://doi.org/10.1016/j.jechem.2022.03.018.

179. Grozovski, V., Kasuk, H., Nerut, J., Härk, E., Jäger, R., Tallo, I., and Lust, E. (2015). Oxygen Reduction at Shape-Controlled Platinum Nanoparticles and Composite Catalysts Based on (100)Pt Nanocubes on Microporous–Mesoporous Carbon Supports. Chemelectrochem *2*, 847–851. https://doi.org/10.1002/celc.201500021.

180. Venarusso, L.B., Boone, C.V., Bettini, J., and Maia, G. (2018). Carbon-supported metal nanodendrites as efficient, stable catalysts for the oxygen reduction reaction. J. Mater. Chem. A *6*, 1714–1726. https://doi.org/10.1039/C7TA08964C.

181. Zaman, S., Wang, M., Liu, H., Sun, F., Yu, Y., Shui, J., Chen, M., and Wang, H. (2022). Carbon-based catalyst supports for oxygen reduction in proton-exchange membrane fuel cells. Trends Chem. *4*, 886–906. https://doi.org/10.1016/j.trechm.2022.07.007.

182. Liu, H., Zhao, J., and Li, X. (2022). Controlled Synthesis of Carbon-Supported Pt-Based Electrocatalysts for Proton Exchange Membrane Fuel Cells. Electrochem. Energ. Rev. *5*, 13. https://doi.org/10.1007/s41918-022-00173-3.

183. Wang, Y.J., Zhao, N., Fang, B., Li, H., Bi, X.T., and Wang, H. (2015). Carbon-Supported Pt-Based Alloy Electrocatalysts for the Oxygen Reduction Reaction in Polymer Electrolyte Membrane Fuel Cells: Particle Size, Shape, and Composition Manipulation and Their Impact to Activity. Chem. Rev. *115*, 3433–3467. https://doi.org/10.1021/cr500519c.

184. Wang, X.X., Swihart, M.T., and Wu, G. (2019). Achievements, challenges and perspectives on cathode catalysts in proton exchange membrane fuel cells for transportation. Nat. Catal. *2*, 578–589. https://doi.org/10.1038/s41929-019-0304-9.

185. Seger, B., and Kamat, P.V. (2009). Electrocatalytically Active Graphene-Platinum Nanocomposites. Role of 2-D Carbon Support in PEM Fuel Cells. J. Phys. Chem. C *113*, 7990–7995. https://doi.org/10.1021/jp900360k.

186. Rey-Raap, N., dos Santos-Gómez, L., and Arenillas, A. (2024). Carbons for fuel cell energy generation. Carbon *228*, 119291. https://doi.org/10.1016/j.carbon.2024.119291.

187. Nair, A.S., and Jafri, R.I. (2023). A facile one-step microwave synthesis of Pt deposited on N & P co-doped graphene intercalated carbon black - An efficient cathode electrocatalyst for PEM fuel cell. Int. J. Hydrogen Energy *48*, 3653–3664. https://doi.org/10.1016/j.ijhydene.2022.10.210.

188. Ji, Z., Perez-Page, M., Chen, J., Rodriguez, R.G., Cai, R., Haigh, S.J., and Holmes, S.M. (2021). A structured catalyst support combining electrochemically exfoliated graphene oxide and carbon black for enhanced performance and durability in low-temperature hydrogen fuel cells. Energy *226*, 120318. https://doi.org/10.1016/j.energy.2021.120318.

189. Şanlı, L.I., Bayram, V., Yarar, B., Ghobadi, S., and Gürsel, S.A. (2016). Development of graphene supported platinum nanoparticles for polymer electrolyte membrane fuel cells: Effect of support type and impregnation–reduction methods. Int. J. Hydrogen Energy *41*, 3414–3427. https://doi.org/10.1016/j.ijhydene.2015.12.166.

190. Quesnel, E., Roux, F., Emieux, F., Faucherand, P., Kymakis, E., Volonakis, G., Giustino, F., Martín-García, B., Moreels, I., Gürsel, S.A., et al. (2015). Graphene-based technologies for energy applications, challenges and perspectives. 2D Mater. *2*, 030204. https://doi.org/10.1088/2053-1583/2/3/030204.

191. Abdolhosseinzadeh, S., Sadighikia, S., and Alkan Gürsel, S. (2018). Scalable Synthesis of Sub-Nanosized Platinum-Reduced Graphene Oxide Composite by an Ultraprecise Photocatalytic Method. ACS Sustain. Chem. Eng. *6*, 3773–3782. https://doi.org/10.1021/acssuschemeng.7b04148.

192. Haghmoradi, N., Sarı, Z.T., Öztürk, E.U., Peri, S., Abdolhosseinzadeh, S., Kaplan, B.Y., and Gürsel, S.A. (2021). Pulsed-UV illumination on graphene oxide: A new strategy in photocatalytic synthesis of electrocatalysts to control the structural and electrochemical properties. Int. J. Energy Res. *46*, 5200–5214. https://doi.org/10.1002/er.7512.

193. Haghmoradi, N., Sarı, Z.T., Kırlıoğlu, A.C., Yarar Kaplan, B., Dedeoğlu, B., Zahedimaram, P., Abdolhosseinzadeh, S., and Alkan Gürsel, S. (2022). Co^{2+}, Fe^{2+}, and Ni^{2+}: Modifiers for Photocatalytic Deposition of Highly Active Pt on Graphene-Based Supports. ACS Appl. Energy Mater. *5*, 13939–13951. https://doi.org/10.1021/acsaem.2c02569.

194. Jamil, M.F., Biçer, E., Yarar Kaplan, B., and Alkan Gürsel, S. (2021). One-step fabrication of new generation graphene-based electrodes for polymer electrolyte membrane fuel cells by a novel electrophoretic deposition. Int. J. Hydrogen Energy *46*, 5653–5663. https://doi.org/10.1016/j.ijhydene.2020.11.039.

195. Abdolhosseinzadeh, S., Mousavi, M., Haghmoradi, N., and Gürsel, S.A. (2019). A Continuous-flow Photocatalytic Reactor for the Precisely Controlled Deposition of Metallic Nanoparticles. J. Vis. Exp. *146*, e58883.

196. Daş, E., Alkan Gürsel, S., Işikel Şanli, L., and Bayrakçeken Yurtcan, A. (2016). Comparison of two different catalyst preparation methods for graphene nanoplatelets supported platinum catalysts. Int. J. Hydrogen Energy *41*, 9755–9761. https://doi.org/10.1016/j.ijhydene.2016.01.111.

197. Daş, E., Alkan Gürsel, S., Işıkel Şanlı, L., and Bayrakçeken Yurtcan, A. (2017). Thermodynamically controlled Pt deposition over graphene nanoplatelets: Effect of Pt loading on PEM fuel cell performance. Int. J. Hydrogen Energy *42*, 19246–19256. https://doi.org/10.1016/j.ijhydene.2017.06.108.

198. Işıkel Şanlı, L., Bayram, V., Ghobadi, S., Düzen, N., and Alkan Gürsel, S. (2017). Engineered catalyst layer design with graphene-carbon black hybrid supports for enhanced platinum utilization in PEM fuel cell. Int.

J. Hydrogen Energy *42*, 1085–1092. https://doi.org/10.1016/j.ijhydene.2016.08.210.

199. Şanlı, L.I., Yarar, B., Bayram, V., and Gürsel, S.A. (2017). Electrosprayed catalyst layers based on graphene–carbon black hybrids for the next-generation fuel cell electrodes. J. Mater. Sci. *52*, 2091–2102. https://doi.org/10.1007/s10853-016-0497-0.

200. Yarar Kaplan, B., Haghmoradi, N., Biçer, E., Merino, C., and Alkan Gürsel, S. (2018). High performance electrocatalysts supported on graphene based hybrids for polymer electrolyte membrane fuel cells. Int. J. Hydrogen Energy *43*, 23221–23230. https://doi.org/10.1016/j.ijhydene.2018.10.222.

201. Daş, E., Kaplan, B.Y., Gürsel, S.A., and Yurtcan, A.B. (2019). Graphene nanoplatelets-carbon black hybrids as an efficient catalyst support for Pt nanoparticles for polymer electrolyte membrane fuel cells. Renew. Energy *139*, 1099–1110. https://doi.org/10.1016/j.renene.2019.02.137.

202. Arıcı, E., Kaplan, B.Y., Mert, A.M., Gürsel, S.A., and Kınayyiğit, Ş. (2019). An effective electrocatalyst based on platinum nanoparticles supported with graphene nanoplatelets and carbon black hybrid for PEM fuel cells. Int. J. Hydrogen Energy *44*, 14175–14183. https://doi.org/10.1016/j.ijhydene.2018.11.210.

203. Tang, X., Zeng, Y., Cao, L., Yang, L., Wang, Z., Fang, D., Gao, Y., Shao, Z., and Yi, B. (2018). Anchoring ultrafine Pt nanoparticles on the 3D hierarchical self-assembly of graphene/functionalized carbon black as a highly efficient oxygen reduction catalyst for PEMFCs. J. Mater. Chem. A *6*, 15074–15082. https://doi.org/10.1039/C8TA02453G.

204. Zhang, C., Feng, Z., Lei, Y., Zhang, X., Gao, W., Sun, L., Liu, Z., Wang, J., Wang, Y., and Wang, C. (2022). Batch synthesis of high activity and durability carbon supported platinum catalysts for oxygen reduction reaction using a new facile continuous microwave pipeline technology. J. Colloid Interface Sci. *628*, 174–188. https://doi.org/10.1016/j.jcis.2022.08.058.

205. Ott, S., Orfanidi, A., Schmies, H., Anke, B., Nong, H.N., Hübner, J., Gernert, U., Gliech, M., Lerch, M., and Strasser, P. (2020). Ionomer distribution control in porous carbon-supported catalyst layers for high-power and low Pt-loaded proton exchange membrane fuel cells. Nat. Mater. *19*, 77–85. https://doi.org/10.1038/s41563-019-0487-0.

206. Wu, Z.P., Caracciolo, D.T., Maswadeh, Y., Wen, J., Kong, Z., Shan, S., Vargas, J.A., Yan, S., Hopkins, E., Park, K., et al. (2021). Alloying–realloying enabled high durability for Pt–Pd-3d-transition metal nanoparticle fuel cell catalysts. Nat. Commun. *12*, 859. https://doi.org/10.1038/s41467-021-21017-6.

207. Li, J., Sharma, S., Liu, X., Pan, Y.T., Spendelow, J.S., Chi, M., Jia, Y., Zhang, P., Cullen, D.A., Xi, Z., et al. (2019). Hard-Magnet $L1_0$-CoPt Nanoparticles Advance Fuel Cell Catalysis. Joule *3*, 124–135. https://doi.org/10.1016/j.joule.2018.09.016.

208. Sawant, K.J., Zeng, Z., and Greeley, J.P. (2024). Origin of Stability and Activity Enhancements in Pt-based Oxygen Reduction Reaction Catalysts via Defect-Mediated Dopant Adsorption. Angew. Chem. Int. Ed. *63*, e202312747. https://doi.org/10.1002/anie.202312747.

209. Yoshida, T., and Kojima, K. (2015). Toyota MIRAI Fuel Cell Vehicle and Progress Toward a Future Hydrogen Society. Electrochem. Soc. Interface *24*, 45–49. https://doi.org/10.1149/2.F03152if.

210. Wang, L., Morales-Collazo, O., Brennecke, J.F., and Jia, H. (2023). Dimeric ionic liquid for improving performance and durability of PEMFCs. J. Power Sources *556*, 232488. https://doi.org/10.1016/j.jpowsour.2022.232488.

211. Herzog, A., Kühl, S., Lu, J., Amitrano, R., Selve, S., Schmidt, J., Merzdorf, T., and Strasser, P. (2024). Synthetic design of active and stable bimetallic PtTi nanoparticle electrocatalysts for efficient oxygen reduction at fuel cell cathodes. J. Mater. Chem. A *12*, 25334–25345. https://doi.org/10.1039/D4TA00364K.

212. Nie, Y., Sun, Y., Meyer, Q., Shiyang, L., Guo, H., Tao, L., Lin, F., Luo, M., Zhang, Q., Gu, L., et al. (2024). Low-Electronegativity Mn-Contraction of PtMn Nanodendrites Boosts Oxygen Reduction Durability. Angew. Chem. Int. Ed. *63*, e202317987. https://doi.org/10.1002/anie.202317987.

213. Wu, Y., Chen, L., Geng, S., Tian, Y., Chen, R., Wang, K., Wang, Y., and Song, S. (2024). PtFe Nanoalloys Supported on Fe-Based Cubic Framework as Efficient Oxygen Reduction Electrocatalysts for Proton Exchange Membrane Fuel Cells. Adv. Funct. Mater. *34*, 2307297. https://doi.org/10.1002/adfm.202307297.

214. Zhang, L., Liu, T., Liu, X., Li, S., Zhang, X., Luo, Q., Ding, T., Yao, T., and Zhang, W. (2024). Highly dispersed ultrafine PtCo alloy nanoparticles on unique composite carbon supports for proton exchange membrane fuel cells. Nanoscale *16*, 2868–2876. https://doi.org/10.1039/D3NR05403A.

215. Yang, H., Ko, Y., Lee, W., Züttel, A., and Kim, W. (2019). Nitrogen-doped carbon black supported Pt–M (M = Pd, Fe, Ni) alloy catalysts for oxygen reduction reaction in proton exchange membrane fuel cell. Mater. Today Energy *13*, 374–381. https://doi.org/10.1016/j.mtener.2019.06.007.

216. Daş, E., Alkan Gürsel, S., and Bayrakçeken Yurtcan, A. (2020). Pt-alloy decorated graphene as an efficient electrocatalyst for PEM fuel cell reactions. J. Supercrit. Fluids *165*, 104962. https://doi.org/10.1016/j.supflu.2020.104962.

217. Cui, C., Gan, L., Heggen, M., Rudi, S., and Strasser, P. (2013). Compositional segregation in shaped Pt alloy nanoparticles and their structural behaviour during electrocatalysis. Nat. Mater. *12*, 765–771. https://doi.org/10.1038/nmat3668.

218. Liang, J., Li, N., Zhao, Z., Ma, L., Wang, X., Li, S., Liu, X., Wang, T., Du, Y., Lu, G., et al. (2019). Tungsten-Doped L10-PtCo Ultrasmall Nanoparticles as a High-Performance Fuel Cell Cathode. Angew. Chem. Int. Ed. *58*, 15471–15477. https://doi.org/10.1002/anie.201908824.

219. Yarar Kaplan, B., Haghmoradi, N., Jamil, E., Merino, C., and Alkan Gürsel, S. (2020). Platinum nanoparticles decorated carbon nanofiber hybrids as highly active electrocatalysts for polymer electrolyte membrane fuel cells. Int. J. Energy Res. *44*, 10251–10261. https://doi.org/10.1002/er.5646.

220. Sevim Yılmaz, M., Kaplan, B.Y., Metin, Ö., and Gürsel, S.A. (2018). A facile synthesis and assembly of ultrasmall Pt nanoparticles on reduced graphene oxide-carbon black hybrid for enhanced performance in PEMFC. Mater. Des. *151*, 29–36. https://doi.org/10.1016/j.matdes.2018.04.041.

221. Harzer, G.S., Orfanidi, A., El-Sayed, H., Madkikar, P., and Gasteiger, H.A. (2018). Tailoring Catalyst Morphology towards High Performance for Low Pt Loaded PEMFC Cathodes. J. Electrochem. Soc. *165*, F770–F779. https://doi.org/10.1149/2.0311810jes.

222. Shen, L., Tu, F., Shang, Z., Ma, M., Xia, Y., Zhao, Z., Zhao, L., Wang, Z., and Shao, G. (2022). Surfactant-assisted synthesis of platinum nanoparticle catalysts for proton exchange membrane fuel cells. Int. J. Hydrogen Energy *47*, 15001–15011. https://doi.org/10.1016/j.ijhydene.2022.03.004.

223. Karuppanan, M., Kim, Y., Gok, S., Lee, E., Hwang, J.Y., Jang, J.H., Cho, Y.H., Lim, T., Sung, Y.E., and Kwon, O.J. (2019). A highly durable carbon-nanofiber-supported Pt–C core–shell cathode catalyst for ultra-low Pt loading proton exchange membrane fuel cells: facile carbon encapsulation. Energy Environ. Sci. *12*, 2820–2829. https://doi.org/10.1039/C9EE01000A.

224. Zhu, S., Yang, L., Bai, J., Chu, Y., Liu, J., Jin, Z., Liu, C., Ge, J., and Xing, W. (2023). Ultra-stable Pt5La intermetallic compound towards highly efficient oxygen reduction reaction. Nano Res. *16*, 2035–2040. https://doi.org/10.1007/s12274-022-4868-3.

225. Liu, J., Liu, S., Yan, F., Wen, Z., Chen, W., Liu, X., Liu, Q., Shang, J., Yu, R., Su, D., and Shui, J. (2022). Ultrathin Nanotube Structure for Mass-Efficient and Durable Oxygen Reduction Reaction Catalysts in PEM Fuel Cells. J. Am. Chem. Soc. *144*, 19106–19114. https://doi.org/10.1021/jacs.2c08361.

226. Zhou, Z., Zhang, H.J., Feng, X., Ma, Z., Ma, Z.F., and Xue, Y. (2024). Progress of Pt and iron-group transition metal alloy catalysts with high ORR activity for PEMFCs. J. Electroanal. Chem. *959*, 118165. https://doi.org/10.1016/j.jelechem.2024.118165.

227. Pan, L., Ott, S., Dionigi, F., and Strasser, P. (2019). Current challenges related to the deployment of shape-controlled Pt alloy oxygen reduction reaction nanocatalysts into low Pt-loaded cathode layers of proton exchange membrane fuel cells. Curr. Opin. Electrochem. *18*, 61–71. https://doi.org/10.1016/j.coelec.2019.10.011.

228. Lim, C., Fairhurst, A.R., Ransom, B.J., Haering, D., and Stamenkovic, V. R. (2023). Role of Transition Metals in Pt Alloy Catalysts for the Oxygen Reduction Reaction. ACS Catal. *13*, 14874–14893. https://doi.org/10.1021/acscatal.3c03321.

229. Zhu, M., Wang, J., and Wu, Y. (2020). Single-atom Catalysts for Polymer Electrolyte Membrane Fuel Cells. Chem. Res. Chin. Univ. *36*, 320–328. https://doi.org/10.1007/s40242-020-0111-5.

230. Wang, X.X., Cullen, D.A., Pan, Y.T., Hwang, S., Wang, M., Feng, Z., Wang, J., Engelhard, M.H., Zhang, H., He, Y., et al. (2018). Nitrogen-Coordinated Single Cobalt Atom Catalysts for Oxygen Reduction in Proton Exchange Membrane Fuel Cells. Adv. Mater. *30*, 1706758. https://doi.org/10.1002/adma.201706758.

231. Shen, H., Thomas, T., Rasaki, S.A., Saad, A., Hu, C., Wang, J., and Yang, M. (2019). Oxygen Reduction Reactions of Fe-N-C Catalysts: Current Status and the Way Forward. Electrochem. Energ. Rev. *2*, 252–276. https://doi.org/10.1007/s41918-019-00030-w.

232. Du, L., Prabhakaran, V., Xie, X., Park, S., Wang, Y., and Shao, Y. (2021). Low-PGM and PGM-Free Catalysts for Proton Exchange Membrane Fuel Cells: Stability Challenges and Material Solutions. Adv. Mater. *33*, 1908232. https://doi.org/10.1002/adma.201908232.

233. Wuan, S., Shui, J.L., Grabstanowicz, L., Chen, C., Commet, S., Reprogle, B., Xu, T., Yu, L., and Liu, D.J. (2013). A Highly Active and Support-Free Oxygen Reduction Catalyst Prepared from Ultrahigh-Surface-Area Porous Polyporphyrin. Angew. Chem. Int. Ed. *52*, 8349–8353. https://doi.org/10.1002/anie.201302924.

234. Fu, X., Zamani, P., Choi, J.Y., Hassan, F.M., Jiang, G., Higgins, D.C., Zhang, Y., Hoque, M.A., and Chen, Z. (2017). In Situ Polymer Graphenization Ingrained with Nanoporosity in a Nitrogenous Electrocatalyst Boosting the Performance of Polymer-Electrolyte-Membrane Fuel Cells. Adv. Mater. *29*, 1604456. https://doi.org/10.1002/adma.201604456.

235. Zhang, X., Mollamahale, Y.B., Lyu, D., Liang, L., Yu, F., Qing, M., Du, Y., Zhang, X., Tian, Z.Q., and Shen, P.K. (2019). Molecular-level design of Fe-N-C catalysts derived from Fe-dual pyridine coordination complexes for highly efficient oxygen reduction. J. Catal. *372*, 245–257. https://doi.org/10.1016/j.jcat.2019.03.003.

236. Xia, D., Yang, X., Xie, L., Wei, Y., Jiang, W., Dou, M., Li, X., Li, J., Gan, L., and Kang, F. (2019). Direct Growth of Carbon Nanotubes Doped with Single Atomic Fe–N4 Active Sites and Neighboring Graphitic Nitrogen for Efficient and Stable Oxygen Reduction Electrocatalysis. Adv. Funct. Mater. *29*, 1906174. https://doi.org/10.1002/adfm.201906174.

237. Wang, Y.C., Lai, Y.J., Song, L., Zhou, Z.Y., Liu, J.G., Wang, Q., Yang, X. D., Chen, C., Shi, W., Zheng, Y.P., et al. (2015). S-Doping of an Fe/N/C ORR Catalyst for Polymer Electrolyte Membrane Fuel Cells with High Power Density. Angew. Chem. Int. Ed. *54*, 9907–9910. https://doi.org/10.1002/anie.201503159.

238. Wan, L., Chen, W., Xu, H., Wang, Y., Yuan, J., Zhou, Z., and Sun, S. (2021). A Mild CO_2 Etching Method To Tailor the Pore Structure of Platinum-Free Oxygen Reduction Catalysts in Proton Exchange Membrane Fuel Cells. ACS Appl. Mater. Interfaces *13*, 45661–45669. https://doi.org/10.1021/acsami.1c14709.

239. Liu, Q., Liu, X., Zheng, L., and Shui, J. (2018). The Solid-Phase Synthesis of an Fe-N-C Electrocatalyst for High-Power Proton-Exchange Membrane Fuel Cells. Angew. Chem. Int. Ed. *57*, 1204–1208. https://doi.org/10.1002/anie.201709597.

240. Li, J., Chen, M., Cullen, D.A., Hwang, S., Wang, M., Li, B., Liu, K., Karakalos, S., Lucero, M., Zhang, H., et al. (2018). Atomically dispersed manganese catalysts for oxygen reduction in proton-exchange membrane fuel cells. Nat. Catal. *1*, 935–945. https://doi.org/10.1038/s41929-018-0164-8.

241. Sibul, R., Kibena-Põldsepp, E., Ratso, S., Kook, M., Sougrati, M.T., Käärik, M., Merisalu, M., Aruväli, J., Paiste, P., Treshchalov, A., et al. (2020). Iron- and Nitrogen-Doped Graphene-Based Catalysts for Fuel Cell Applications. Chemelectrochem *7*, 1739–1747. https://doi.org/10.1002/celc.202000011.

242. Kırlıoğlu, A.C., Ölmez, B., Rahbarshendi, F., Buldu-Akturk, M., Yürüm, A., Alkan Gürsel, S., and Yarar Kaplan, B. (2024). Scalable nano-sized Fe-N-C catalysts for fuel cells: Evaluating the impact of iron precursors and CeO_2 addition. Mater. Res. Bull. *179*, 112952. https://doi.org/10.1016/j.materresbull.2024.112952.

243. Yang, X., Wang, Y., Zhang, G., Du, L., Yang, L., Markiewicz, M., Choi, J. y., Chenitz, R., and Sun, S. (2020). SiO_2-Fe/N/C catalyst with enhanced mass transport in PEM fuel cells. Appl. Catal. B Environ. *264*, 118523. https://doi.org/10.1016/j.apcatb.2019.118523.

244. Wan, X., Liu, X., Li, Y., Yu, R., Zheng, L., Yan, W., Wang, H., Xu, M., and Shui, J. (2019). Fe–N–C electrocatalyst with dense active sites and efficient mass transport for high-performance proton exchange membrane fuel cells. Nat. Catal. *2*, 259–268. https://doi.org/10.1038/s41929-019-0237-3.

245. Liu, S., Li, C., Zachman, M.J., Zeng, Y., Yu, H., Li, B., Wang, M., Braaten, J., Liu, J., Meyer, H.M., III., et al. (2022). Atomically dispersed iron sites with a nitrogen–carbon coating as highly active and durable oxygen reduction catalysts for fuel cells. Nat. Energy *7*, 652–663. https://doi.org/10.1038/s41560-022-01062-1.

246. Yin, S., Chen, L., Yang, J., Cheng, X., Zeng, H., Hong, Y., Huang, H., Kuai, X., Lin, Y., Huang, R., et al. (2024). A Fe-NC electrocatalyst boosted by trace bromide ions with high performance in proton exchange membrane fuel cells. Nat. Commun. *15*, 7489. https://doi.org/10.1038/s41467-024-51858-w.

247. Liu, J., Wan, X., Liu, S., Liu, X., Zheng, L., Yu, R., and Shui, J. (2021). Hydrogen Passivation of M–N–C (M = Fe, Co) Catalysts for Storage Stability and ORR Activity Improvements. Adv. Mater. *33*, 2103600. https://doi.org/10.1002/adma.202103600.

248. Kasuk, K.A., Nerut, J., Grozovski, V., Lust, E., and Kucernak, A. (2024). Design and Impact: Navigating the Electrochemical Characterization Methods for Supported Catalysts. ACS Catal. *14*, 11949–11966. https://doi.org/10.1021/acscatal.4c03271.

249. Wu, J., Yuan, X.Z., Wang, H., Blanco, M., Martin, J.J., and Zhang, J. (2008). Diagnostic tools in PEM fuel cell research: Part I Electrochemical techniques. Int. J. Hydrogen Energy *33*, 1735–1746. https://doi.org/10.1016/j.ijhydene.2008.01.013.

250. Vega-Granados, K., and Alonso-Vante, N. (2023). Quantifying the Activity of Electrocatalysts. In Electrocatalysis for Membrane Fuel Cells, N. Alonso-Vante and V. Di Noto, eds.. https://doi.org/10.1002/9783527830572.ch12.

251. Hashimasa, Y., and Numata, T. (2015). Comparison of test results on load cycle durability of polymer electrolyte fuel cell cathode catalysts. Int. J. Hydrogen Energy *40*, 11543–11549. https://doi.org/10.1016/j.ijhydene.2015.04.031.

252. Tang, H., Qi, Z., Ramani, M., and Elter, J.F. (2006). PEM fuel cell cathode carbon corrosion due to the formation of air/fuel boundary at the anode. J. Power Sources *158*, 1306–1312. https://doi.org/10.1016/j.jpowsour.2005.10.059.

253. Sun, Y.Y., Liu, S., Hou, Y.K., Li, G.R., and Gao, X.P. (2019). In-situ surface modification to stabilize Ni-rich layered oxide cathode with functional electrolyte. J. Power Sources *410–411*, 115–123. https://doi.org/10.1016/j.jpowsour.2018.11.015.

254. Chung, D.Y., Lopes, P.P., Farinazzo Bergamo Dias Martins, P., He, H., Kawaguchi, T., Zapol, P., You, H., Tripkovic, D., Strmcnik, D., Zhu, Y., et al. (2020). Dynamic stability of active sites in hydr(oxy)oxides for the oxygen evolution reaction. Nat. Energy *5*, 222–230. https://doi.org/10.1038/s41560-020-0576-y.

255. Pivovar, B.S., and Kim, Y.S. (2007). The Membrane–Electrode Interface in PEFCs: I. A Method for Quantifying Membrane–Electrode Interfacial

Resistance. J. Electrochem. Soc. *154*, B739. https://doi.org/10.1149/1.2740005.

256. Kim, Y.S., Einsla, M., McGrath, J.E., and Pivovar, B.S. (2010). The Membrane–Electrode Interface in PEFCs: II. Impact on Fuel Cell Durability. J. Electrochem. Soc. *157*, B1602. https://doi.org/10.1149/1.3481577.

257. Kim, Y.S., and Pivovar, B.S. (2010). The Membrane–Electrode Interface in PEFCs: IV. The origin and implications of interfacial resistance. J. Electrochem. Soc. *157*, B1616. https://doi.org/10.1149/1.3481581.

258. Dao, D.V., Adilbish, G., Le, T.D., Lee, I.H., and Yu, Y.T. (2019). Triple phase boundary and power density enhancement in PEMFCs of a Pt/C electrode with double catalyst layers. RSC Adv. *9*, 15635–15641. https://doi.org/10.1039/C9RA01741K.

259. Wang, Y.C., Huang, W., Wan, L.Y., Yang, J., Xie, R.J., Zheng, Y.P., Tan, Y.Z., Wang, Y.S., Zaghib, K., Zheng, L.R., et al. (2022). Identification of the active triple-phase boundary of a non-Pt catalyst layer in fuel cells. Sci. Adv. *8*, eadd8873. https://doi.org/10.1126/sciadv.add8873.

260. Deng, X., Zhang, J., Fan, Z., Tan, W., Yang, G., Wang, W., Zhou, W., and Shao, Z. (2020). Understanding and Engineering of Multiphase Transport Processes in Membrane Electrode Assembly of Proton-Exchange Membrane Fuel Cells with a Focus on the Cathode Catalyst Layer: A Review. Energy Fuels *34*, 9175–9188. https://doi.org/10.1021/acs.energyfuels.0c02101.

261. O'Hayre, R., Barnett, D.M., and Prinz, F.B. (2005). The Triple Phase Boundary: A Mathematical Model and Experimental Investigations for Fuel Cells. J. Electrochem. Soc. *152*, A439. https://doi.org/10.1149/1.1851054.

262. Breitweiser, M., Klingele, M., Vierrath, S., Zengerle, R., and Thiele, S. (2017). Tailoring the Membrane-Electrode Interface in PEM Fuel Cells: A Review and Perspective on Novel Engineering Approaches. Adv. Energy Mater. *8*, 1701257. https://doi.org/10.1002/aenm.201701257.

263. Meyer, Q., Liu, S., Ching, K., Da Wang, Y., and Zhao, C. (2023). Operando monitoring of the evolution of triple-phase boundaries in proton exchange membrane fuel cells. J. Power Sources *557*, 232539. https://doi.org/10.1016/j.jpowsour.2022.232539.

264. Jiménez-García, J.C., Robledo Flores, D.F.F., Acosta, R.H., Velasco, M. I., Franceschini, E.A., and Mariscal, M.M. (2024). Water behavior at PEMFC triple phase boundary: Exploring ionomer and catalytic layer effects via molecular dynamic simulations and NMR experiments. Int. J. Hydrogen Energy *52*, 65–71. https://doi.org/10.1016/j.ijhydene.2023.10.097.

265. Li, Y., Wu, Z., Wang, C., Yu, X., Gao, W., Wang, B., Wu, C., Yao, Y., Yang, J., and Zou, Z. (2024). Engineering Triple-Phase Boundary in Pt Catalyst Layers for Proton Exchange Membrane Fuel Cells. Adv. Funct. Mater. *34*, 2310428. https://doi.org/10.1002/adfm.202310428.

266. Dhanda, A., O'Hayre, R., and Pitsch, H. (2009). EIS Analysis of the Triple Phase Boundary Model. ECS Trans. *19*, 23–31. https://doi.org/10.1149/1.3268159.

267. Dhanda, A., Pitsch, H., and O'Hayre, R. (2011). Diffusion Impedance Element Model for the Triple Phase Boundary. J. Electrochem. Soc. *158*, B877. https://doi.org/10.1149/1.3596020.

268. Koh, J.K., Jeon, Y., Cho, Y.I., Kim, J.H., and Shul, Y.G. (2014). A facile preparation method of surface patterned polymer electrolyte membranes for fuel cell applications. J. Mater. Chem. A *2*, 8652–8659. https://doi.org/10.1039/C4TA00674G.

269. O'Hayre, R., Lee, S.J., Cha, S.W., and Prinz, F.B. (2002). A sharp peak in the performance of sputtered platinum fuel cells at ultra-low platinum loading. J. Power Sources *109*, 483–493. https://doi.org/10.1016/S0378-7753(02)00238-0.

270. Klingele, M., Breitwieser, M., Zengerle, R., and Thiele, S. (2015). Direct deposition of proton exchange membranes enabling high performance hydrogen fuel cells. J. Mater. Chem. A *3*, 11239–11245. https://doi.org/10.1039/C5TA01341K.

271. Wehkamp, N., Breitwieser, M., Büchler, A., Klingele, M., Zengerle, R., and Thiele, S. (2016). Directly deposited Nafion/TiO_2 composite membranes for high power medium temperature fuel cells. RSC Adv. *6*, 24261–24266. https://doi.org/10.1039/C5RA27462A.

272. Dang, Q.K., Henkensmeier, D., Krishnan, N.N., Jang, J.H., Kim, H.J., Nam, S.W., and Lim, T.H. (2014). Nafion membranes with a porous surface. J. Membr. Sci. *460*, 199–205. https://doi.org/10.1016/j.memsci.2014.03.003.

273. Wang, Z., and Nagao, Y. (2014). Effects of Nafion impregnation using inkjet printing for membrane electrode assemblies in polymer electrolyte membrane fuel cells. Electrochim. Acta *129*, 343–347. https://doi.org/10.1016/j.electacta.2014.02.133.

274. Ahn, J.H., You, T.S., Lee, S.M., Esken, D., Dehe, D., Huang, Y.C., and Kim, D.W. (2020). Hybrid separator containing reactive, nanostructured alumina promoting in-situ gel electrolyte formation for lithium-ion batteries with good cycling stability and enhanced safety. J. Power Sources *472*, 228519. https://doi.org/10.1016/j.jpowsour.2020.228519.

275. Kim, S.M., Kim, C.H., Kim, Y., Kim, N., Lee, W.J., Lee, E.H., Kim, D., Park, S., Lee, K., Rivnay, J., and Yoon, M.H. (2018). Influence of PEDOT:PSS crystallinity and composition on electrochemical transistor performance and long-term stability. Nat. Commun. *9*, 3858. https://doi.org/10.1038/s41467-018-06084-6.

276. Cheng, N., Shao, Y., Liu, J., and Sun, X. (2016). Electrocatalysts by atomic layer deposition for fuel cell applications. Nano Energy *29*, 220–242. https://doi.org/10.1016/j.nanoen.2016.01.016.

277. Meyer, Q., Zeng, Y., and Zhao, C. (2019). In Situ and Operando Characterization of Proton Exchange Membrane Fuel Cells. Adv. Mater. *31*, 1901900. https://doi.org/10.1002/adma.201901900.

278. Tang, K., Meyer, Q., White, R., Armstrong, R.T., Mostaghimi, P., Da Wang, Y., Liu, S., Zhao, C., Regenauer-Lieb, K., and Tung, P.K.M. (2022). Deep learning for full-feature X-ray microcomputed tomography segmentation of proton electron membrane fuel cells. Comput. Chem. Eng. *161*, 107768. https://doi.org/10.1016/j.compchemeng.2022.107768.

279. Xue, D., and Zhang, J.N. (2024). Recent progress of antipoisoning catalytic materials for high temperature proton exchange membrane fuel cells doped with phosphoric acid. Ind. Chem. Mater. *2*, 173–190. https://doi.org/10.1039/D3IM00101F.

280. Kumar, R., Prabakaran, A., Gaigole, P.M., Esakkiammal, U., Divya, N., Sherje, N., and Ragu Nathan, S. (2024). Advancements in Proton Exchange Membrane Fuel Cells Improving Efficiency and Durability. E3S Web Conf. *591*, 06001. https://doi.org/10.1051/e3sconf/202459106001.

281. Alabi, A.S., Popoola, A.P.I., Popoola, O.M., Mathe, N.R., and Abdulwahab, M. (2023). Materials for electrocatalysts in proton exchange membrane fuel cell: A brief review. Front. Energy Res. *11*. https://doi.org/10.3389/fenrg.2023.1091105.

282. Liu, W., Liu, D., Wan, X., and Shui, J. (2025). Functional additives for proton exchange membrane fuel cells. EnergyChem *7*, 100144. https://doi.org/10.1016/j.enchem.2025.100144.

283. Zhao, L., Ren, Y., Shi, X., Liu, H., Yu, Z., Gao, J., and Zhao, J. (2025). Unveiling the unexpected sinking and embedding dynamics of surface supported Mo/S clusters on 2D MoS2 with active machine learning. Smart Mol. *3*, e20240018. https://doi.org/10.1002/smo.20240018.

284. Grandi, M., Rohde, S., Liu, D.J., Gollas, B., and Hacker, V. (2023). Recent advancements in high performance polymer electrolyte fuel cell electrode fabrication – Novel materials and manufacturing processes. J. Power Sources *562*, 232734. https://doi.org/10.1016/j.jpowsour.2023.232734.

285. Pramitha, A., Hegde, S.S., Bhat, B.R., George, S.D., Sudhakar, Y.N., and Raviprakash, Y. (2023). Properties of Mn_3O_4 thin film electrodes prepared using spray pyrolysis for supercapacitor application. Mater. Chem. Phys. *307*, 128213. https://doi.org/10.1016/j.matchemphys.2023.128213.

286. Waldrop, K., Slack, J.J., Gumeci, C., Parrondo, J., Dale, N., Reeves, K.S., Cullen, D.A., More, K.L., and Pintauro, P.N. (2023). Electrospun

Nanofiber Electrodes for High and Low Humidity PEMFC Operation. J. Electrochem. Soc. *170*, 024507. https://doi.org/10.1149/1945-7111/acb8e2.

287. Towne, S., Viswanathan, V., Holbery, J., and Rieke, P. (2007). Fabrication of polymer electrolyte membrane fuel cell MEAs utilizing inkjet print technology. J. Power Sources *171*, 575–584. https://doi.org/10.1016/j.jpowsour.2007.07.017.

288. Agyekum, E.B., Ampah, J.D., Wilberforce, T., Afrane, S., and Nutakor, C. (2022). Research Progress, Trends, and Current State of Development on PEMFC-New Insights from a Bibliometric Analysis and Characteristics of Two Decades of Research Output. Membranes *12*, 1103–1135. https://doi.org/10.3390/membranes12111103.

289. Hydrogen Council (2023). Hydrogen Insights 2023. https://hydrogencouncil.com/wp-content/uploads/2023/05/Hydrogen-Insights-2023.pdf.